THE ORGANIZATION OF SPATIAL VISION IN THE JUVENILE LEMON SHARK (*NEGAPRION BREVIROSTRIS*): RETINOTECTAL PROJECTION, RETINAL TOPOGRAPHY, AND IMPLICATIONS FOR THE VISUAL ECOLOGY OF SHARKS

By

ROBERT EDWARD HUETER

A DISSERTATION PRESENTED TO THE GRADUATE SCHOOL
OF THE UNIVERSITY OF FLORIDA IN
PARTIAL FULFILLMENT OF THE REQUIREMENTS
FOR THE DEGREE OF DOCTOR OF PHILOSOPHY

UNIVERSITY OF FLORIDA

1988

ACKNOWLEDGMENTS

The many problems of conducting physiological research on living sharks could only have been overcome with the generous assistance of many people. I first extend my deepest appreciation and gratitude to my major professor, Dr. Horst Schwassmann, one of the original "mappers" from a time when technology was second to technique. His initial skepticism about the project was always tempered with an undercurrent of strong support, which soon became enthusiastic encouragement as the project progressed. I have learned much from him, not only in electrophysiology, histology, and sensory biology, but also in appreciating the historical perspective of scientific endeavors--not to mention the many splendors of the fish eye. For all of these things, I am deeply grateful.

I also express my sincere appreciation to Dr. Paul Linser and Dr. William Dawson of my supervisory committee. Both of them generously opened up their laboratories to me so that I could successfully complete this project. Dr. Linser's support of my work during my tenure at the Whitney Laboratory was extraordinary, literally keeping this project afloat, and to him I am deeply grateful for that support as well as his expertise, his patience, and his friendship. Much of the same also applies to Dr. Dawson, whose vision laboratory opened my own eyes to so many wonderful possibilities, and whose interest in my studies and support of this project were instrumental in its success.

Dr. David Evans and Dr. Carter Gilbert, the two other members of my committee, have been among the most influential teachers in my university education, and I thank them for their knowledge, their inspiration by example, and their friendship.

To the following, I am deeply indebted for their assistance and expertise in the collection and maintenance of sharks in captivity. Frank Murru and Don Chittick of Sea World of Florida supervised the collecting of my experimental animals, furnished transport equipment, and provided advice on captive maintenace of the sharks. Billy Raulerson at the Whitney Laboratory, and Robert Ingman and Charlie Jabaly at the zoology department in Gainesville helped solve the problems of keeping sharks in limited facilities.

Special thanks are extended to the following people at the Whitney Laboratory for their assistance: Drs. Mike Greenberg and Barry Ache for support and technical help; Margaret Perkins for technical and moral support; and Lynn Milstead and Jim Netherton for illustration and photographic work. Back in Gainesville, I thank Ron Parmer for technical assistance, and Minnie Hawthorne deserves special mention for her help in the pursuit of the perfect retinal wholemount.

Financial assistance for this project was provided by the following sources: the Lerner-Gray Fund for Marine Research, a Sigma Xi Grant-in-Aid, and the Department of Zoology at the University of Florida.

Finally, personal thanks are extended to my friend and colleague Dr. Joel Cohen for his constant encouragement, expertise, and special abstract service; to all of my friends in the zoology department for their help and uncommon friendship; and, as always, to my family, for their steadfast understanding and support.

TABLE OF CONTENTS

Abstract of Dissertation Presented to the Graduate School
of the University of Florida in Partial Fulfillment of the
Requirements for the Degree of Doctor of Philosophy

THE ORGANIZATION OF SPATIAL VISION IN THE JUVENILE LEMON SHARK (NEGAPRION BREVIROSTRIS): RETINOTECTAL PROJECTION, RETINAL TOPOGRAPHY, AND IMPLICATIONS FOR THE VISUAL ECOLOGY OF SHARKS

By

Robert Edward Hueter

April 1988

Chairman: Horst O. Schwassmann
Major Department: Zoology

In an effort to understand the organization of spatial vision and its role in the visual ecology of sharks, the retinotectal projection, retinal cone distribution, and retinal ganglion cell distribution were mapped in the juvenile lemon shark. Retinotectal mapping was electrophysiologically conducted in live sharks using a perimetry device that simulated the left visual field. Tectal unit responses evoked by photic stimuli were recorded in the contralateral optic tectum at an average depth of 496 μm below the tectal surface. The overall projection pattern reveals an orderly point-to-point relationship such that dorsal visual field projects to medial tectum, ventral field projects to lateral tectum, rostral field projects to rostral tectum, and caudal field projects to caudal tectum, as in almost all other vertebrates. This confirms the mesencephalic tectum as the primary center for spatial visual input in elasmobranchs.

Retinal cell topography was mapped using a retina wholemount technique. The retinotectal projection pattern, cone distribution, and ganglion cell distribution are all organized into a prominent visual streak, a horizontal band of proportionately greater retinal cell density and retinotectal magnification. This streak is located within about 15° above and 15° below the horizontal meridian in the visual field. Three times more tectum is devoted to vision in the streak than to peripheral vision, and receptive fields of tectal units are smaller and more regular in shape inside the streak than in the periphery. Ganglion cell and cone densities increase from less than 500 ganglion cells/mm^2 and less than 500 cones/mm^2 peripherally to over 1500 ganglion cells/mm^2 and about 6500 cones/mm^2 inside the streak.

The visual streak of the juvenile lemon shark conforms with the terrain theory of visual streak function. According to this theory, the streak enhances spatial vision along the visual horizon in animals whose habitats are dominated by a two-dimensional horizontal terrain. In the juvenile lemon shark, the locomotory mode of constant patrolling over the benthos may further add to the adaptive value of the visual streak in this species.

INTRODUCTION

Physiological Ecology of Vision

The sensory systems of animals constitute the selective channels through which animals perceive their world and gain information about their environment. All that an animal learns of its surroundings must pass through the filters of one or more of its senses. To make best use of available resources, be they food, protection from predators, or reproductive opportunities, an animal's sensory systems must be no less exquisitely molded by the forces of natural selection than its locomotory design, respiratory rate, or reproductive strategy.

From this premise, it follows that a study of the ways in which sensory systems are attuned to the environments in which they operate yields at least two interrelated kinds of insights into animals' lives. The first of these is the body of significant sensory stimuli for a particular species. Careful examination of an animal's sensory machinery can reveal the key stimuli selected for by that species. The discoveries of bombykol olfactory receptors in the antennae of the silkworm moth (Schneider, 1971), movement-sensitive ganglion cells in the frog retina (Lettvin et al., 1959), and the ultrasensitivity of ampullary electroreceptors in chondrichthyan fishes (Murray, 1962) have identified some of the specific extrinsic features that are smelled, watched,

and listened for in an animal's daily life. They present a picture of how the animal itself perceives its own environment.

The second insight gained by these studies is a comparative understanding of how species' senses are designed to accommodate the total range of environmental information available to them, perhaps leading to more refined explanations of species success. Both types of insights are concerned with the linkage between animal and environment, and with the utilization of sensory information as an environmental resource. With the diversification of sensory systems through an evolutionary process of adaptive radiation (Ali, 1978), sensory resources are subdivided among species, just as food and living space are partitioned within ecological niches.

In attempting to comprehend the remarkable diversity of adaptations and complexities found in the sensory systems of animals, it is useful to consider the concept of the "sensory niche." A sensory niche can be defined as the total range of environmental information that is detected and monitored by the combined sensory systems of a species. It is an ecological expression of the sampling strategies used by a species in selecting out specific sensory information relevant to species survival. The boundaries of the niche within a particular sensory environment are set by the filtering characteristics of the specific sensory systems involved, such as frequency response in hearing or chromatic vs. achromatic vision. In this way, the sensory niche represents an animal's total perceived environment, which is a subset of its broader physical environment.

Few investigators have maintained this perspective in the past, although there are exceptions (e.g. Hughes, 1977; Jaeger, 1978; Wehner,

1987). Yet it seems apparent that research on the functional performance of a sensory system can truly be a study of the "sensory physiological ecology" of a species. As a viable, recognized subdiscipline within biology, such a field unfortunately does not yet exist, although the concept of "sensory ecology" has been defined and was the subject of at least one major symposium (Ali, 1978). But from the somewhat more limited standpoint of strictly neural elements in sensory systems, we do have a viable concept of second choice in pursuing such research: neuroethology, the neural basis of animal behavior. Although neuroethology is historically rooted in studies of brain physiology (Ewert, 1980), the field has today grown to include research with implications not only for animal behavior in a pure ethological sense, but also for animal life history and ecology as well.

The role of vision in the life of animals has received special attention from neuroethologists, because of at least two factors. One of these is that vision is the dominant sense in humans, and so we have a natural curiosity about how other species see the world, and if their vision is "as good" or "better" than our own.

The second factor involves the special characteristics of the visual sensory channel. Unlike some of the other senses, vision operates with discrete stimuli having extremely precise temporal and spatial properties, and these features are specifiable and quantifiable to a high degree. This increases the information-carrying capacity of the visual channel, and, in some respects, it helps to simplify the work of neuroethologists in interpreting experiments on animal vision.

Topography of Vertebrate Vision

The Midbrain Visual Pathway

An emergent property in the design of many sensory systems is the theme of a topographic representation of the sensory umwelt at points within the central nervous system of an animal (Ulinski, 1984). For the somatosensory system or sense of touch, for example, this "map" concept takes on the form of a somatotopic projection, which in humans is symbolically represented by the bizarre "homunculus" relating skin surfaces to projection sites on the cerebral cortex (Penfield and Rasmussen, 1950).

For the visual system, this type of topographic map is called the retinotopic projection, relating points within the visual field to their corresponding representations in the retina and brain. As with the somatotopic map, the proportional representation of sensory areas in the retinotopic projection pattern conforms with the relative spatial importance of zones within the visual field to the animal. In other words, the map indicates what areas of an animal's visual field are being looked at with a greater investment of neural components, with the implication that the details of such areas are somehow of greater visual importance to the animal. So, in a sense, the retinotopic map shows how the animal itself sees the visual space around it.

To tap into this central projection of the visual world, then, is to gain some comprehension of the handling of spatial information in the major visual pathways of a species. Projection patterns emerging from studies of these pathways can then serve as guides for understanding the topography of spatial vision in an animal, and help to define the particular "visual niche" occupied by that species within a community.

Beginning approximately two decades ago, a major theme in visual science took shape in which the central pathways of vision in vertebrates are divided into primarily two different visual systems (Schneider, 1969). The first pathway--and probably the "older" of the two, evolutionarily speaking--projects from the retina to the mesencephalic optic tectum or "midbrain roof" (superior colliculus in mammals), with postsynaptic continuations to other sites in the CNS, including spinal cord and medulla (myelencephalon) and thalamus (diencephalon). This retinotectal projection is the dominant visual pathway in nonmammalian vertebrates.

The second pathway, most highly developed in mammals, projects from the retina to the diencephalon (lateral geniculate nucleus), where it synapses with pathway continuations to the telencephalon (striate cortex in mammals). Many efferent connections are made from visual centers in the cortex, including pathways back to the diencephalon and mesencephalon.

In both pathways, the primary crossing of optic nerve fibers to the opposite side (contralateral projections) occurs between retina and mesencephalon or diencephalon. For the first pathway, this decussation of fibers between retina and mesencephalon is complete in all nonmammalian vertebrates. In other words, the primary retinotopic projection in lower vertebrates is found in the contralateral optic tectum. But in mammals, the decussation of fibers in the dominant pathway between retina and lateral geniculate nucleus is partial, presumably a modification for enhanced binocular vision (Pettigrew, 1986b).

The functional significance of these two dissociated pathways has been explored particularly within the past 20 years, but as early as

1946, the groundwork was being laid to probe this dichotomy. Working with cats, Hess et al. (1946) used electrical stimulation of the superior colliculus to elicit behavioral correlates of midbrain function. By delivering physiological levels of stimulation to a single superior colliculus in the cat brain, Hess et al. observed rapid, distinctive head and eye turning movements symmetrically opposite to the side stimulated. This spatial response was interpreted as being a function of decussating visual pathways projecting from the eyes to the contralateral superior colliculi.

Perhaps the most important aspect of the work of Hess et al. (1946) was that they attempted to explain the functional significance of this midbrain pathway in terms of a reflex response, the "visuelle Greifreflex," or visual grasp reflex. According to Hess, the midbrain pathway provides for a rapid reflex to the perception of objects in motion, so that eyes and head are abruptly turned to "grasp," or fixate on, objects that appear instantaneously in the peripheral visual field. This reflex is mediated by corresponding tectospinal pathways projecting to motor nuclei connecting with ocular, neck, and upper chest muscles. The implication of the findings of Hess et al. was that, at least in mammals, the midbrain pathway controls primary orienting movements towards just-detected objects in the contralateral visual field, especially moving objects at the periphery.

The work of Hess et al. was followed by stimulation studies on the optic tecta of lower vertebrates. Both Akert (1949) and Leghissa (1951) studied species of fishes to examine the visuomotor responses to tectal stimulation. Akert, using trout (Salmo sp.), demonstrated motor responses comparable to the visual grasp reflex seen in cats, elicited by

stimulation of the contralateral optic tectum. Akert stated more explicitly the function of the reflex: an object appearing in the periphery of the visual field can be scrutinized with optimum acuity through involuntary change of ocular position, to align the target with higher acuity zones in the central visual field.

Akert furthermore described the systematic correlation between the coverage of areas of visual space on the retina and the representation of those areas on the fish tectum, with experimental histological tracing of optic fibers. The correspondence of sensory afferents with motor efferents in the tectum, Akert said, pointed to a functional relationship between the perception of an object in visual space and responsive turning movements toward such an object. Thus, Akert elaborated on Hess et al.'s theme not only by extending it to the midbrain visual pathway of vertebrates in general, but also by investigating the functional, topographic projection patterns of that pathway.

Leghissa (1951) explored the same correlation between specific eye movements and contralateral tectal stimulation in goldfish (Carassius auratus). He also found a correspondence between stimulated tectal areas and resulting shifts in the visual field by directed eye movements. Later, Ewert (1967) demonstrated that toads (Bufo bufo) also make turning movements in response to contralateral tectal stimulation. Thus, similar functions were uncovered for midbrain pathways in at least fishes, amphibians, and mammals.

From the studies of Hess, Akert, Leghissa, Ewert, and others, therefore, emerged a generalized theme of the vertebrate midbrain pathway as a mediator of visual information involving the spatial location of objects arising in the visual field. This theme added a more

functional basis to the previously reported retinotectal projection patterns, explored anatomically beginning with Lubsen (1921) and electrophysiologically beginning with Apter (1945). This functional basis was rooted in the discovery of responsive orienting movements, which could be elicited by stimulation, either natural or experimental, of tectospinal pathways.

Further studies on various vertebrate groups have demonstrated that, in general, the midbrain tectum or superior colliculus receives a precisely ordered retinal projection preserving the topographic order of the retina and visual field, and the midbrain structures furthermore send efferent connections directly to brain stem and spinal motor centers (Ingle, 1973).

Retinotectal Projection Patterns

Although the use of electrophysiological mapping techniques to trace neural pathways dates back at least to the 1870's, they remain a valuable approach to the understanding of whole macroscopic patterns of neural projections, especially when combined with neuroanatomical techniques (Schlag, 1978). Vision researchers seized upon this methodology especially in the 1950's and 1960's, when a host of reports appeared in the wake of Apter's mapping of the retinotopic projection on the superior colliculus of the cat (Apter, 1945). Since then, precise retinotopic projection patterns as revealed by electrophysiological mapping have been described for species of bony fishes (Jacobson and Gaze, 1964; Schwassmann and Kruger, 1965a,b; Schwassmann, 1968; Schwassmann and Krag, 1970), amphibians (Gaze, 1958; Gaze and Jacobson, 1962; Gaze et al., 1963; Ewert and Borchers, 1971), reptiles (Heric and Kruger, 1965; Gaither and Stein, 1979; Stein and Gaither, 1981), birds (Hamdi and

Whitteridge, 1954), and mammals (Hamdi and Whitteridge, 1953; Siminoff et al., 1966; Pettigrew, 1986a).

The two classes of vertebrates missing from this survey are the agnathans (lampreys and hagfishes) and the chondrichthyans (sharks, skates and rays, and chimeras). Visual evoked potentials have been recorded from the mesencephalon of lampreys (Veselkin, 1966; Karamian et al., 1966), but precise retinotectal topography has not been mapped. This is not so surprising considering the minute size of the lamprey brain. But what is less understandable is the complete omission of chondrichthyan species from the list, in spite of the large size and accessibility of the elasmobranch tectum, and the strategic phylogenetic position of the group in vertebrate evolution (Bullock, 1984). The entire class has simply been ignored as the field has moved on to other topics, such as retinotectal specificity and regeneration (e.g. Sharma, 1972; see Schmidt, 1982) and integration of multimodal input in the vertebrate mesencephalon. The latter has been the subject of study in a number of species, including elasmobranchs (Platt et al., 1974; Schweitzer, 1986), teleosts (Bastian, 1982), reptiles (Hartline et al., 1978; Stein and Gaither, 1981), and birds (Knudsen, 1985).

The elasmobranchs notwithstanding, the basic patterns of retinotectal projection and retinal structure in fishes have been well studied, as fishes have long served as models for visual science. As the oldest general group of vertebrates, the fishes were first to evolve the vertebrate eye, and, judging by the remarkable constancy of structure in the eyes of all vertebrates, the fish eye became a blueprint for vertebrate vision. Fishes display the full range of specializations in vertebrate retinal anatomy and physiology, including rod and cone photoreceptors,

high acuity zones such as foveas and visual "areas," and mechanisms of light and dark adaptation (Walls, 1942).

As previously stated, the primary topographic map of the visual pathway between retina and brain in fishes is the retinotectal projection, and fish retinotectal topography has been most precisely investigated using extracellular microelectrode recordings at the tectum during photic stimulation of the retina (Schwassmann, 1975; Vanegas, 1983). Where equal areas of the visual field have proportionately equal representation on the tectal surface, the retinotectal projection pattern is called linear (Schwassmann, 1968). A linear projection pattern is indicative of uniform, unspecialized spatial vision, in which no particular region within an animal's visual field receives greater attention to detail than any other region. Such a linear pattern has been found in four species of freshwater teleosts: largemouth bass, Micropterus salmoides; bluegill, Lepomis macrochirus; carp, Cyprinus carpio; and goldfish, Carassius auratus (Schwassmann and Kruger, 1965a; Jacobson and Gaze, 1964).

On the other hand, nonlinear patterns indicating regions in the visual field receiving magnification of the retinotectal projection--that is, a proportionately greater amount of tectum devoted to a given portion of the visual field--are found in vertebrates with some type of heterogeneity in their spatial vision. These animals are specialized for potentially greater visual acuity along certain lines of sight, or visual axes, within their visual fields. In freshwater fishes, few nonlinear patterns have been found. The surface-swimming "four-eyed fish" (Anableps microlepis) possesses a horizontally oriented band of retinotectal magnification, affording it enhanced visual capabilities

within the region of its visual field just above the water surface (Schwassmann and Kruger, 1965b). Fernald (pers. comm.) has recently found preliminary evidence of some retinotectal heterogeneity in the African cichlid Haplochromis burtoni, a freshwater teleost in which visual signalling and recognition play an important role in the animal's lifestyle (Fernald, 1977).

In contrast to the freshwater fishes, most (if not all) marine fishes whose retinotectal patterns have been mapped have shown varying types of retinotectal nonlinearities, mostly consisting of temporal retinal areas with magnified tectal representations (Schwassmann, 1975). This heterogeneity reaches a peak in the serranid fishes (sea basses), one of the few teleost families with foveate retinas (Walls, 1942). The fovea, a morphological depression in certain vertebrate retinas including human, is an adaptation associated with higher visual acuity. In three species of the Pacific serranid Paralabrax, Schwassmann (1968) found a more than five-fold retinotectal magnification of the ten degree-wide area surrounding the fishes' visual axes, which run from their rostral visual fields to their caudally positioned foveas. Paralabrax is a visually orienting fish, with adaptations for specialized spatial acuity that include binocular convergence of both eyes to fixate visual targets, keyhole-shaped pupils, and sighting grooves in the snout, all of which act in concert with the primary visual axis intersecting the fovea (Schwassmann, 1968).

Nonlinearities in the retinotectal projection pattern of a species, therefore, are accompanied by certain specializations in visual behavior, ocular morphology, and most notably retinal topography. Since the retinotectal pathway represents the projection of retinal ganglion cell

fibers to the midbrain roof, it follows that heterogeneities in the projection pattern might reflect topographic differences in ganglion cell distribution across the retina. This ganglion cell topography, in turn, could reasonably be expected to reflect spatial heterogeneities in the original light-sensing mosaic, the photoreceptor layer. Thus, topographic surveys of ganglion and photoreceptor cell densities, when conducted in conjunction with retinotectal mapping, can further define the neural bases for specializations in spatial vision of a species.

Retinal Topography

As the light-detecting tissue in which the photic image is transduced into electrochemical signals, the retina is composed of a highly ordered meshwork of neurons and glia. The neural elements include the primary photoreceptive cells (rods and cones), interneurons such as the bipolar and horizontal cells, and the tertiary-level ganglion cells whose axons exit the retina via the optic nerve. Since these various cells are responsible for the detection and initial encoding of the retinal image, it follows that the spatial organization and activity patterns of retinal neurons impose certain limits on virtually every aspect of the performance of the overall visual system, including visual sensitivity, temporal response, color vision, and spatial resolution.

According to Hughes (1977), as far back as 1604 Johannes Kepler acknowledged that human peripheral vision is less acute than central vision, and Kepler cited variations in retinal structure along with poor peripheral optics as being responsible for the differences. The role of the fovea in human central vision was brought to the forefront by Müller (1856), who further emphasized the differences in retinal organization,

not only across the human retina, but also between species. This laid the groundwork for comparative studies of vertebrate retinal adaptations for high resolution vision, later punctuated by the works of Franz (1934), Walls (1942), Rochon-Duvigneaud (1943), Polyak (1957), and Duke-Elder (1958).

Quantitative studies of retinal topography, particularly of the ganglion cell and photoreceptor layers, have recently come into prominence, but as early as 1935 Østerberg mapped the densities of rod and cone cells across the human retina. Later, Van Buren (1963) provided a quantititative description of ganglion cell topography in human retina. More recently, Dawson and Maida (1984) compared Østerberg's and Van Buren's data with visual acuity data and found very high correlations between the cone and ganglion cell densities (r=0.99), ganglion cells vs. acuity (0.99), and cones vs. acuity (0.98). Although there are some exceptions (Hughes, 1977), the distributional patterns of cones and ganglion cells in vertebrates retinas in general are strongly correlated, with peak densities in both indicating regions of specialization for spatial vision for a particular species.

With the application of retinal wholemounting (flatmounting) techniques (Stone, 1981), topographic mapping of the cone and ganglion cell populations of primarily mammalian retinas has been upgraded from previous studies utilizing sectioning methods. Actually, wholemounts were first used by Schultze in 1866 to study retinal organization in a variety of diurnal and nocturnal vertebrates, and this eventually led to the formulation of the Duplexity Theory of rod and cone function (see Polyak, 1957). This theory today underlies all studies of the functional significance of photoreceptor distributions. It states that the cones mediate

chromatic, high acuity, low sensitivity, "photopic" vision in bright light, whereas the rods mediate achromatic, low acuity, high sensitivity, "scotopic" vision in dim light.

Since the work of Schultze in 1866, studies on the relationship between comparative retinal topography and the visual ecology of animals have been conducted primarily on mammals over the past two decades, perhaps following in the wake of Walls' (1942) writings emphasizing the evolutionary adaptations of comparative ocular design. The most compelling overview of this subject since Walls is that of Hughes (1977), which, although written as a review of the mammalian literature, occasionally dealt with nonmammalian vertebrates as well. More recently, Stone (1983) has also addressed the relationship between retinal topography and comparative visual function, in his review of ganglion cell classification in mammals. Both of these reviews emphasized differential organization of the retina along taxonomic lines, although Stone's position is less adaptationist and phylogenetically flexible than that of Hughes.

For fishes, analogous studies have been comparatively few. Kahmann (1934, 1936) compiled a list of foveate species of marine fishes, and Tamura (1957), Tamura and Wisby (1963), and Fernald (1983) demonstrated a correlation between retinal regions of higher cone and ganglion cell density with the axis of accommodative lens movements in teleosts. This primary line of sight, the visual axis *per se*, was hypothesized to specify the fish's zone of optimum resolving power, loosely referred to as visual acuity. Using psychophysical methods to measure contrast threshold in goldfish, Hester (1968) found lower monocular field thresholds that corresponded with retinal areas of higher cone density, which he

roughly mapped from sectioned goldfish retina. Results consistent with this were later obtained with goldfish using psychophysically measured visual discrimination tasks as well (Penzlin and Stubbe, 1977).

Topographic maps of cone density in three species of the cichlid Haplochromis were produced by van der Meer and Anker (1984), and they discussed the ecological significance of retinal structure in these fishes, but only with respect to the relationship between cone size and ambient light levels during feeding activity. On the other hand, cone density and ecologically relevant resolving power have been explored in the bluegill sunfish (Lepomis macrochirus) across ontogenetic lines (Hairston et al., 1982). In these fish, continuous retinal growth throughout life produces a decreasing intercone spacing, measured in minutes of visual angle, such that larger fish are able to discriminate and capture smaller prey than juvenile fish. This study was significant not only for its ramifications for the visual ecology of feeding in fishes, but also for its support of the Helmholtzian view that retinal resolving power, and ultimately visual acuity, are fundamentally limited by the spacing between adjacent cones in the retina (von Helmholtz, 1924).

Finally, the most thorough treatment of the linkage between cone density, ganglion cell density, retinotectal projection pattern, and visual axis in fishes has been through the studies of Schwassmann (1968) and Schwassmann and Meyer (1971) on the marine serranid Paralabrax. Schwassmann (1968) mapped the double cone and ganglion cell distributions across the sea bass retina, and demonstrated a precise topographical correlation between these retinal features and the retinotectal projection pattern from visual field to midbrain tectum. With the

subsequent confirmation by Schwassmann and Meyer (1971) that the major accommodative axis in these fish coincides with their specialized retinal and retinotectal zones, the situation for foveate teleosts was clarified: lens movement, retinal topography, and retinotectal projection are matched in register with each other to afford enhanced spatial vision along the fish's visual axis, which is a behaviorally and ecologically relevant line of sight for the species.

Topography of Spatial Vision in Sharks

Tectal Anatomy and Physiology

In most chondrichthyan fishes, the mesencephalic tectum is well developed into two bilateral lobes (Fig. 1), each of which enclose expansions of the ventricular cavity (Smeets et al., 1983). The shark tectum is the primary termination site for retinofugal fibers. In all sharks studied to date, the decussation of these fibers to the contralateral tectum is complete, with the exception of extremely weak ipsilateral projections to hypothalamic, thalamic, and pretectal sites. These investigated shark species include the squalomorph Squalus acanthias (Northcutt, 1979), and the galeomorphs Ginglymostoma cirratum (Ebbesson and Ramsey, 1968; Luiten, 1981), Hemiscyllium (=Chiloscyllium) plagiosum (Jen et al., 1983), Scyliorhinus canicula (Smeets, 1981; Repérant et al., 1986), Galeocerdo cuvieri (Ebbesson and Ramsey, 1968), and Negaprion brevirostris, the lemon shark (Graeber and Ebbesson, 1972a). The majority of these studies used degeneration techniques to trace retinofugal pathways, while the more recent studies utilized more sensitive autoradiographic methods to follow anterograde transport of tritiated compounds.

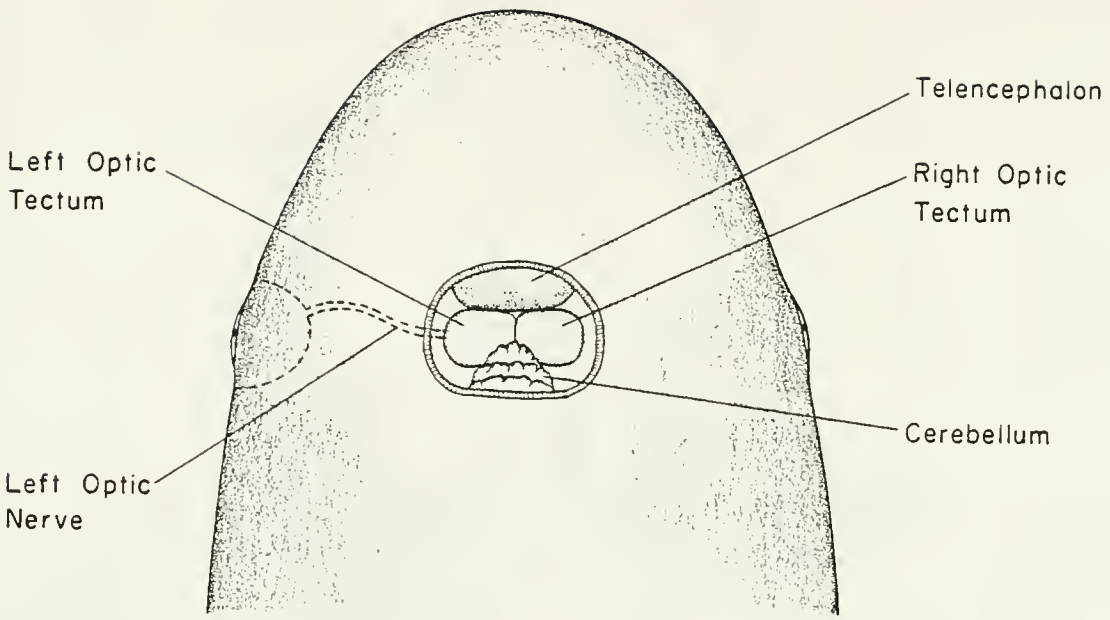

Fig. 1. Schematic diagram of position of mesencephalic optic tecta in cranium of juvenile lemon shark. Ganglion cell fibers from retina of left eye cross over completely underneath the brain and project to the roof of the right optic tectum.

Because the elasmobranch tectum is not nearly as distinctly layered as the intensively studied tectum of teleost fishes, anatomical nomenclature of the shark tectum has been a subject of confusion. Beginning with Houser (1901), the elasmobranch tectum has been subdivided by different authors into between 3 and 13 multiple laminae and zones. The four-stratum nomenclature of Ariëns-Kappers et al. (1936) dominated the literature for about 30 years, but with more attention focused on elasmobranch neuroanatomy in the 1970's, at least six new nomenclatures appeared. Recent attempts to consolidate these descriptions have been published by Northcutt (1978) and Repérant et al. (1986).

What does appear to be generally agreed upon, however, is the basic pattern of optic fiber pathway and termination within the elasmobranch tectum. Contrary to the situation with teleosts, the optic fibers of sharks do not enter the tectum from its external surface, but rather project within the deep tectum and turn outward towards the dorsal zone, terminating in the superficial layers (Northcutt, 1977; Repérant et al., 1986). Thus, although differentiation of specific tectal layers is poor compared with that of teleosts, it seems clear that the site of optic fiber termination is strictly limited to the outer tectal zone in all sharks studied, as well as in the skates Raja clavata and R. eglanteria (Witkovsky et al., 1980).

For this reason, and for the sake of simplicity within the scope of my study, I am choosing to adopt the streamlined nomenclature of Northcutt (1977, 1978), who recognized three tectal zones: superficial, central, and periventricular. In this system, the optic fibers run through the upper central and lower superficial zones, and terminate predominately, if not entirely, in the superficial tectal zone (Northcutt,

1978). It is in this superficial zone, therefore, that electrophysiological mapping of the retinotectal projection pattern should be conducted. Fortunately, the superficial zone is also the tectal region most accessible for microelectrode recording.

Studies on the physiology of the elasmobranch tectum, especially on single unit or multi-unit "hash" responses evoked by photic stimuli, have been few and far between. Gilbert et al. (1964) first demonstrated that evoked potentials to light flashes could be recorded at single sites in the tectal of small lemon sharks (Negaprion brevirostris) and bonnethead sharks (Sphyrna tiburo), and similar studies on other elasmobranch species were reported by Karamian et al. (1966) and Veselkin and Kovačević (1973). Platt et al. (1974) described averaged potentials evoked by photic stimulation in Raja, Torpedo, Trygon, Scyliorhinus, and Mustelus, such potentials being primarily large, slow waves with little spatial localization within the mesencephalon. Bullock (1984) mentioned having recorded presumably similar responses in the tecta of the sharks Carcharhinus melanopterus and Negaprion acutidens (the lemon shark of the Indo-Pacific), and the rays Rhinobatos, Platyrhinoidis, and Potamotrygon.

Bullock (1984) summarized the body of literature available on tectal physiology in elasmobranchs, and, as previously indicated, drew attention to the omission of reports on elasmobranch retinotectal topography. In doing so, he repeatedly called for new studies on single-unit characteristics and the topographical representation of the visual field on the tectum.

Retinal Topography

Attention to the topographical organization of shark retina has no doubt been hindered by the view, widely held until recently, that the

elasmobranchs as a rule possess all-rod retinas. Although there were several early reports of duplex retinas in elasmobranchs (see Gruber and Cohen, 1978), the cone-free viewpoint was expressed in the influential writings of Schultze (1866), Verrier (1930), Walls (1942), Rochon-Duvigneaud (1943), and Duke-Elder (1958), and this view prevailed. The result was a general characterization of sharks as functioning visually with pure rod retinas, and thus being "poorly adapted for distinguishing the details and color of an object" but "well equipped . . . for differentiating an object, particularly a moving one, from its background" (Gilbert, 1963: p. 321). The idea that sharks were strictly specialized for nocturnal vision, with poor resolving power and achromatic vision under photopic conditions, became ingrained in the literature and was perpetuated as recently as 1975 (Wolken, 1975).

However, since 1963, when Gruber et al. published conclusive evidence of cones in the retina of the lemon shark (Negaprion brevirostris), many researchers have confirmed the presence of cones in a wide variety of elasmobranchs, comprising at least 24 species in 10 families (summarized by Gruber and Cohen, 1978). The only exception that has held up appears to be the all-rod retina of the skate Raja, which has thus served as a model for vertebrate visual studies in which cone function is absent (e.g. Dowling and Ripps, 1970).

Although no researcher to date has systematically plotted cone distribution across a shark retina, rod-to-cone ratios are often reported from sectioned tissue. Gruber et al. (1963) reported a rod:cone ratio of 12:1 in their tangential sections from the "posterior pole" of lemon shark retina. Since then, reported rod:cone ratios in shark retina have ranged from a low of 4:1 in the white shark, Carcharodon carcharias

(Gruber et al., 1975), to a high of 100:1 in the smooth dogfish, Mustelus canis (Stell and Witkovsky, 1973b). Only five reports, however, have presented evidence of any topographical heterogeneity in cone density across the retinas of sharks. In four out of the five, lower rod:cone ratios (and thus higher cone concentrations) were found in central retina vs. peripheral retina, as follows: 7:1 vs. 12:1 in Ginglymostoma cirratum (Hamasaki and Gruber, 1965); 7:1 vs. 13:1 also in G. cirratum (Wang, 1968); 20:1 vs. 50:1 in Hemiscyllium (=Chiloscyllium) plagiosum (derived from Yew et al., 1984); and 4:1 vs. 10:1 in Carcharodon carcharias (Gruber et al., 1975; Gruber and Cohen, 1985). Cohen (1980) mentioned a rod:cone ratio of 5:1 in the "dorsal" retina of the lemon shark, as opposed to the 12:1 count reported by Gruber et al. (1963) and Wang (1968), but Cohen did not further specify the retinal location of this higher cone concentration.

Because all of these studies utilized histological sections selected at random from arbitrarily divided regions of shark retina, very little functional significance can be inferred from these data on rod:cone ratios, other than the implication that some shark species may have regional retinal specializations for spatial vision. Certainly, the finding of a higher cone concentration in basically "central" vs. "peripheral" retina is not surprising in a duplex retina.

On the other hand, somewhat better topographic information is available on ganglion cell distribution in sharks, if only in three species. Franz (1931) described the eyes of Scyllium (=Scyliorhinus) canicula and Mustelus laevis (=mustelus) as both containing a linear area centralis, visible in the dark-adapted eye as a narrow horizontal band in which the retinal cells are smaller and more densely concentrated than outside of

the area. From vertical sections, Franz estimated the ganglion cell concentration in Mustelus increases from 800 cells/mm^2 in the periphery to 2500 cells/mm^2 inside the band. However, Stell and Witkovsky (1973a), although not disagreeing with the relative proportions in total cell density from outside to inside the band, questioned whether these cells in Mustelus were all ganglion cells, suggesting that as many as 90% of the cells counted by Franz could have been neuroglia.

The only other quantitative study of ganglion cell topography in sharks was reported by Peterson and Rowe (1980) for the horn shark, Heterodontus francisci. Using a wholemount method combined with cresyl violet staining, Peterson and Rowe plotted the density of putative ganglion cells at 1 mm intervals across five horn shark retinas. They reported that the ganglion cell layer of Heterodontus is composed primarily of cells averaging about 16 μm in soma diameter, with a peak distribution that forms a horizontally extended band across the retina from nasal to temporal periphery, not unlike the situation in Scyliorhinus and Mustelus reported by Franz (1931). However, the peak density of ganglion cells in Heterodontus is 500 cells/mm^2 in the midline of the band, and density drops off to between 50 and 100 cells/mm^2 at the dorsal and ventral periphery.

These various reports of topographic heterogeneities in the cone and ganglion cell populations of shark retinas are summarized in Table 1. Few of these authors addressed the functional importance of the observed retinal heterogeneities, but Gruber and Cohen (1985) speculated that the increase in cone density in the white shark central retina is indicative of a diurnally adapted species. No study has identified a visual axis per se in any shark species based upon retinal topography. The

Table 1. Previous reports of regional specializations in cone and ganglion cell distributions in shark retinas.

Specialization	Species	Source
Higher cone concentration in "central" retina	*Ginglymostoma cirratum*	Hamasaki and Gruber (1965) Wang (1968)
	Hemiscyllium (=*Chiloscyllium*) *plagiosum*	Yew et al. (1984)
	Carcharodon carcharias	Gruber and Cohen (1985)
Higher cone concentration in "dorsal" retina	*Negaprion brevirostris*	Cohen (1980)
Higher ganglion cell concentration along horizontal meridian	*Scyllium* (=*Scyliorhinus*) *canicula*	Franz (1931)
	Mustelus laevis (=*mustelus*)	Franz (1931)
	Mustelus canis	Stell and Witkovsky (1973a)
	Heterodontus francisci	Peterson and Rowe (1980)

significance of the horizontal bands of higher ganglion cell density reported by Franz (1931) in Scyliorhinus and Mustelus was later discussed by Munk (1970) and Hughes (1977); the implications of these studies, particularly in relation to the retinal topography of the lemon shark, will be taken up later in the Discussion.

Studies of Spatial Visual Performance

Although an extensive body of research on the visual systems of sharks has emerged in the last twenty years, very little information exists on their capabilities for handling spatial information. Controlled experiments to test visual discrimination in sharks began in the early 1960's with simple instrumental conditioning techniques, but never progressed substantially beyond that initial stage. The difficulties of working with sharks under long-term, controlled conditions have been documented (Myrberg, 1976; Gruber and Myrberg, 1977), and these have restricted whole-animal studies of shark vision to only a few laboratories with proper facilities. Unfortunately, visual acuity has not been studied in any of these laboratories.

Attempts to train sharks under somewhat controlled conditions to locate a target for food reward, potentially using visual cues, were first reported by Clark (1959). She was able to train adult lemon sharks to press a white 41 cm square target to obtain food, and later Clark (1961, 1963) also trained lemon sharks to visually discriminate between a square vs. a diamond, and between a white square vs. one with vertical black and white stripes. But she did not quantify such factors as visual angle, contrast, or luminance of the targets during these experiments, and so the significance of the work was restricted to a

basic demonstration that sharks could learn certain visually mediated tasks--which, at the time, was nevertheless newsworthy.

The studies that followed took a similar approach, emphasizing behavioral traits such as acquisition and retention rather than the limits of visual performance. Wright and Jackson (1964) used Clark's technique to train juvenile lemon and bull (Carcharhinus leucas) sharks to press a white 15 cm square target for food, but no discrimination tasks between targets were involved. With similar instrumental conditioning techniques, Aronson et al. (1967) trained juvenile nurse sharks (Ginglymostoma cirratum) to discriminate between illuminated vs. not illuminated 6 x 11 cm targets. The sharks in this study learned the task as effectively and as quickly as teleosts (cichlids) and mammals (mice) trained under similar conditions, putting to rest the passé notion that sharks were untrainable, unpredictable experimental subjects.

Using aversive conditioning with electric shock, Tester and Kato (1966) trained juvenile Pacific reef blacktip (Carcharhinus melanopterus) and gray reef (C. menisorrah = amblyrhynchos) sharks to avoid certain visual targets, and thereby visually discriminate between horizontal vs. vertical white rectangles, and between a white square or white circle vs. a white triangle. No attempt was made to find a threshold for visual discrimination of these shapes.

The only other laboratory to report the use of visual discrimination tasks in shark behavioral studies was that of Graeber and his colleagues (Graeber, 1978). Experimenting with juvenile nurse sharks in an operant conditioning Y-maze paradigm, Graeber trained the sharks to select a vertically striped vs. a horizontally striped black and white door to obtain a food reward. In this set-up, the stripes were each

5 cm wide, with each target consisting of three black and three white stripes. The sharks were forced to choose between targets from a distance of no less than 15 cm away. By my calculations, this corresponds to a visual angle of 19° for a half-period of the grating (width of one stripe at minimum viewing distance), or less than 0.03 cycles per degree (c/deg). This is certainly not a task requiring high visual acuity relative to the capabilities of other vertebrates. However, there is no way to know at what distance from the targets, between 15 cm and 2 m away, that the sharks discriminated the stripe pattern, and Graeber did not push the sharks to threshold.

Graeber's work has drawn more attention for his use of this discrimination paradigm to assess visual function in nurse sharks after ablation of brain structures. Graeber and Ebbesson (1972b) and Graeber et al. (1973) stated that, in at least one shark, bilateral tectal ablation did not prevent the learning of the visual discrimination task, although the shark bumped into the aquarium walls and objects earlier in the postoperative period. The researchers suggested that recovery of visual function had been mediated possibly by some other area of the CNS, and they suspected telencephalic involvement, which they later investigated (Graeber et al., 1978). In any case, Graeber's findings raised questions about the specific role of the shark optic tectum in processing spatial visual information.

I have previously attempted to estimate the potential resolving power of the juvenile lemon shark eye, based upon retinal magnification factor calculated from a schematic eye for the species, and using rough measurements of the photoreceptor mosaic obtained from the literature (Hueter, 1980). That prediction, for the finest visual resolution of a

grating target like that used in Graeber's tests, was a visual angle of 4.1' of arc, which is more than two orders of magnitude finer than the conditions of the Graeber test. This perhaps underscores the need for more stringent testing of visual discrimination in both intact and ablated sharks before we can draw specific conclusions about mesencephalic vs. telencephalic control of visual function.

The Juvenile Lemon Shark

Biology of the Lemon Shark

From the previous review of the literature, it is evident that we are a long way from understanding the fundamentals of spatial vision in sharks, much less its role in the physiological ecology of shark species. A comparative wealth of information exists on such features as absolute sensitivity, adaptation dynamics, ocular morphology, and cellular structure and physiology in certain elasmobranch visual systems, but the spatial organization of those systems--retinal topography, retinotectal projection patterns, functional acuity, etc.--has so far eluded us. In fact, discussions of shark vision almost never mention the concept of a true visual axis, due to the lack of information in this arena and to the confusion surrounding whether or not sharks can accommodate (Sivak, 1978). This has in turn crippled the effectiveness of studies to assess the visual performance of sharks, and has frustrated efforts to characterize the optics and resolving power of the shark eye (Hueter and Gruber, 1982). And yet, in order to understand how sharks see their world, and how they function within this visual niche to orient, navigate, feed, and reproduce, we must begin to address these neglected issues.

There are approximately 300 species of living sharks presently described (Compagno, 1977). My choice of the juvenile lemon shark (Negaprion brevirostris) as a model species to begin answering these questions was based on several factors. Most important of these was that extensive optical, anatomical, electrophysiological, and psychophysical studies of the visual system in this animal have been conducted (e.g. Gruber, 1967, 1975; Cohen et al., 1977; Hueter, 1980), and retinal projections and tectal anatomy have been previously described for this species (Graeber and Ebbesson, 1972a).

In addition, the juvenile lemon shark offers certain advantages for laboratory study. In Florida, it is available nearly year-round, particularly on the flats of Florida Bay in south Florida, and compared with other species is relatively transportable from the collecting site to the laboratory. Specific recommendations for maintaining this shark in captivity for research purposes have been worked out (Gruber and Keyes, 1981). Furthermore, the lemon shark is among the few shark species with the ability to pump water over the gills and continue to respire while resting, which makes it more amenable to confinement in the laboratory than most other species.

Another consideration in choosing the lemon shark is its phyletic position among the selachians: as a carcharhinid, it is a member of the dominant group of galeomorph sharks, which comprise 73% of all living shark species (Compagno, 1977). Thus, the lemon shark is not a bad choice as representative of the mainstream of shark evolution. Furthermore, as with other carcharhinids, the lemon shark grows to a large size (over 3.5 m), is predatory from birth, and resides in warm coastal waters, and so is considered potentially dangerous to man. Of the 267

cases from the international Shark Attack File in which the species of shark could be identified, six cases cited a lemon shark as the attacker (Baldridge, 1974).

The lemon shark is a common inshore species ranging in the western Atlantic from New Jersey to southern Brazil (Compagno, 1984), and the juveniles are often the most abundant shark in the shallow coastal waters of Florida Bay and the Florida Keys (Springer, 1950). According to Gruber and Stout (1983), the lemon shark is a slow-growing, late-maturing, long-lived species, reaching sexual maturity in no less than 12 yr. Mature females may reproduce every other year (Clark and von Schmidt, 1965), giving birth to an average of 11 pups after a gestation period of about 1 yr (Gruber and Stout, 1983). The adult sharks are less abundant in the shallower waters of Florida Bay in the latter six months of the year (Springer, 1950), presumably because the spring and early summer reproductive season is over. The juveniles remain in the Florida Bay shallows for at least their first year, in which they grow approximately 15 cm from their birth size of about 60 cm total length (Gruber and Stout, 1983). The only potential predators of the juveniles are larger sharks, and the young sharks probably continue to reside in shallow waters around the Florida Keys until they reach sexual maturity, when they assume a somewhat more offshore distribution.

On the flats of Florida Bay, the juveniles are active predators feeding primarily on fishes and some crustaceans. Springer (1950) observed juvenile lemon sharks feeding on mullet (Mugil spp.), and Starck (1968) mentioned parrotfishes (Sparisoma spp.) as being particularly prominent among their stomach contents. Both authors also noted the presence of crustaceans in the diet, as did Gruber (1981), who found

crawfish (Florida spiny lobster, Panulirus spp.), crabs, "and, curiously, lots of turtle grass" (p. 57) in lemon shark stomachs. The last item may be related to incidental ingestion of benthic vegetation during the sharks' pursuit of crustacean prey: bonnethead sharks (Sphyrna tiburo), which also inhabit the Florida Bay shallows and feed heavily on small spiny lobster, often show large amounts of turtle grass in their stomach contents as well (G. Parsons, pers. comm.).

Adult lemon sharks continue to feed on fishes and crustaceans, with some evidence of specialization on stingrays (Gruber, 1981). Among the prey items taken by lemon sharks throughout its distribution, Compagno (1984) lists mainly teleosts (sea catfishes, mullet, jacks, croakers, porcupine fishes, cowfishes), followed by elasmobranchs (guitarfish, stingrays, and eagle rays), crustaceans (crabs, crawfish, barnacles, and amphipods), molluscs (conchs), and occasional sea birds.

It is clear that the juvenile lemon sharks are patrolling over the flats in very shallow water, seeking their food on or just over the bottom. Although the adults move into deeper water, they remain primarily benthic feeders, and they retain the bottom-resting trait. Even where lemon sharks are common, they are not normally seen at the surface among other surface-swimming sharks (Springer, 1950).

Contrary to the common generalization, neither juvenile nor adult lemon sharks appear to be restricted to nocturnal periods of activity. Starck (1968) reported that active feeding of the juveniles in Florida Bay occurs both night and day, especially at low tide, and Gruber (1982) found that sonic-tagged lemon sharks are almost equally active during day and night in the field. Activity peaks occur at dawn and dusk, when the sharks show a 67% increase in rate of movement, oriented towards the

rising and setting sun (Gruber, 1982). This indicates that the lemon shark is crepuscular like some other reef shark species, but continues to be equally active throughout the day and night (Gruber, 1981).

Visual System Features

The habits of the lemon shark would seem to call for a versatile, duplex visual system that can adapt to both photopic and scotopic conditions. In fact, behavioral and electrophysiological studies of juvenile lemon sharks in the laboratory have revealed extensive evidence of duplex visual function, from the standpoints of spectral sensitivity, dark adaptation dynamics, color vision, and other features (reviewed by Gruber, 1975).

The eyes of the juvenile lemon shark are mounted laterally on its relatively broad head, with only a small degree of binocular overlap between the two monocular visual fields. But as the shark swims, the side-to-side motion of the head gives the animal an essentially 360° sweep of the horizontal visual field. Small, compensatory eye movements, similar to those observed by Harris (1965) in the spiny dogfish (Squalus acanthias), appear to adjust for turning of the head during swimming, most likely to maintain some stability of the retinal image.

Externally visible features of the eye include an active vertical-slit pupil, which contracts to a thin slit under photopic conditions (full light adaptation), and dilates to a near-circular aperture under scotopic conditions (full dark adaptation). The nictitating membrane, a feature that the lemon shark shares with other carcharhinids, is a type of third eyelid which can be retracted across the eye in response to physical or chemical irritants, but not normally in response to light (Gruber and Schneiderman, 1975).

Intraocular organization of the lemon shark eye is fairly typical of vertebrate eyes. The sclera is supported by a thick cartilagenous layer, and the nutritive choroid contains an occlusible tapetum lucidum, whose reflective plates are actively exposed under scotopic conditions. The nearly spherical, crystalline lens is the sole refractive element in the eye (Hueter, 1980). The lens is supported by a dorsal suspensory ligament and the ventral pseudocampanule, said to function as a protractor lentis muscle in lens accommodation (Walls, 1942). However, efforts to confirm this mechanism in the lemon shark eye have so far failed (Sivak, 1974; Hueter, 1980).

The retina is not vascularized and contains no obvious landmarks other than the optic disc (corresponding to the shark's blind spot), which marks the point of exit of the ganglion cell fibers via the optic nerve from retina to brain. There is no fovea, and no specialized area has been previously described in this species.

In histological sections, cones are readily differentiated from rods on the basis of size, shape, and staining characteristics (Gruber and Cohen, 1978). Rods are much longer than cones, with a combined outer and inner segment length of 32 μm and a nonvarying diameter of less than 3 μm for the rods in fixed, dehydrated tissue. Cones are 19 μm long and have inner segments approximately 5 μm in diameter in histological sections. The cone outer segment is tapered, with a mid-length diameter of 2.5 μm. The tips of the cone outer segments reach up to the level of the rod ellipsoids, which are smaller than the cone ellipsoids located beneath (Cohen, 1980; Gruber et al., 1963).

Rod:cone ratios have been estimated for the lemon shark retina in three studies, although none of these studies systematically surveyed

cone density across the whole retina. Both Gruber et al. (1963) and Wang (1968) stated that the rod:cone ratio in young and adult lemon sharks appeared to be a uniform 12:1. However, as previously mentioned, Cohen (1980) indicated finding some heterogeneity in this ratio, with counts reaching 5:1 in so-called "dorsal" retina. In the absence of thorough topographic surveys of either cone or ganglion cell density, and without evidence of an axis of lens accommodatory movement, no primary visual axis *per se* has been described for the lemon shark.

Cohen (1980) described the ganglion cells of the lemon shark retina as falling into two classes. The first type are small, spherical cells measuring 8-10 μm in diameter and containing irregularly shaped, eccentrically located nuclei. The second type are giant ganglion cells, measuring 20-30 μm in diameter and containing spherical nuclei with distinct nucleoli. Contrary to most other vertebrates, whose ganglion cell axons are nonmyelinated until they exit the eye and enter the optic nerve, these axons in elasmobranchs, including the lemon shark, are myelinated within the retina throughout the nerve fiber layer (Cohen, 1980). Extracellular recordings made from ganglion cells of lemon shark retina have revealed three types of units based upon response to the onset and offset of a light stimulus (Cohen and Gruber, 1985). In these recordings, OFF units--those cells responding only to the offset of a light--are the most numerous, comprising 63% of units classified in Cohen and Gruber's study. ON units, responding only to the onset of a light, made up 18% of the units, and ON-OFF units, responding to both the onset and offset of a light, made up 19% of all units studied. Receptive field sizes of all of these cells ranged from 0.85 to 1.45 mm in diameter on the retina (Cohen, 1980), which corresponds to a

visual angle of between 5.2 and 8.8° given a retinal magnification factor of 0.164 mm/° from the lemon shark schematic eye (Hueter and Gruber, 1982).

Graeber and Ebbesson (1972a) used degeneration techniques to follow the pathways of retinal projection and tectal anatomy in the lemon shark. They reported that the optic fibers undergo complete decussation, with the exception of a very small number of fibers terminating ipsilaterally in the hypothalamus. As the optic tract enters the thalamus, the great majority of fibers turn dorsolaterally and remain in a compact lateral tract, eventually terminating in the contralateral optic tectum. The few remaining scattered fibers, according to Graeber and Ebbesson, appear to ascend directly to the dorsal tectum.

All entering optic fibers penetrate the superficial tectal zone (stratum griseum et fibrosum superficiale of Graeber and Ebbesson) from underneath, and terminate in this zone out to the periphery of the tectum. Compared with the highly differentiated layering of the teleost optic tectum, the lemon shark tectum is not as distinctly laminated, with the densest termination of fibers in the internal superficial zone. Some recognizable lamination of tectal neurons, especially in the lower periventricular zone, has been briefly described in the lemon shark by Klatzo (1967). However, the comparatively diffuse nature of tectal organization in the lemon shark led Graeber and Ebbesson (1972a) to question the role of the tectum in shark vision, and spurred their studies of tectally ablated nurse sharks. Precise electrophysiological mapping of the retinotectal projection would help to shed light in this area.

Objectives of the Study

The primary purpose of this study was to determine if sharks, as exemplified here by the juvenile lemon shark, have within their visual system any topographically nonlinear representations of their visual field that would indicate a visual axis or axes for specialized spatial vision. Should such differentiation exist, the functional significance of this nonlinear sampling strategy in the visual ecology of the lemon shark requires attention. To this end, I sought the following major objectives:

(1) To map the precise retinotectal projection of the visual field of the lemon shark onto its optic tectum utilizing electrophysiological techniques, and thereby produce the first map of the retinotectal projection in a chondrichthyan species;

(2) To map the relative distributions of cone and ganglion cell density across the lemon shark retina as indicators of topographic heterogeneity in retinal organization, in order to provide an anatomical basis for the spatial pattern of the retinotectal projection; and

(3) To assess the implications of such topographic organization of spatial vision for the visual ecology of the lemon shark, taking into consideration the demands of habitat and lifestyle on the visual system of this shark species.

MATERIALS AND METHODS

Animal Collection and Maintenance

Collection

Data were collected from a total of 46 juvenile lemon sharks, approximately 40% males and 60% females, during the course of the study. Mean size of the sharks was 70 cm total length (TL), 60 cm fork length (FL), 56 cm precaudal length (PCL), and 2.1 kg body mass, with ranges of 63-90 cm TL, 52-79 cm FL, 49-71 cm PCL, and 1.2-4.9 kg. This size range corresponds to an age of less than two years after birth (Gruber and Stout, 1983).

The animals were collected in the Florida Keys, with the assistance of personnel of the Sea World Marine Science and Conservation Center on Long Key, Florida, in an area of Florida Bay approximately 10 km NNE of the Long Key facility. This area is a major pupping and nursery ground for the lemon shark, and the juveniles are relatively abundant over the turtle grass flats and around the mangrove islands there throughout most of the year. Only during the three months between mid-January and mid-April are the juvenile sharks somewhat difficult to find in this region, until the newborn pups begin to appear in spring.

Natural chemical attractants were used to lure the sharks to the collecting boat in shallow water (less than 1 m depth) over the grass

flats, by chumming with a mesh bag containing cut fish parts and blood. Sharks usually appeared in the chum line swimming toward the boat within 20-30 min after chumming was begun. When a shark was within 4-5 m away from the boat, a circular hoop of fencing wire, measuring 1.5 m in diameter and 0.6 m in height, was thrown over the freely swimming shark. The trapped shark was then dip-netted from inside the hoop to a live-well in the boat, in which it was transported back to the Long Key facility. With these methods, the sharks experienced a minimum of trauma and physiological stress, much less than would be produced with hook-and-line or cast-net capture techniques.

At Long Key, the sharks were allowed to adjust to captivity in a 55,000 l aquarium containing filtered, recirculating seawater. After 2-3 days in captivity, the sharks were prophylactically treated with the addition of 2.0 ppm dimethyl (2,2,2-trichloro-1-hydroxyethyl) phosphanate (Dylox) to the aquarium seawater. This chemical, which degrades in seawater after 24-36 hr, controls skin infections of Vibrio bacteria and monogenetic trematodes (Dermopitherius sp.), both of which can cause major problems for lemon sharks kept in captivity (Gruber and Keyes, 1981). Following a recovery after prophylaxis of several days, the sharks began feeding in captivity, and were ready for overland transport to the laboratory within a week after being collected.

Transport and Maintenance Systems

Up to ten juvenile sharks at a time were transported live and unanesthetized from Long Key to the Whitney Marine Laboratory in St. Augustine, Florida, an 8 hr drive. The sharks were carried by truck either in a 300 l transport box provided by Sea World of Orlando or in the Whitney Laboratory's 500 l transport box. The Sea World box was equipped

with a 100% O_2 constant bubbler and seawater filtration, both driven by a 12 V automobile battery. The Whitney Lab box had an O_2 bubbler and a 12 V seawater pump to recirculate the tank water without filtration. In both cases, all animals survived the 8 hr transport and began feeding again in captivity within several days.

At the Whitney Laboratory, the sharks were maintained for up to several months in a shallow, semi-natural seawater pond averaging about 1 m in depth, in an enclosed area of the pond approximately 15 m long by 9 m wide. This pond was part of the Laboratory's open, flow-through seawater system. The seawater in the pond was sand-filtered Atlantic ocean water, 34-35 ppt salinity and 23°C average temperature. The water temperature ranged from a high of 28°C in August to a low of 14°C in February, but this did not seem to affect the survival of the captive sharks or the success of the mapping experiments. The only noticeable effect due to temperature was sluggishness and very low food intake by the sharks during the coldest periods.

The pond was not shaded and received a natural daily cycle of sunlight. Underwater visibility in the pond was typically about 3-4 m. The bottom consisted of coarse mud and sand covered with algae, and was free of obstructions. Other fishes were excluded from the shark enclosure to ensure that food intended for the sharks was not taken by other pond residents.

During the course of the study, no sharks died in captivity in the shark pond, and no animals exhibited any external signs of serious disease or parasitic infestation during their several weeks' to several months' residence in the pond. All animals fed, and the longer residents showed obvious growth after a few months in captivity.

Food and Feeding

I fed the juvenile lemon sharks a variety of fresh and frozen, thawed food items. Following Springer's (1950) observation that these sharks feed on mullet in Florida Bay, I prepared cut pieces of fresh striped mullet (Mugil cephalus), including bone, skin, and fin parts, as a main food item for the lemon sharks. Mullet is a relatively oily fish, and in a small, closed aquarium system is not a practical food item due to its introduction of oily contaminants which produce a surface scum in the aquarium. In a large, open system, however, this is not a problem, and the juvenile lemon sharks readily fed on the cut mullet.

In addition to mullet, the following teleosts were also fed to the sharks as fresh, cut pieces in varying amounts: bluefish (Pomatomus saltatrix), killifish (Fundulus spp), crevalle jack (Caranx hippos), and ladyfish (Elops saurus). The only fish that was tried as a fresh food item and was rejected by the sharks was hardhead catfish (Ariopsis felis), delivered as filleted pieces with skin on, a curious finding in light of Compagno's (1984) inclusion of sea catfish in the diets of lemon sharks.

When fresh fish was not available in sufficient amounts, portions of frozen, thawed fish or invertebrates were fed to the sharks. Among the frozen fishes, the following species were delivered as food items in decreasing order of usage: striped mullet, Atlantic thread herring (Opisthonema oglina), Atlantic mackerel (Scomber scombrus), Atlantic menhaden (Brevoortia tyrannus), and Atlantic bumper (Chloroscombrus chrysurus). The sharks also readily fed on frozen, thawed squid and penaeid shrimp, and these invertebrates were often used to augment the

fish food items. In addition, to guard against vitamin deficiencies particularly in the frozen foods, I added a standard multivitamin supplement (formulated for humans) to the sharks' food at the dosage of one tablet per shark (about 40 mg per kg body mass) each week.

Fresh or frozen food was delivered in 20-50 g pieces on the following schedule: one day of heavy feeding to satiation in a single session, one day of light feeding in one session, one day of fasting, then repeat. With this schedule, which is comparable but not identical to the 3- to 4-day feeding cycles observed by Longval et al. (1982) in juvenile lemon sharks in captivity, my animals' interest in food remained high. Their maximum weekly consumption conformed approximately to the figure of about 25% body mass of wet weight food reported for young lemon sharks in captivity by Gruber (1980).

Preparation for Experiments

Sharks selected for experimentation were transferred from the pond to an outdoor, 3800 l seawater tank prior to the day of each experiment, for greater ease of handling on the day of the experiment. Sharks were removed from the pond by confining them to a shallow shoreline with a beach seine, and then dip-netting them from the pond to the concrete tank. Inside dimensions of the rectangular tank were 2.6 m long by 2.0 m wide, with a water depth of about 0.8 m. The corners were smoothed out with plywood boards to promote circular water flow and guide the sharks' swimming movements away from the walls. The tank seawater was part of the same open, flow-through system supplying the pond. Water flow in the tank was clockwise from surface to bottom at a rate of about 30 l/min, turning over the tank water about every 2 hr. The tank was shaded from direct sunlight most of the day, and the sharks experienced

a naturally timed cycle of daytime and nighttime illumination. I continued to feed animals in the tank along the schedule previously described, prior to their use in experiments.

To minimize the amount of bleeding during pre-experimental surgery by promoting rapid clotting capabilities, experimental animals were given a vitamin K supplement 8-10 hr prior to surgery. I administered an intramuscular injection of Aquamephyton (Merck Sharp & Dohme), an aqueous colloidal solution of vitamin K_1, at a dosage of 2 mg per kg body mass (about 3.5 mg per shark). This treatment significantly increased the success of surgical procedures and electrophysiological experiments on the following day.

Retinotectal Mapping Experiments

Surgical Preparation

Experimental animals were transferred from the outdoor shark tank to the laboratory, where preparatory surgery and vision experiments were conducted. The shark was anesthetized with a knock-down dose of 1:1000 (1 g/l seawater) of ethyl m-aminobenzoate (Sigma), also called tricaine methanesulfonate (MS-222, Sandoz; or Finquel, Ayerst), or ethyl p-aminobenzoate, also called benzocaine (Sigma), delivered via a seawater sprayer directed through the gills (Gilbert and Wood, 1957). When the shark ceased to struggle and slowed all ventilatory movements, it was transferred to a surgical arena, where it was placed on a regulated flow of aerated seawater from a 50 l reservoir containing 1:10,000 (0.1 g/l) tricaine/benzocaine anesthetic, delivered via a fitted plastic mouthpiece. At this point the shark was also curarized to block neuromuscular

activity, with an intramuscular injection of 1.5 mg curare per kg body mass delivered in a solution of 3 mg/ml saline.

An approximately 2 x 3 cm patch of skin centered over the chondrocranium between the eyes was removed using a small rotary saw (Dremel) and scalpel. Bleeding from vessels in the cut skin was stopped using an electrocoagulator (Sybron). Cranial cartilage overlying the midbrain is relatively soft in the juveniles, and was cut, shaved, and clipped away carefully with scalpel and rongeurs, exposing the outer meninges. Some larger blood vessels in this tissue were electrocoagulated at the edge of the chondrocranial opening, and the tissue was cut and moved to the side, exposing the cerebellum overlying the midbrain. The cerebellum was gently retracted, and cerebrospinal fluid (CSF) was aspirated out of the cranial cavity. Slow seepage of CSF kept the midbrain surfaces moist throughout the experiment. To fully expose the dorsal surface of the right tectum, an adjustable retractor was positioned to spread apart the telencephalon-tectum boundary and tectum-cerebellum boundary. Wedges of Gelfoam (Upjohn) were inserted in spaces around and beneath the tectum where necessary, and between the dorsal chondrocranium and the cut skin to control bleeding. Extreme care was taken to avoid abrasion of the tectal surface and damage to the extensive vascular supply of the brain and chondrocranium.

Mapping Chamber

The shark was transferred from the surgical arena, on an acrylic plastic (Plexiglas) adjustable platform lined with polyurethane foam, to a Plexiglas mapping chamber (Fig. 2). This chamber was designed as a modified version of the type developed by Schwassmann (1975) for retinotectal mapping in teleosts. The paralyzed, anesthetized shark was

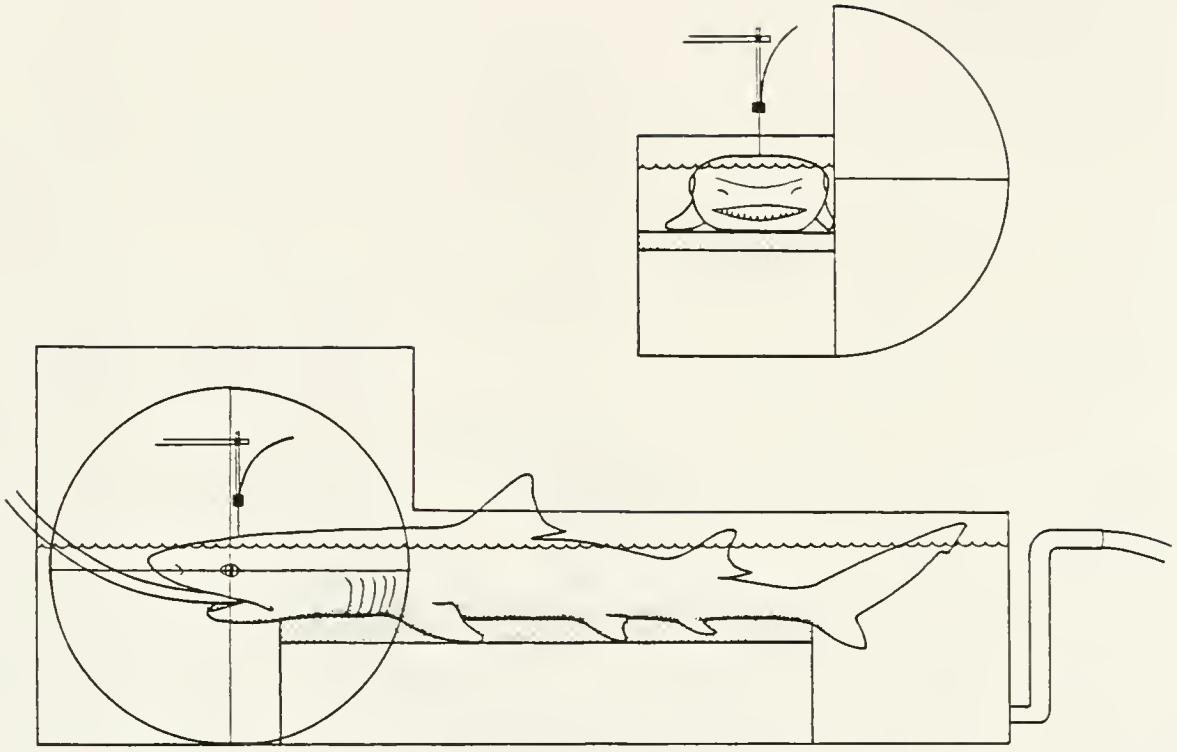

Fig. 2. Experimental chamber for mapping retinotectal projection in sharks. Top, rostral view; bottom, left side view. The paralyzed, anesthetized shark receives a constant supply of oxygenated seawater. The shark's eye is underwater and the cranial preparation is in air, with the recording electrode mounted above. The left eye is positioned at the center of the water-filled hemisphere representing the 180° left visual field. Photic stimuli are presented and receptive fields of visual units are mapped on the hemispheric surface. Apparatus adapted from Schwassmann (1975).

positioned in the seawater-filled, clear plastic chamber, so that its left eye was located at the geometric center of a water-filled hemisphere vertically mounted to the side of the holding tank. The shark was restrained on the platform in fixed position with a head clamp, hard plastic mouth tube, and three body straps. A regulated flow of seawater (approximately 2 l/min) containing 1:20,000 (0.05 g/l) tricaine/benzocaine anesthetic was continuously delivered through the mouth tube over the shark's gills. This seawater supply was gravity-driven from an 80 l reservoir in which 100% O_2 was bubbled, and the supply was recirculated throughout the experiment, using a 12 V DC submersible pump to periodically refill the reservoir.

The seawater level in the holding tank was positioned at least 1 cm above the shark's eye but below the surgical opening into the cranium, using an adjustable standpipe. With this water level, the surgical preparation was kept free of seawater without interfering with the underwater optics of the left eye, so that the water-filled hemisphere simulated the 180° left visual field of the shark underwater. A slight angular error is introduced in the simulation of the visual field due to the small difference in refractive index between water (1.33 for the distilled water inside the hemisphere, 1.34 for the seawater in the holding tank) and plastic (1.48) in the hemisphere and tank wall. Schwassmann and Kruger (1965a), however, have calculated that this error is only about one degree of arc at the extreme periphery, decreasing to zero at the center of the visual field, and so I ignored it in mapping.

A coordinate system marked on the outer surface of the hemisphere consisted of the 0° horizontal and vertical meridians intersecting at

the center of the visual field, with field lines parallel to the two meridians at 10° intervals. The left visual field was thus represented from 90° dorsal to 90° ventral and 90° rostral to 90° caudal on the hemispheric surface.

Eye position was carefully checked for proper alignment of the eye's optical axis with the hemisphere in the following ways. First, the center of the pupil was positioned at the intersection of cross hairs marking the hemispheric center and drawn on the common wall between the holding tank and hemisphere. (The cross hairs were interrupted near the ocular margin so that they did not occlude the visual field.) This alignment was checked to coincide with the crossing of the 0° horizontal and vertical meridians on the outer surface of the hemisphere. Next, the pitch of the head was adjusted by aligning the vertical slit pupil with the vertical cross hairs. The yaw of the head was also adjusted by evenly aligning the corneal surface with the holding tank wall as viewed dorsally, with an aqueous separation of about 1-3 mm between the cornea and wall. When ocular position was acceptable, the head clamp and body restraints were tightened to prevent head movements. No suturing of the eye was necessary, as the shark showed no evidence of eye movements during the experiment.

As a final check on ocular position, I located the left optic disc (optic nerve head) by visualizing it via a direct ophthalmoscope placed on the hemispheric surface, and mapped the disc's representative location on the hemisphere through the ophthalmoscope. For the juvenile lemon shark, the optic disc is located about 30° ventral and 10° rostral to the optical axis on the retina (Hueter, 1980), or about 30° dorsal and 10° caudal in the visual field, and the disc position of the shark

was checked to approximate these coordinates. The disc location was later rechecked periodically throughout the experiment to verify that ocular position had not changed.

Refractive error of the shark's eye was not optically corrected for, even though I have previously shown (Hueter, 1980) that juvenile lemon sharks are somewhat hypermetropic (farsighted), averaging +2.76 diopters (D) of refractive error. This ametropia would distort the apparent size of receptive fields, but not affect the relative center-to-center distribution of fields, which was the critical mapping criterion. Even so, calculations using the schematic eye for the juvenile lemon shark (Hueter, 1980) show that ametropic blur would increase the apparent size of receptive fields by a relatively small margin: 1% distortion of a field 10° wide, 2% distortion of a 5° field, and 12% distortion of a 1° field. Since the ganglion cell receptive fields mapped in these experiments were generally on the order of 5-10°, I chose to ignore refractive error, as have other workers (e.g. Schwassmann and Kruger, 1965a; Heric and Kruger, 1965).

Photic Stimuli

Stimuli used for mapping were presented on the outer surface of the hemisphere, in front of a diffusely reflecting screen located approximately 30 cm from the hemisphere. A tungsten incandescent light source illuminated the screen, producing a white background behind the hemisphere with a mean luminance of approximately 1.6 logfL (136.4 cd/m^2), as measured with a SEI photometer. The remaining peripheral illumination in the room was kept low (less than 1 lux). Adaptive state of the shark during the mapping experiment remained in the photopic range, based on pupillary configuration and photometric estimates of retinal illuminance.

Throughout the experiment, the pupillary aperture remained at a size (about 18 mm^2) and configuration (slightly dilated slit) illustrated by Gruber (1967) for juvenile lemon sharks after 0-3 min of dark adaptation following intense light adaptation. In the course of dark adaptation in lemon sharks, there is less than a one log unit change in sensitivity within the first three minutes, compared with an ultimate adaptive change of six log units when fully dark-adapted (Gruber, 1975). Furthermore, retinal illuminance in the mapping experiments, given a pupillary area of 18 mm^2, a medial ("posterior") nodal distance of 9.398 mm in the juvenile lemon shark eye (Hueter, 1980), and luminance of 136.4 cd/mm^2, was estimated to be well over 7000 trolands (Brown et al., 1987), which is beyond the region of rod saturation for human vision (Wyszecki and Stiles, 1967). Thus it seems unlikely that the shark became scotopic under the conditions of the mapping experiment.

Visual stimuli eliciting the best tectal responses for mapping purposes were circular black discs, with diameters subtending 5° or 10° of visual angle when positioned on the hemispheric surface. The discs were mounted on clear glass rods, so that they could be manipulated freely over the hemisphere from well outside of a unit's receptive field. Also occasionally used in delimiting the edges of receptive fields were a black card mounted on a glass rod or a black bar. Under routine conditions, however, the discs alone were used to locate and define receptive field positions in the mapping experiments.

Electrodes and Instrumentation

The recording electrodes were insulated, stainless steel microelectrodes with 2-4 μm-wide tips, and 5-10 MΩ resistance (at 22 Hz) as determined with a WPI F-29 volt-ohmmeter. The microelectrodes were homemade

from insect pins (BioQuip) electrolytically sharpened and insulated with Insl-x, based upon the method of Green (1958). If necessary, the tips were opened by immersing them for an instant in ethanol, until a resistance of approximately 7 MΩ was obtained. The sharpened, insulated pins were mounted in 23-gauge syringe needles (with connectors removed), and gold-over-nickel/copper miniature connectors (Amphenol) were crimped on to the needles. Electrodes were tested by recording from teleost tectum before conducting the shark experiments. The use of metal-filled glass micropipettes as mapping electrodes was also attempted, but these were ineffective in consistently penetrating the relatively tough meningeal layer overlying the shark tectum, and thus they were unsuitable for lengthy mapping experiments.

The stainless steel microelectrodes were mounted in a hydraulic microdrive with digital display (Haer), which provided remotely controlled stepping of electrode depth (z-position) at steps of 10, 5, or 1 μm. The microdrive head was mounted in a manual x-y micromanipulator (Prior), calibrated in 0.1 mm steps, which was used to set the position of the electrode across the tectal surface. This arrangement allowed calibrated movements of the electrode in three planes (x-y-z). The orientation of the electrode and shark were aligned with respect to each other so that the electrode was perpendicular to the dorsal surface of the tectum, and the x-y movement of the electrode was parallel to the sagittal and transverse planes through the brain. After proper alignment, the electrode mount was firmly anchored in place to the laboratory bench. The cranial preparation and electrode position could be observed throughout the experiment via a binocular surgical microscope (Zeiss) mounted over the mapping chamber. Blood flow through tectal vessels was

monitored through this microscope as a periodic check on the animal's condition during the experiment.

After ocular, tectal, and electrode orientations were secured in proper alignment, I used the electrode to plot tectal position for reference purposes, in two ways. First, the four dimensional limits (rostral, caudal, medial, lateral) of the right tectum were located with the electrode tip, and their corresponding x-y coordinates were recorded. Second, I selected a distinctive, easily identifiable melanophore from the pattern of such cells distributed over the tectal surface, and plotted its position with the electrode, as Jacobson (1962) did for reference purposes in the frog tectum. These five reference points could be reconfirmed throughout the course of the experiment as a check on head movement. Furthermore, the melanophore site's corresponding receptive field was plotted on the hemisphere as a reference field, and I periodically returned the electrode to that site to confirm that its corresponding field position had not changed.

Conventional amplification, audio-monitoring, and visual display methods were used to record unit activity. Single-ended input was used from the electrode to an AC preamplifier (Grass P15) mounted near the preparation and grounded to the seawater bath, the metal retractor in the cranium, the micromanipulator, and the binocular microscope. The preamplifier gain was set at 1000X, the high cutoff filter at 10 kHz, and the low cutoff filter at 100 Hz. The output signal from the preamplifier was passed through a 60-Hz T notch filter and then split to an audio monitor (Grass AM4), a nonstorage oscilloscope (Tektronix 502A), and a dual-beam storage oscilloscope (Tektronix 5115). The audio monitor and nonstorage oscilloscope were used during the routine mapping

procedure. For permanent records, photographs were taken from the storage oscilloscope screen with an oscilloscope camera (Tektronix C-5A), using the output from a silicon photocell to track movement of the photic stimulus through a unit's receptive field.

Mapping Procedure

I based my mapping technique on that developed by Schwassmann and Kruger (1965a,b) and Schwassmann (1968, 1975) for teleost fishes. After setting the desired x-y position of the electrode, it was lowered to the tectal surface by manually cranking down the stage of the micromanipulator. When the tip made contact, I switched to the microdrive unit to slowly penetrate the tectum. As the electrode was advanced through the tectum perpendicular to the dorsal surface, I stimulated the left eye with a broad photic stimulus, usually a moving flashlight beam, until the level of maximum unit activity in the tectum was obtained.

The spatial area on the hemispheric surface in which unit activity was affected--the unit's receptive field--was delimited with the discrete photic stimuli described previously. The boundaries of this field were determined by moving the stimulus (a 10° or 5° black circular disc against a white background) in small steps over the hemispheric surface, and marking the outer edges of the responsive area with a colored pen. This area, outside of which no response of the unit was observed, constituted the receptive field for the electrode position at specific x-y-z coordinates, and these coordinates were recorded with a unit number matching that of the corresponding delimited field on the hemispheric surface. The electrode was then withdrawn, and mapping continued at the next tectal site.

In this way, the dorsal tectal surface was mapped in 0.5 mm steps. In a complete mapping experiment, a grid of equally spaced electrode sites, each 0.5 mm away from the next site along a rostral-caudal or medial-lateral transect, is obtained. A 6 x 8 mm tectal surface can potentially yield up to 150 such recording sites, but due to time constraints this was impractical. The maximum number of surface sites that I successfully recorded from in one experiment was 76, and that experiment ran for over 24 hr. Most of the successful mapping experiments ran for 10-14 hr.

As with teleosts (Schwassmann, 1975), a portion of the ventral visual field was found to project to the lateral wall of the shark tectum, and this region was mapped by penetrating the electrode beyond overlying surface sites to these deeper units. The medio-lateral and rostro-caudal coordinates for these deep sites were the same as for the overlying sites, and their depths below the tectal surface were recorded.

Special characteristics of receptive fields, such as directional selectivity and unit classification into ON, OFF, or ON-OFF units, were occasionally noted during mapping. Since the steel electrodes primarily recorded multi-unit responses, and the photic stimuli and adaptive state were not rigidly standardized, the comparability of these data between experiments or to other studies is diminished. As long as spatial orientation of the electrode and preparation is preserved, however, the critical mapping criterion of the center-to-center distribution of receptive fields can be accurately assessed.

During the course of the experiment, the needle of a syringe containing 3 mg/ml of curare was situated in the shark's dorsal musculature, and curare was injected if necessary at the first sign of body movement.

Since curare is metabolized, this was sometimes necessary about every 3 hr. The standing anesthetic level of 1:20,000 tricaine/benzocaine was sufficient throughout even the longest experiment. These drugs have the additional benefits of decreasing blood pressure, and thus the amount of bleeding, and reducing spontaneous activity of visual units, making the determination of receptive field boundaries more precise. On the other hand, tricaine and benzocaine have been shown to adversely affect retinal function by inhibiting dark adaptation in frogs (Rapp and Basinger, 1982; Hoffman and Basinger, 1977), newts (LaTouche and Kimeldorf, 1978), and even juvenile lemon sharks (Hamasaki and Bridges, 1965), probably by blocking the regeneration of rhodopsin (Rapp and Basinger, 1982). There is no evidence, however, that these drugs can affect the topographic relationships in the retinotectal projection pattern.

At the conclusion of the mapping experiment, the receptive fields plotted on the hemisphere were transcribed to a data sheet, on which was printed a two-dimensional representation of the hemispheric surface, and the x-y coordinates of corresponding electrode positions were plotted on graph paper.

Histology

Fixation

Experimental animals to be sacrificed for histology were maintained under anesthesia and dark-adapted for approximately 1 hr prior to enucleation of eyes, to permit easier separation of the retina from the retinal epithelium after fixation. The eyes were excised under dim red light, and the shark was sacrificed with an overdose of tricaine/benzocaine.

A small quantity of 10% formalin-saline was injected into the vitreous of each eye through the optic disc (Hebel, 1976). The saline used in this fixative was an elasmobranch balanced saline ("Ringer's") solution formulated by D.H. Evans (after Forster et al., 1972), and is shown in Table 2. This fixative yielded excellent results exceeding those typically obtained with formalin fixation.

The eyes were immersed in 10% formalin-saline, where they remained for at least several weeks in fixative before dissection. Natural landmarks in the eyes (pupillary shape, optic disc location) allowed the identification of left vs. right eye and correct orientation of each eye during later dissection of the retina.

Retinal Wholemounts

Techniques for preparing retinal wholemounts (flatmounts) were adapted from guidelines described by Stone (1981). After fixation, the eye was opened at the corneo-scleral margin, and the retina was dissected free from the retinal epithelium in elasmobranch Ringer's. To preserve spatial orientation, small knicks were made in the dorsal-most and ventral-most retina prior to removing the anterior segment, using the dorsal and ventral pupillary corners as guides. The isolated retina was then floated onto a large, gelatinized, glass coverslip (48 x 65 x 1 mm), and was radially cut a minimum number of places around the border to achieve flattening of the retina onto the coverslip. With a fine camel's hair brush and small wedges of filter paper, I gently brushed the retina down onto the coverslip (photoreceptor layer down) and removed excess liquid and remaining vitreous.

The tissue was next cleared in 100% dimethyl sulfoxide (DMSO). This clearing agent is miscible in both aqueous and organic phases, and

Table 2. Elasmobranch balanced saline (Ringer's) solution of D.H. Evans (after Forster et al., 1972).

	g/l
NaCl	16.35
KCl	0.45
$CaCl_2 \cdot 2H_2O$	0.74
$MgCl_2 \cdot 6H_2O$	0.61
Na_2SO_4	0.07
$NaH_2PO_4 \cdot 2H_2O$	0.16
$NaHCO_3$	0.67
Urea	21.00
Trimethylamine oxide (TMAO)	7.99
Glucose	0.90
Polyvinylpyrrolidone (PVP)	30.00

does not induce the artifacts of tissue shrinkage that are produced with xylene-clearing and alcohol-dehydration methods (Grace and Llinás, 1985). Curcio et al. (1987) have recently described a technique for using DMSO-clearing of retinal wholemounts to analyze photoreceptor and ganglion cell topography. I utilized their technique with some modifications, as follows. Several drops of DMSO were placed on the flattened retina, and a second large, but nongelatinized coverslip was positioned over the tissue. This "sandwich" was then placed in a dish containing DMSO, with a small weight (about 100 gm) sitting on top of the dish lid and lightly pressing down on the sandwich, to maintain flattening. The retina was allowed to clear in DMSO for about three days.

After clearing, the overlying coverslip was carefully separated from the retina, excess DMSO was removed, and the retina was saturated with glycerol. A new large coverslip was applied, and the edges of the sandwich were sealed with lacquer, resulting in a cleared, nondehydrated, unstained wholemount with relatively long shelf life (Curcio et al., 1987). Shrinkage of the tissue using this technique is minimal, compared with the approximately 10% linear shrinkage usually associated with xylene-alcohol techniques. In fact, Curcio et al. (1987) reported a small net expansion of 3.2%, primarily due to a water rinse step which I omitted. Recently, Dawson et al. (1987) have utilized the same flatmounting technique as mine to count ganglion cells in human retina, and they found negligible shrinkage of the tissue, based upon the size retention of erythrocytes in the finished flatmount.

The wholemounted retinas were examined with a Reichert Biovert microscope, using Nomarski differential interference contrast (NDIC) optics and strain-free Neofluor 40X or 63X flat-field objectives. One 10X

eyepiece contained a linear scale calibrated with a 100 μm calibration slide. The other 10X eyepiece contained a cross-hair reticle dividing the field into four quadrants. The microscope stage was equipped with x-y scales for determining viewing location on the tissue to the nearest 0.1 mm.

An outline map was made of each retina on graph paper, using the microscope and calibrated scales to trace the coordinates of the flat-mount features. This map was then used to specify sampling sites at which photoreceptor and ganglion cell counts were subsequently made, and these data were recorded at their corresponding locations on the map. Orientation of the retina was preserved using the dorsal and ventral cuts and optic disc as landmarks. Cell counts were converted to cells/mm^2, and isodensity contours were drawn following the guidelines of Stone (1981).

RESULTS

Retinotectal Mapping

Responsive Layer and Receptive Fields

Retinotectal projection maps, either complete or partial, were recorded with 20 animals. Initially, my success in getting a shark through the surgery and obtaining a usable map was low, less than 50%. But after gaining considerable experience with the surgical preparation (especially control of bleeding), depth of anesthesia, choice of electrode, and the electrophysiological technique, the experimental procedure became routine.

Recording depth of maximum unitary response to photic stimuli is subject to variables which include size of the animal, specific location on the tectum, and the degree of dimpling of the tectal surface as the electrode is advanced (Schwassmann, 1968). The last factor is influenced by the shape of the electrode tip and the toughness of the meninges overlying the tectal surface. I attempted to circumvent the problems of dimpling by resetting the electrode to the tectal surface after each initial penetration, and then beginning depth measurements from that point.

With this adjustment, the average depth of maximum response for all tectal surface sites from the 20 experiments was 496 μm below the surface. For the central tectal site alone from each of the 20 sharks, average depth of maximum response was 470 μm (with a range of 260-680 μm).

Typical discharges of these "tectal units" in response to photic stimuli are shown in Fig. 3. Signal-to-noise ratio was acceptable for mapping purposes, as typical recorded responses were approximately 50 μV bursts over a background noise of about 10 μV. Occasionally, discharges of 70-80 μV were recorded; rarely, these discharges reached 100-120 μV in some isolated tectal units. With the steel microelectrodes, the great majority of recordings were not from isolated single units, but rather were multi-unit bursts, pooling the responses of two or more units with overlapping receptive fields (RF's). This limits the efficacy of determining specific RF properties beyond the mapping criterion of center-to-center distribution. Furthermore, such factors as adaptive state of the animal, background luminance, and depth of anesthesia may influence the properties of visual receptive fields.

With this proviso, the following RF characteristics were noted. OFF units predominated, but examples of ON-OFF and ON units were also found. Strong directional selectivity of stimulus movement through a unit's RF was occasionally observed and noted, although time constraints of the mapping experiments would not permit a systematic unit-by-unit evaluation. However, in those few units analyzed, no particular pattern of directional selectivity with RF location in the visual field was found.

On the other hand, location in the visual field did affect the size and shape of tectal unit RF's. Far peripheral RF's beyond about 60° in the dorsal, caudal, and ventral visual fields were larger (10° or occasionally more) and more irregular in border shape than centrally located RF's. Closer to the optical axis, receptive fields were roughly a circular shape subtending about 5-10°. Along the 0° horizontal meridian

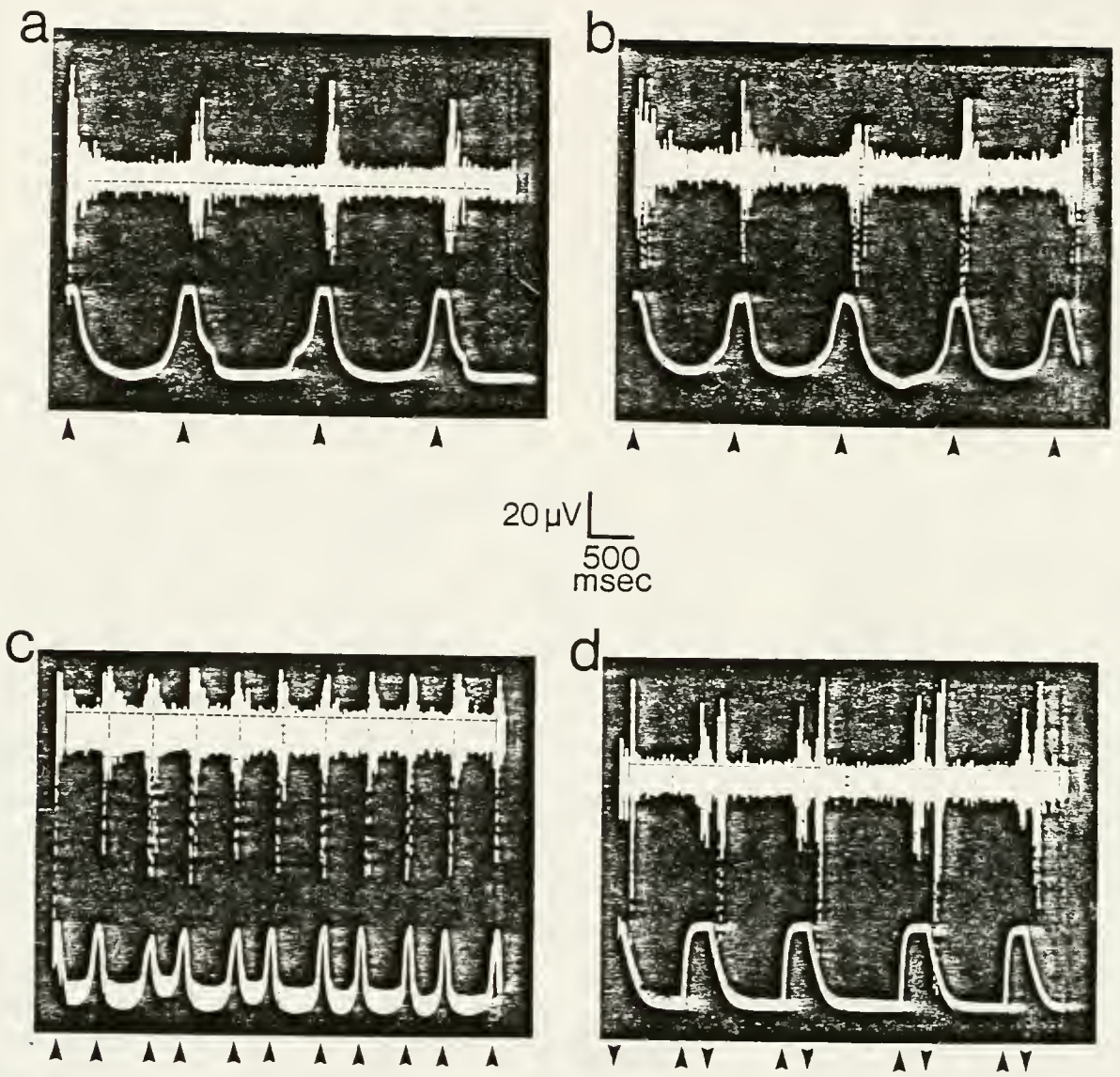

Fig. 3. Extracellular recordings from tectal units in lemon shark tectum in response to photic stimuli. In each case, the top trace shows unit discharges, the bottom trace shows stimulus change in the unit's receptive field as monitored by a photocell. In a, b, and c, the units are centrally located OFF units firing in response to the passage of a 10° black disc through their receptive fields (arrows) against a white background. In d, the unit is an ON-OFF unit responding to both the onset (arrow up) and offset (arrow down) of light.

(visual horizon), however, unit RF's took on a pronounced elliptical shape, with vertical minor axes subtending about 5° or less, and horizontal major axes subtending about 7-10°.

Retinotectal Topography

General projection pattern. As many as 97 different tectal units were plotted in the most complete mapping experiment on a single shark. Even in partial mapping experiments, the general topographic orientation of the visual field map as superimposed on the contralateral tectum was clear: the dorsal visual field (VF) projects to the medio-dorsal tectal surface, the rostral (anterior, nasal) VF projects to the rostro-dorsal tectal surface, the caudal (posterior, temporal) VF projects to the caudo-dorsal tectal surface, and the ventral VF projects to the lateral tectal surface. (To visualize this, it is useful to think of the hemispheric bubble that simulates the left visual field, turn it inside out, and overlay it with that orientation on the right optic tectum.) With the inversion of the visual field on the retina, this means that the dorsal retina projects to the lateral tectum, the ventral retina projects to the medial tectum, the rostral (nasal) retina projects to the caudal tectum, and the caudal (temporal) retina projects to the rostral tectum.

Topographic maps. Seven selected examples of actual data maps from the 20 experiments are shown in Figs. 4-10. Each figure shows the left visual field as a plane projection of the hemispheric surface. The shark's right tectum is shown in dorsal view, with medio-lateral (M-L) or rostro-caudal (R-C) electrode transects corresponding to the receptive fields located on the hemispheric surface. Both visual field and tectum are oriented as in Fig. 2, with the shark facing to the left.

Fig. 4. Topographical position of receptive field (RF) centers in the left visual field (left) and corresponding electrode tracks on the right optic tectum (right) of the lemon shark. Data map from experiment #10. The shark was oriented within the visual field as depicted in the lower portion of Fig. 2. The visual field is marked off in 10° parallel horizontal and vertical field lines, which appear curved in this plane projection. The visual field center, marked by an X, is at the intersection of the 0° horizontal and vertical meridians. The corresponding position of the optic disc (O.D.) is shown mapped onto the visual field, this being the shark's blind spot. Only RF positions are shown, not true sizes or shapes. The tectum is represented in dorsal view as if the shark were facing to the left, as during the experiment. Electrode locations were spaced equidistantly at 0.5 mm intervals along medio-lateral (M-L) transects positioned 1 mm apart, except where indicated on the tectal surface. The dorsal (D) visual field projects to the medial tectum, the ventral (V) visual field projects to the lateral tectum, the rostral (R) visual field projects to the rostral tectum (not mapped in this experiment), and the caudal (C) visual field projects to the caudal tectum. Units with a subscript (a, b) represent deep, lateral wall units recorded below the corresponding tectal surface units.

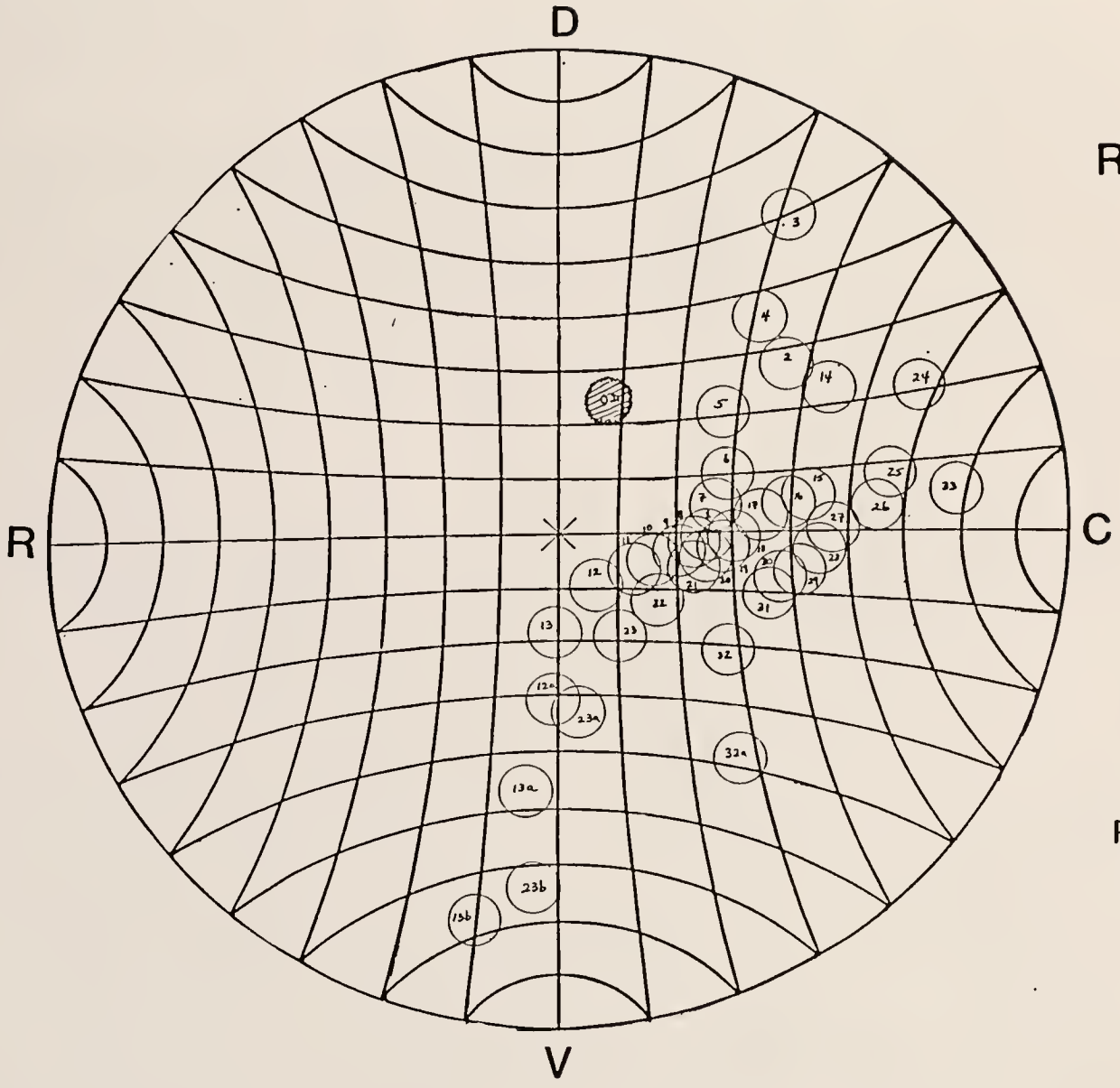

RF positions only

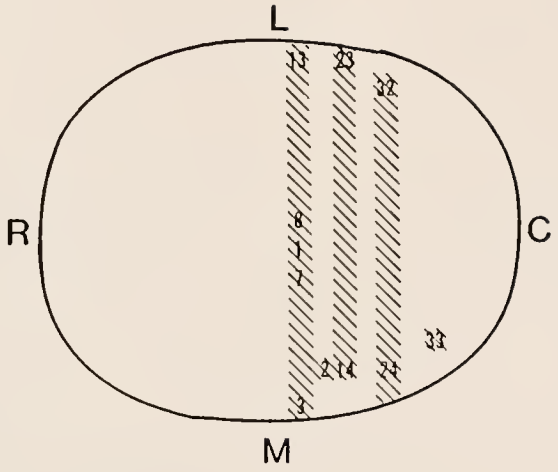

Fig. 5. Data map from experiment #20. Retinotectal projection from the rostro-ventral visual field to the rostro-lateral tectum. RF positions only, not true sizes or shapes.

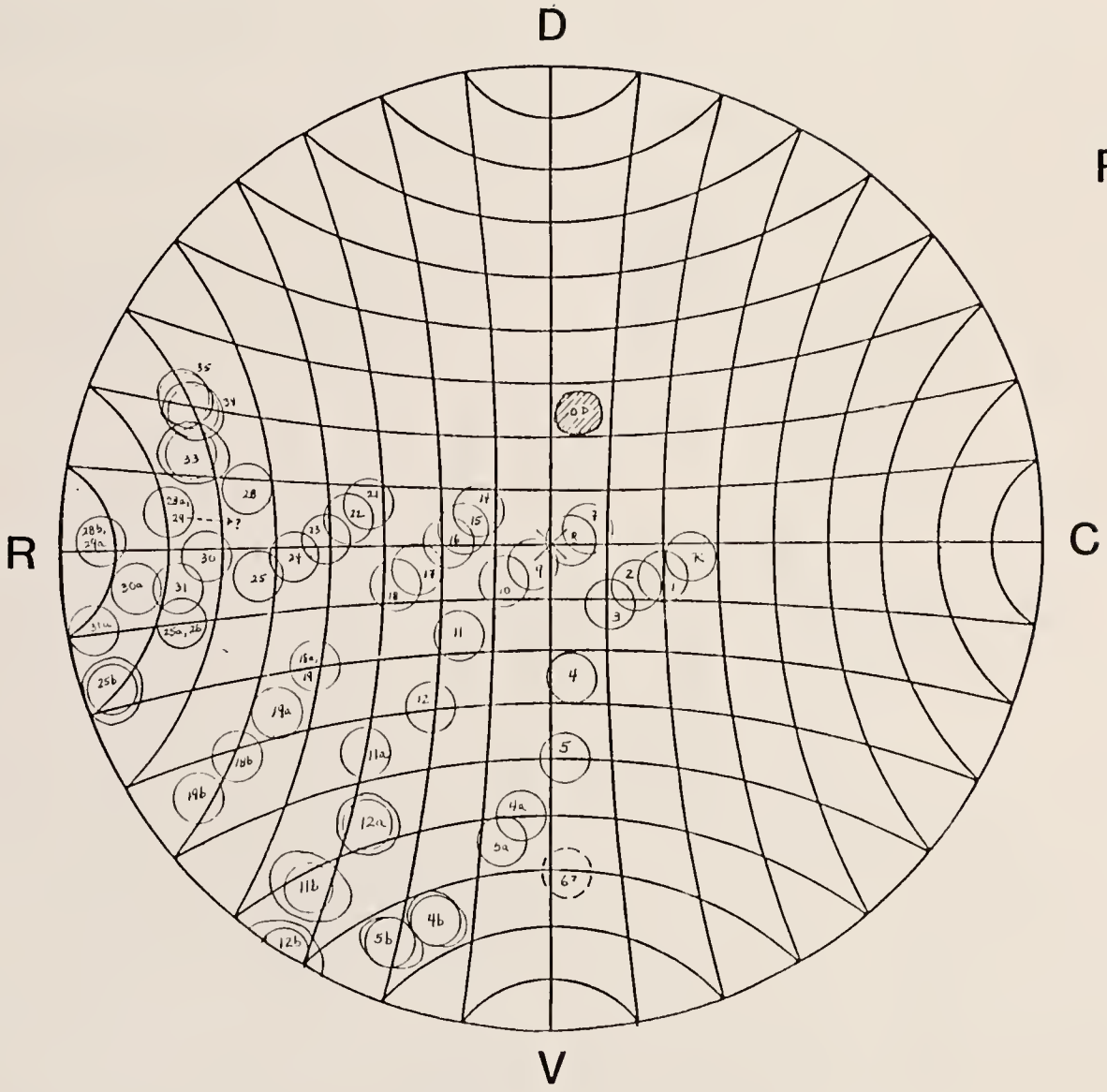

RF positions only

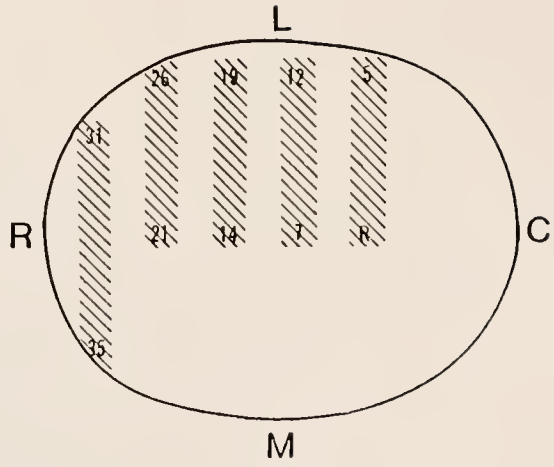

Fig. 6. Data map from experiment #13. Complete mapping experiment covering most of the tectal surface with 1 mm-spaced electrode transects. Electrode positions within transects are 0.5 mm apart. The single, curved line represents the approximate border between units projecting to the rostro-lateral wall of the tectum (marked with subscripts a-d) and those projecting to the dorsal tectal surface. Units 29-32/64-67 were replicate mappings. RF positions only, not true sizes or shapes (except unit 63).

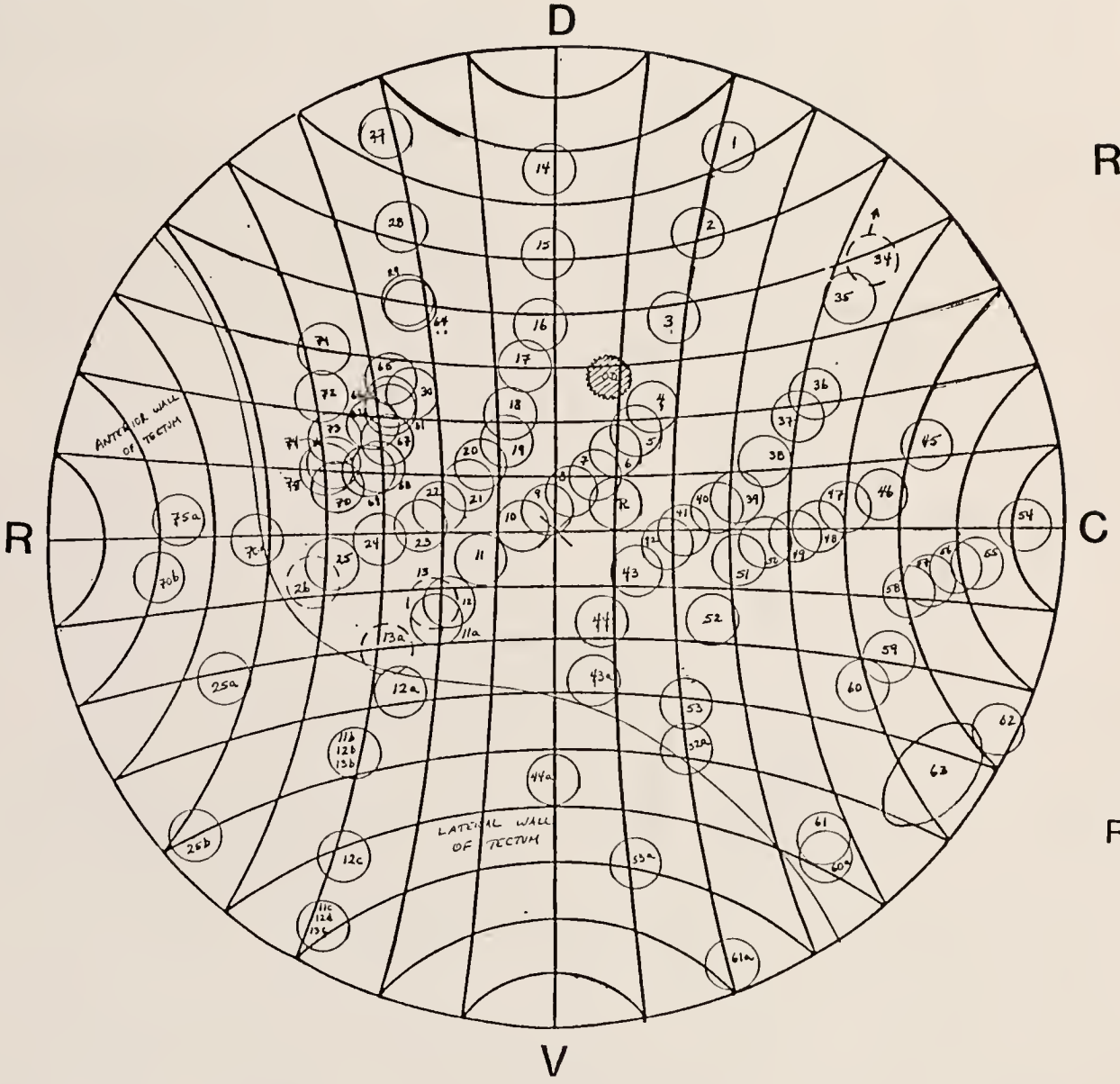

RF positions only

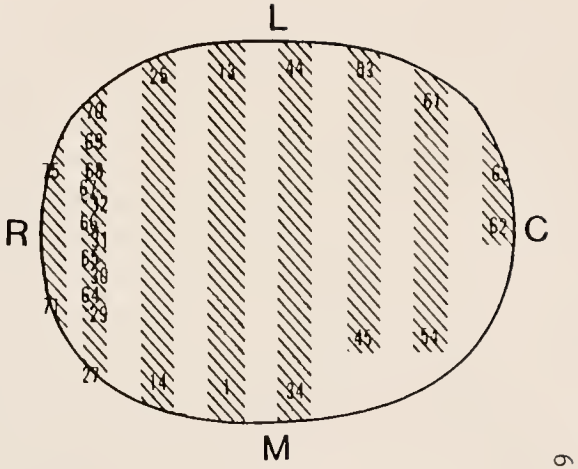

Fig. 7. Data map from experiment #16. Single M-L transect of electrode positions spaced 0.5 mm apart and corresponding RF's in visual field. True RF sizes, shapes, and positions. Note compression of RF's through the horizontal meridian and the elliptical shape of these RF's with stronger responding centers (small circles). Peripheral unit RF's are larger and spaced farther apart.

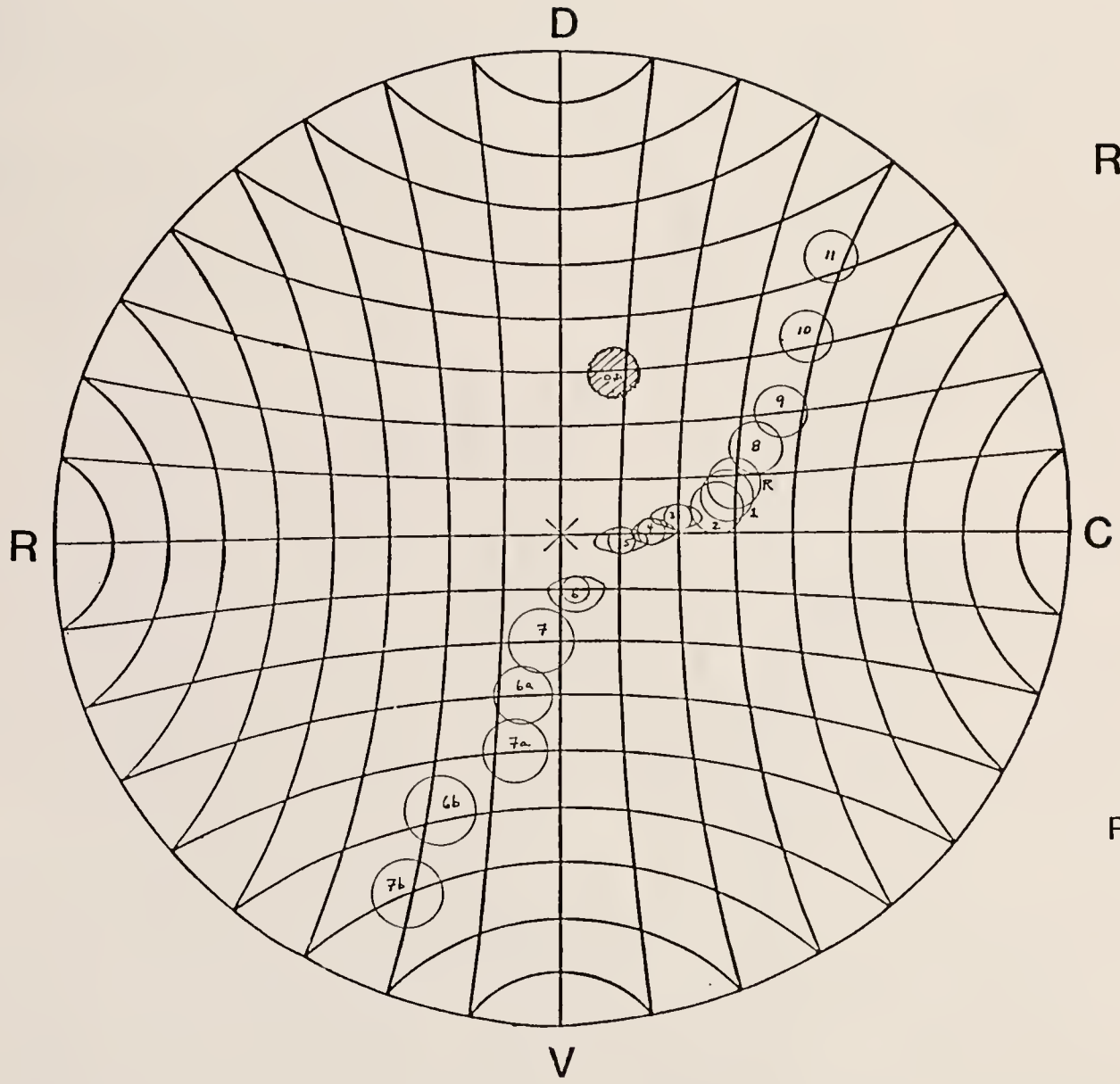

RF sizes/shapes

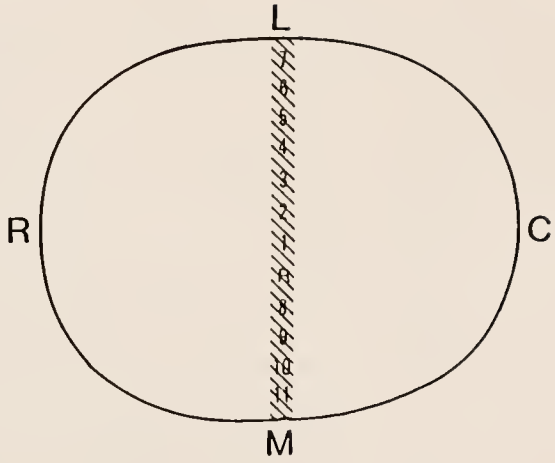

Fig. 8. Data map from experiment #15. Rostro-caudal transect of electrode positions with some caudo-lateral tectal units spaced 0.5 mm apart. True RF sizes, shapes, and positions. A blood vessel on the tectal surface between units 8 and 9 caused the recording gap in the transect.

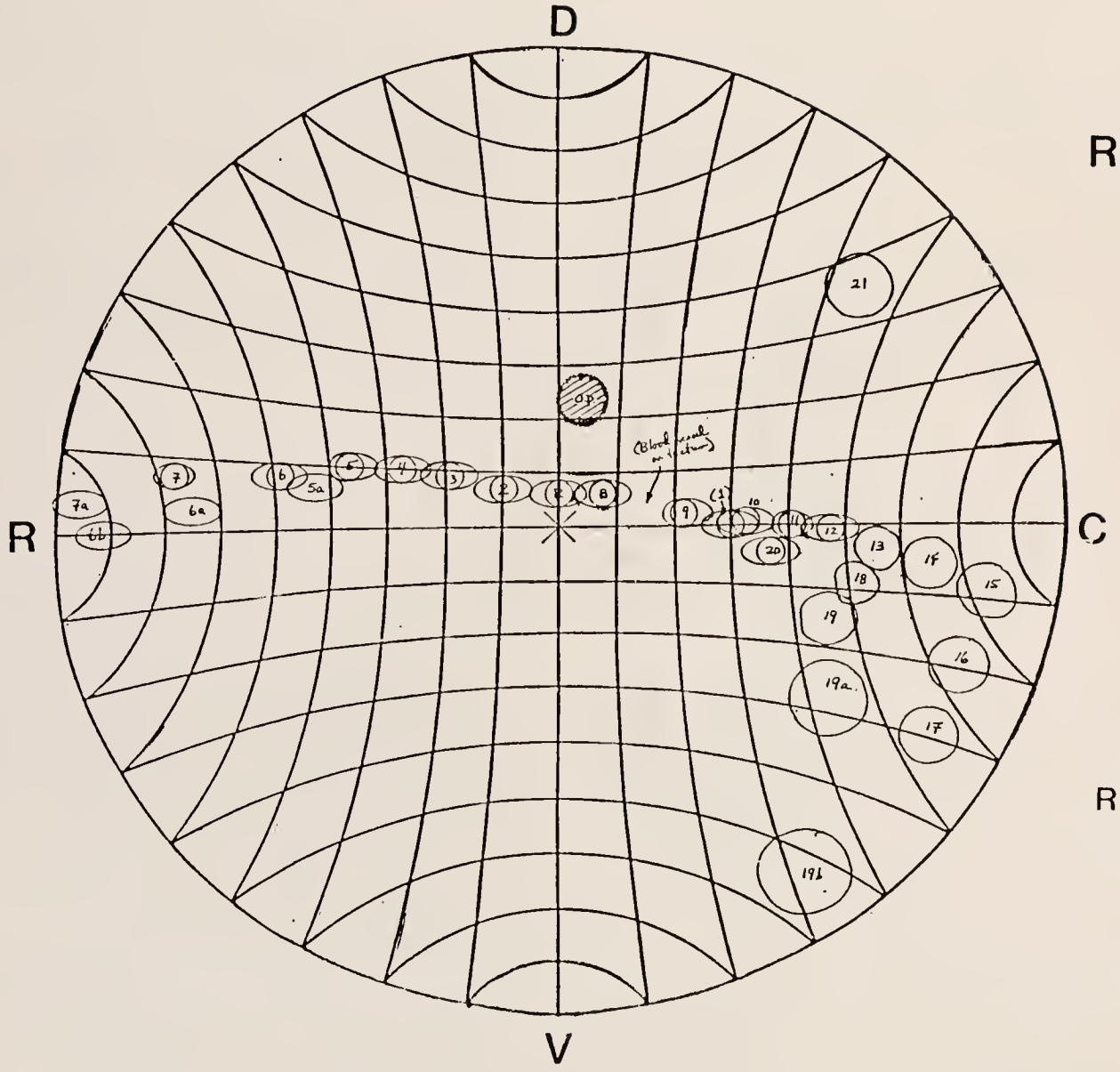

RF sizes/shapes

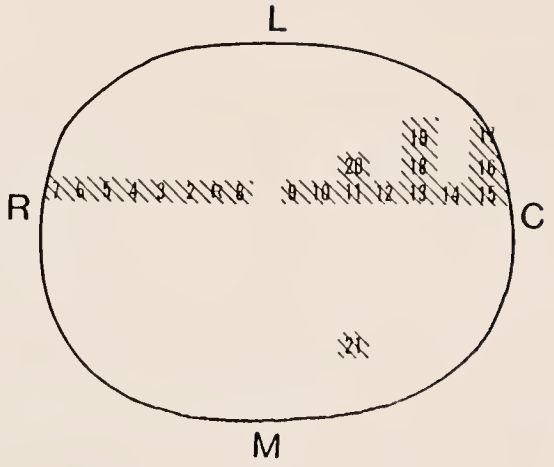

Fig. 9. Data map from experiment #19. True RF sizes and shapes, except units 24-26 (position only). Projection from rostro-ventral visual field and other selected areas.

RF sizes/shapes
(except units 24–26)

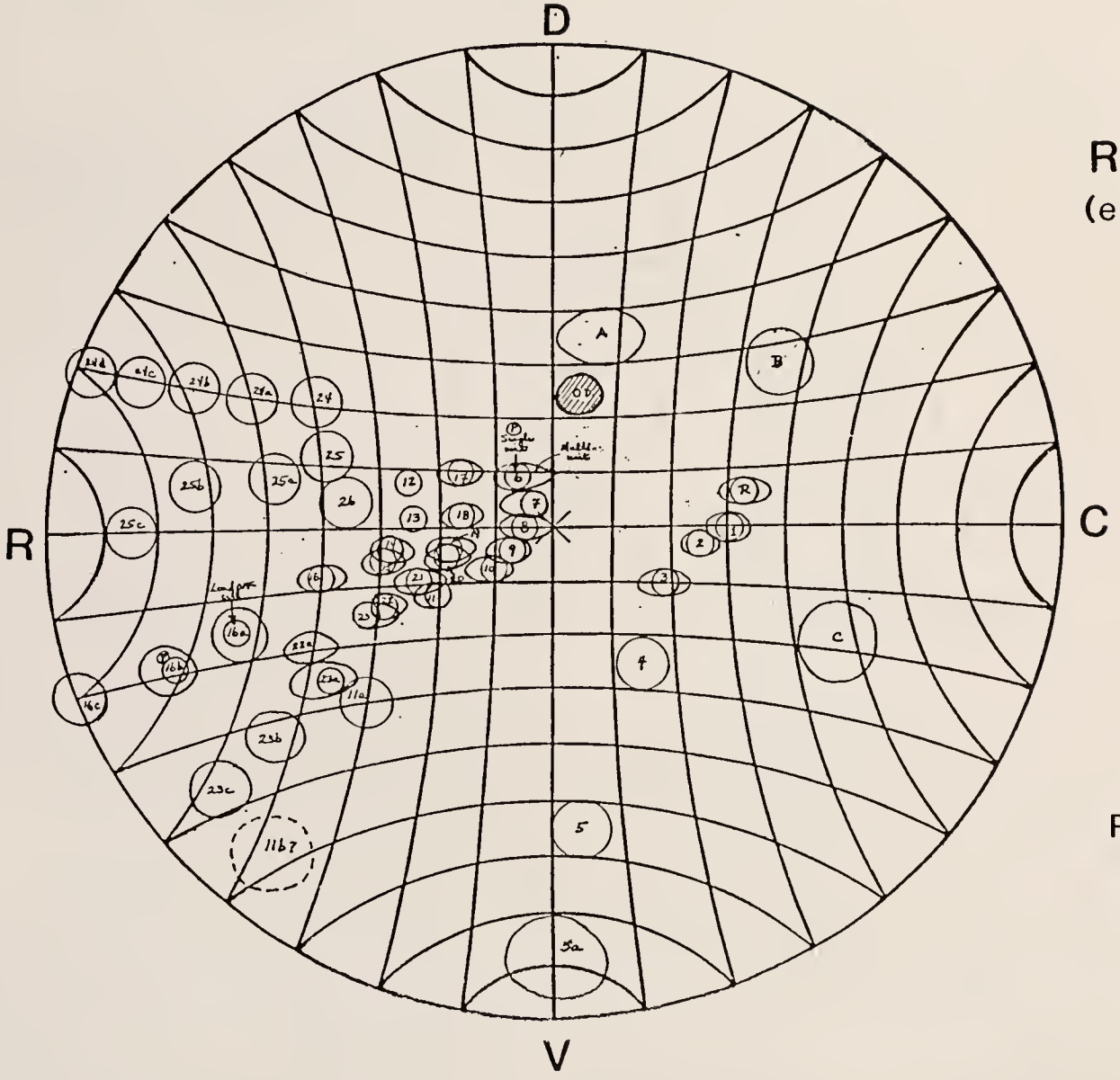

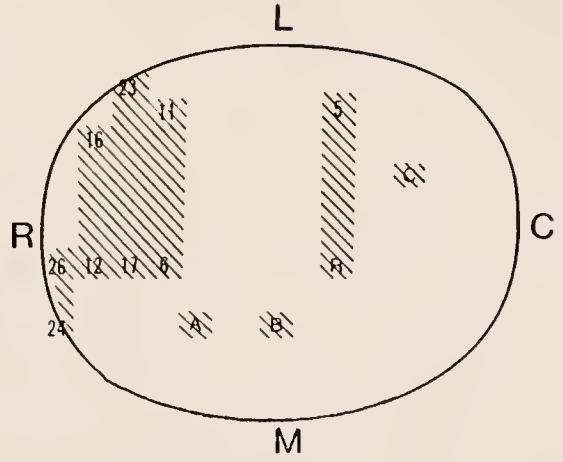

Fig. 10. Data map from experiment #17. Two medio-lateral transects across the tectal surface and down the tectal wall. True RF sizes, shapes, and positions.

RF sizes/shapes

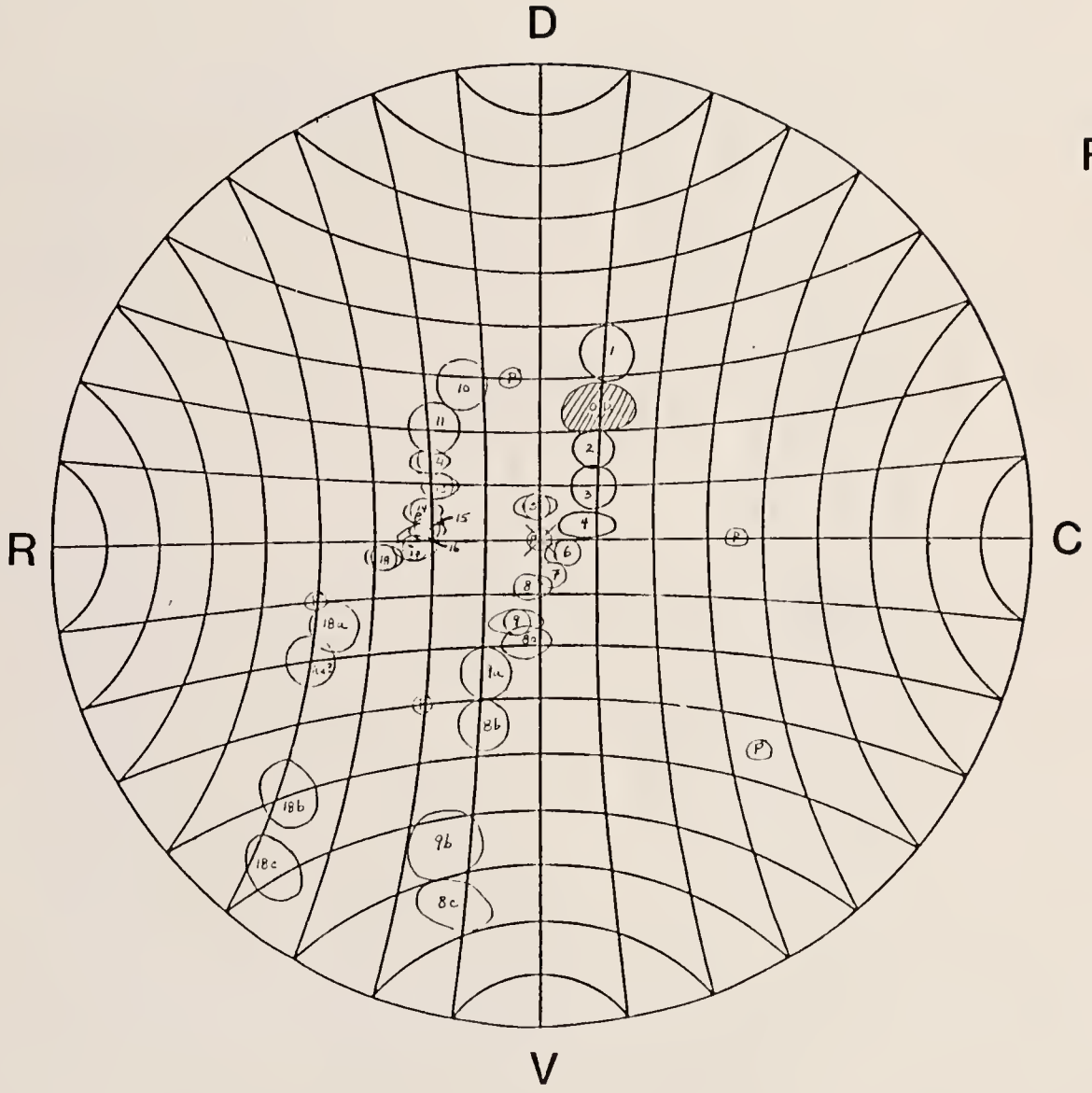

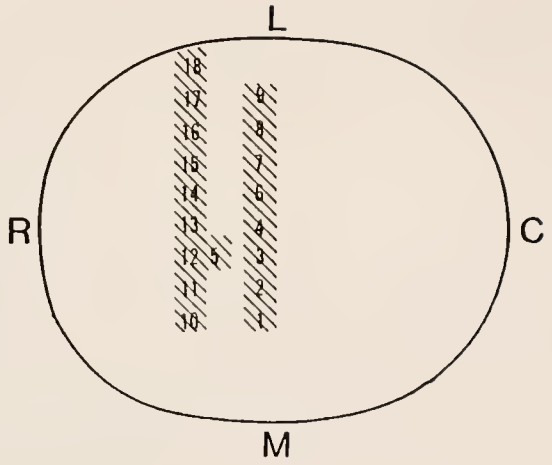

With few exceptions where indicated on the figures, neighboring electrode sites along a single M-L or R-C transect were spaced an equidistant 0.5 mm from each other. This means that absolute shifts in RF position, measured in degrees of visual angle, are spatially comparable between electrode sites along a given transect, and between transects. Thus, any nonlinearities in the shark retinotectal projection would be expressed as a compression or expansion of the spacing between RF centers corresponding to equidistant recording sites. A totally linear projection, then, would reveal a completely uniform distribution of RF positions, and any nonuniformity in this pattern would be indicative of a nonlinear projection.

In Figs. 4-6, only the RF center positions, as represented by circular fields with numbers corresponding to the accompanying tectal recording sites, are mapped. Fig. 6 shows the results of the most complete single mapping experiment. RF positions as well as sizes and shapes, as determined under experimental conditions, were mapped in the experiments depicted in Figs. 7-10. In each case, the optic disc (O.D.) was located and mapped by ophthalmoscope, and the disc's corresponding location is shown in the dorso-caudal quadrant of the visual field.

The first characteristic that is apparent in the data maps is the nonorthogonal nature of the RF positions as the tectum is traversed. Proceeding from medial to lateral tectum, there is a movement of corresponding RF locations that first descends in a slightly rostral direction, but then abruptly "twists" forward as the central visual field is approached (Figs. 4, 6, 7). Following a 45° procession of RF's through this central region, there is a symmetrical twist back, such that ventral field RF's are aligned more or less parallel with the dorsal field RF's.

The forward descent of RF positions with medio-lateral movement across the tectum indicates that the visual field map represented on the tectal surface is rotated about 20° clockwise from the precise sagittal and transverse planes of the tectum. In other words, my M-L electrode transects were oriented about 20° off the representative D-V field lines overlying the tectal surface. These lines apparently run somewhat caudally when proceeding from the medial to the lateral tectum. This in itself has no functional importance in terms of spatial visual organization, for the precise alignment of the tectal map is not indicative of any nonlinear specialization, merely a developmental result. But the nonorthogonal twisting of RF positions through the central visual field, across the rostro-caudal horizontal meridian, hints at some sort of nonlinearity in this region.

Returning to the dorsal visual field (Fig. 4, 6, 7), the RF positions are spaced relatively far apart, as much as 20° but typically about 15° per 0.5 mm shift on the tectum, and their distribution is more or less uniform with equidistant sampling of the medial tectal surface. Thus, the dorsal visual field is projected linearly on the lemon shark tectum.

The ventral visual field (Figs. 4-10) is similar to the dorsal field in that the projection also appears to be relatively linear with widely spaced receptive fields. This is a much more difficult region to map, however, due to the location of corresponding tectal units (numbered with subscripts a-d in Figs. 4-10) on the rostro-lateral wall of the tectum rather than on the dorsal tectal surface. To reach these sites, I had to penetrate successively below the surface down through this wall with the electrode, until unit activity was picked up and receptive fields could be mapped.

This difference in sampling technique most likely introduces a small spatial distortion in the ventral map, the extent of which is difficult to correct for exactly, but several points should be considered. First, although some workers have attempted to correct for tectal curvature (e.g. Siminoff et al., 1966), this correction has been relatively minor and has not significantly changed the overall projection pattern, leading subsequent workers (e.g. Schwassmann, 1968) to reject the need for correction.

Second, the shark tectum does not turn under and curve medially under the optic ventricles, as in teleosts (Schwassmann, 1975), but rather ends on the lateral wall. This minimizes the positional sampling error of the deep rostro-lateral sites in shark tectum compared with teleost tectum, and it also explains differences in the order of RF's in the ventral visual fields of the lemon shark vs. teleosts. For example, in Fig. 7, the order of RF's descending through the ventral field corresponds first to tectal unit #6 (the next-to-last surface point), then #7 (last surface point), then #6a (in this case, 1.04 mm below #6), #7a (0.81 mm below #7), #6b (0.90 mm below #6a), and finally #7b (1.00 mm below #7a). The comparable order in a teleost map would be 6-7-7a-6a (with no deeper "b" points), because of the infolding of the the teleost tectum (compare with the serranid map in Schwassmann, 1968).

Finally, in reconstructing the actual spacing of deep recording sites as represented on the shark's rostro-lateral tectal surface, I found that geometric distortion was minimized because the deep points were approximately 1 mm below overlying points, and successive surface points on the lateral tectal wall were 0.5 mm apart. This resulted in a near-preservation of the 0.5 mm spacing in the surface sampling grid, such that ventral unit mapping should be comparable to dorsal unit mapping.

In consideration of these various points, I chose to incorporate the ventral RF positions into the composite retinotectal map as is, without correction. No retinotectal magnification or other nonlinearity is therefore detected in the lemon shark's lower ventral field.

However, there is obvious magnification present in the horizontal expanse of the central visual field, which projects to the central dorsal roof of the tectum where no curvature distortion is involved. In Figs. 4-7 and 10, a clear compression of RF positions can be seen in the horizontal band running approximately 15° above and 15° below the horizontal meridian. Within this band, where the RF procession twists (to accommodate the greater input of tectal units?), the spacing of successive RF centers is about 5°, which is about one-third of the visual angle subtended by the spacing between the most peripheral units. This band appears to extend unbroken from nearly 90° rostrally (Fig. 5) to 90° caudally (Fig. 6), although specification of the extreme rostral end is compromised by the difficulties of reaching the corresponding projection sites on the rostral tectal wall.

Not only are there differences in RF spacing between inside and outside of the band, but the sizes and shapes of receptive fields appear to be different as well (Figs. 7-10), as previously mentioned. Peripheral units have large, somewhat irregular receptive fields, whereas units within the band have notably smaller receptive fields subtending about 5° or less vertically and 7-10° horizontally, resulting in a characteristic elliptical shape oriented parallel to the band itself. These RF's appeared to contain somewhat more responsive centers, circumscribed by a 5° circle (indicated in Figs. 7-10), as expressed by the amount of unit activity inside the circular center (strong, discrete spikes) vs. between

circular center and elliptical border (weaker "hash") vs. outside of the ellipse (no response).

Composite maps. Figs. 11-14 represent an attempt to pool the results of all 20 mapping experiments into a series of composite maps. These maps incorporate only positional data of the RF centers plotted in the 20 experiments, as these RF's would project to the theoretical "average" shark tectum measuring 7 mm x 5.5 mm (R-C x M-L), yielding 137 surface and 32 subsurface recording sites (Fig. 11). The composite maps were produced by piecing together the standardized results of the most complete mapping experiments in order to summarize the general projection pattern.

Fig. 12 shows the left visual field with the complete representation of RF centers corresponding to the electrode locations plotted in Fig. 11. The single, curving line in Fig. 12 marks the approximate border between the area of the visual field projecting to the dorsal tectal surface and the area projecting to the rostro-lateral wall. The stippled zone encloses the horizontal band of compression of the receptive fields.

By connecting the RF centers plotted in Fig. 12--in other words, by reconstructing the theoretical M-L and R-C electrode transects as in an ideal mapping experiment--the map shown in Fig. 13 is obtained. The 10° visual field lines have been removed from this map to avoid confusion. In this figure, the nonlinearity in the transition of the RF distribution through the horizontal band can be clearly seen.

Finally, by transferring the 10° visual field lines of Fig. 12 as they pass through the RF distribution onto the recording site grid of Fig. 11, a composite map of the projection of the left visual field onto

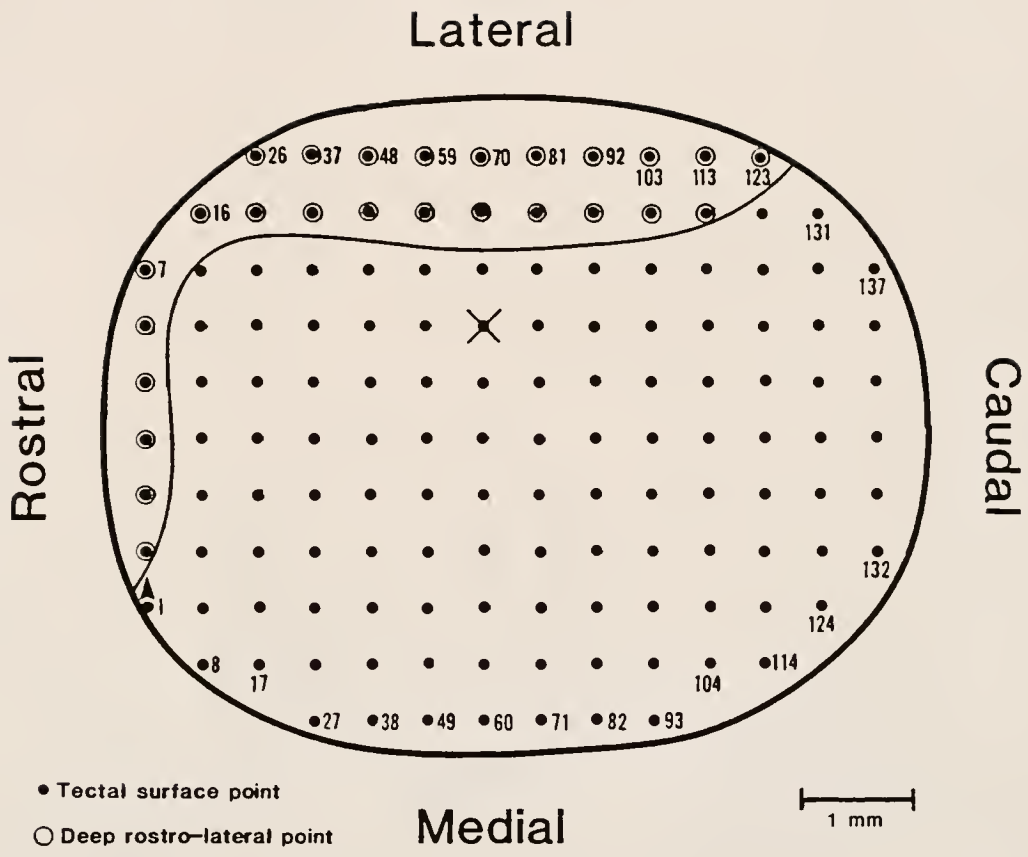

Fig. 11. Dorsal view of right optic tectum of juvenile lemon shark covered by complete grid of 0.5 mm-spaced electrode sites. The unit numbers correspond to the RF centers plotted in Fig. 12. The curved line represents the underlying rostro-lateral tectal wall. The X (unit 67) is the site receiving input from the center of the visual field (geometric center of the retina).

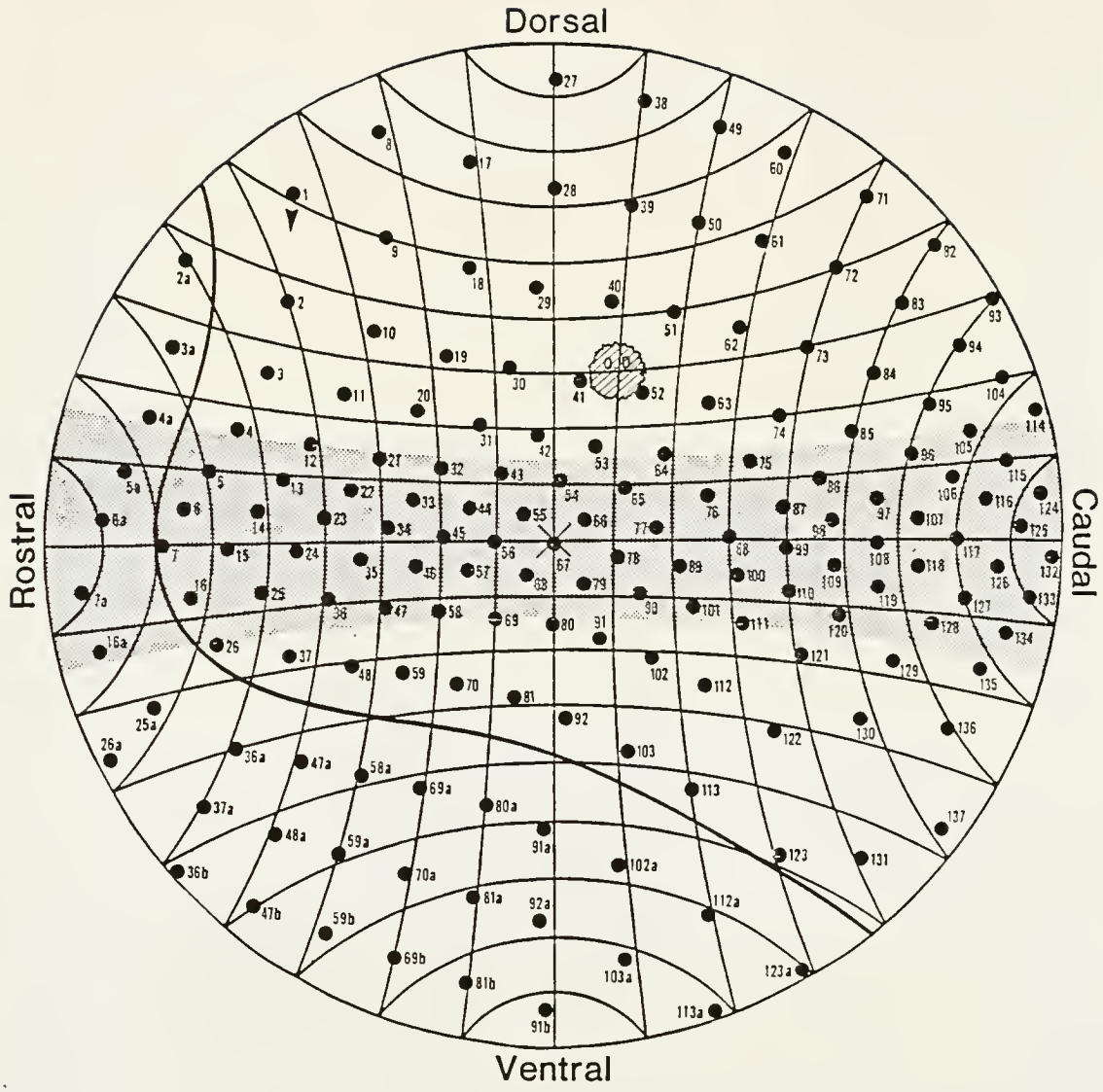

Fig. 12. Composite map of the locations of RF centers in the left visual field of the lemon shark projecting to the corresponding electrode sites plotted in Fig. 11. The approximate border between units projecting to the dorsal tectal surface and deep rostro-lateral units (numbered with subscripts a or b) is shown by the single, curving line. The horizontal band of RF compression is indicated within 15° dorsal and 15° ventral to the horizontal meridian.

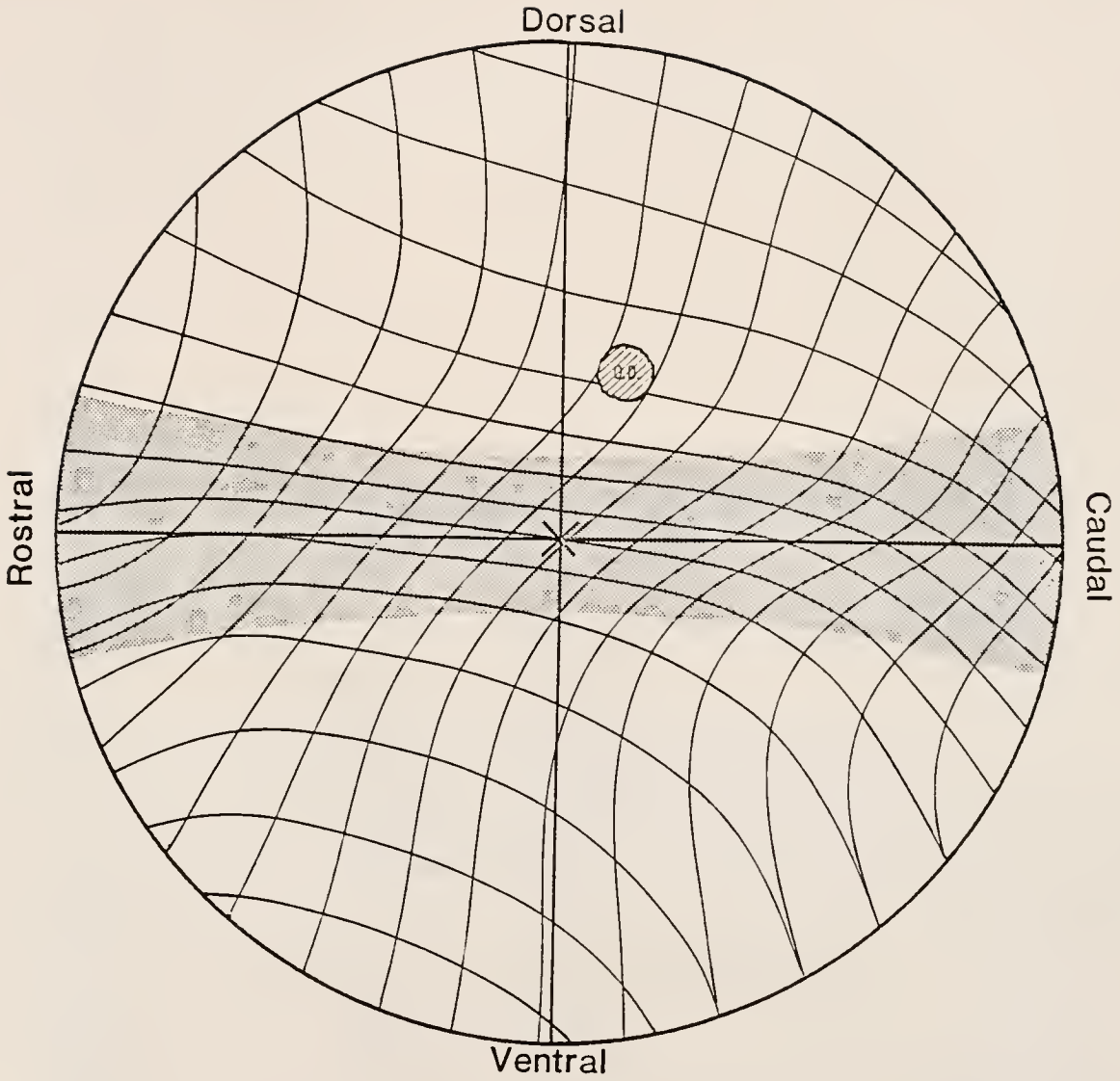

Fig. 13. Composite visual field map of lines connecting neighboring RF centers plotted in Fig. 12. These lines represent idealized, continuous sampling along the M-L and R-C tectal transects of Fig. 11. Except for the horizontal and vertical meridians, the 10° field lines have been removed to avoid confusion. The concentration of tectal representation into the horizontal band within 15°D and 15°V is clearly seen in this composite.

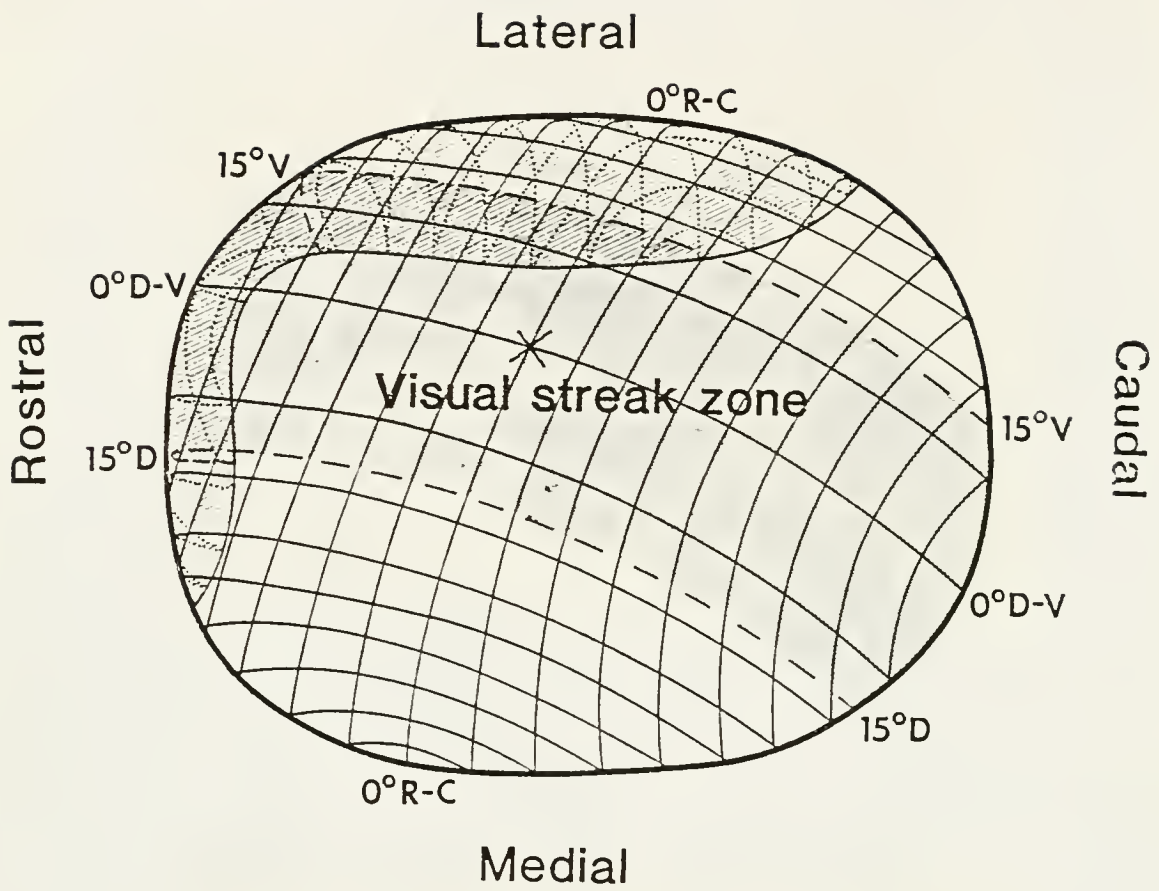

Fig. 14. Retinotectal projection of the left visual field onto the surface of the right optic tectum in the juvenile lemon shark. Horizontal and vertical meridians are labeled 0°D-V and 0°R-C, respectively. Their intersection, marked by an X, represents the visual field center. The extreme rostral and ventral visual field is shown wrapping under the dorsal tectal surface onto the rostro-lateral tectal wall. Retinotectal magnification of the visual streak between 15°D and 15°V is such that 52% of the total tectal surface is devoted to this visual area representing only 26% of the total visual field.

the right optic tectum is obtained (Fig. 14). Now the retinotectal magnification of the visual field contained within the 15°D and 15°V field lines, hereafter referred to as the "visual streak," is clearly evident. Calculations show that this visual streak, which comprises only 26% of the entire hemispherical visual field, is represented by 52% of the available tectal surface, including the rostro-lateral wall. The remaining 74% of the visual field, hereafter referred to as the "peripheral field," is represented by only 48% of the tectal surface. This means that the ratio of proportional representation on the tectum of the visual streak (52/26 = 2.00) vs. the peripheral field (48/74 = 0.65) is 2.00/0.65 = 3.08. Thus, averaged across the entire visual field, about three times more tectal surface area receives input from units within the visual streak than from equivalent areas of the peripheral visual field.

Retinotectal magnification factor. This concept of proportional representation is typically expressed in terms of the retinotectal magnification factor (not to be confused with the retinal magnification factor, or RMF), calculated as the number of micrometers on the tectal surface per degree of visual field coverage (Jacobson, 1962). For most peripheral dorsal and ventral projection areas (e.g. units #14 and 15 in Fig. 6), this number averages about 500 μm/15° = 33 μm/°. For the visual streak, this number is 500 μm/5° = 100 μm/°. Thus, the ratio of retinotectal magnification factors is in agreement with the surface area computations: three times more tectum is devoted to vision in the visual streak than to peripheral vision.

Retinal Topography

Photoreceptor and Ganglion Cell Identification

Results of the DMSO-cleared retinal wholemounts combined with NDIC microscopy were generally excellent for the photoreceptors and within acceptable limits for the ganglion cells. These results far surpassed my previous attempts to visualize photoreceptors and ganglion cells using cresyl violet staining and conventional optics. The advantage of NDIC optics on unstained tissue is that the microscopist can focus up and down, often through many tissue layers (Figs. 15-18), and visualize the three-dimensional surfaces of cells and processes at successive levels without significant light attenuation. This greatly assists in identifying cell types, a benefit that unfortunately does not translate as well into a static, two-dimensional micrograph.

DMSO-clearing yielded particularly good results with the shark photoreceptor layer, the architecture of which can be otherwise susceptible to the shrinkage effects of xylene-clearing and alcohol-dehydration. Occasionally, at the edges of the retinal wholemounts, a teased-out grouping of neighboring photoreceptors was visible in isolation (Fig. 16). Cones were readily identifiable in such side views on the basis of size, shape, and position in the photoreceptor layer. Their length from the outer limiting membrane to the tip of the outer segment was 20 µm, and the widest diameter of the cone inner segment was about 5 µm, consistent with Cohen's (1980) report of a cone inner segment width of 5.1 µm in juvenile lemon shark retina. Gruber et al. (1963) reported a cone length of 19 µm and a width of 4.7 µm, which indicates that their dehydrated tissue had undergone a 5-6% shrinkage.

Fig. 15. (a) Flatmount view with Nomarski differential interference contrast (NDIC) optics of outer nuclear layer containing the nuclei of rod and cone photoreceptors in the wholemounted lemon shark retina. (b) Bipolar cell nuclei of inner nuclear layer located directly beneath view in (a). White bars = 10 µm.


a

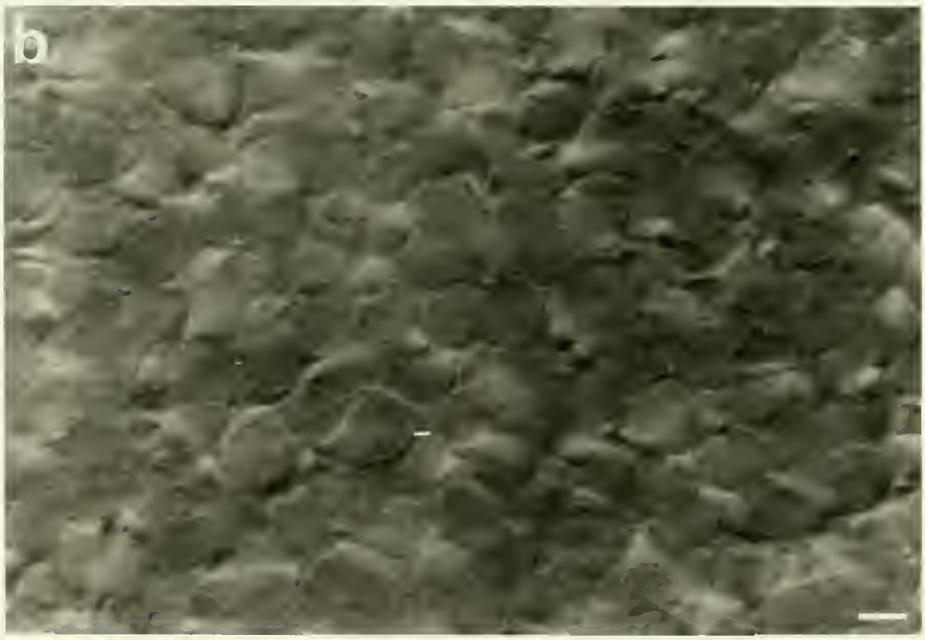
b

Fig. 16. (a) Isolated grouping of rod and cone photoreceptors from lemon shark retina. A single cone can be clearly seen, including its outer and inner segments with prominent ellipsoid (arrow). The white lines mark the level of the rod ellipsoids at which counts of cone density were made in flatmount view (see Fig. 17). The photoreceptor nuclei lie just below the outer limiting membrane. (b) Focusing deeper, a Müller cell process (arrow) supporting the photoreceptor group is seen. NDIC optics. White bars = 10 µm.

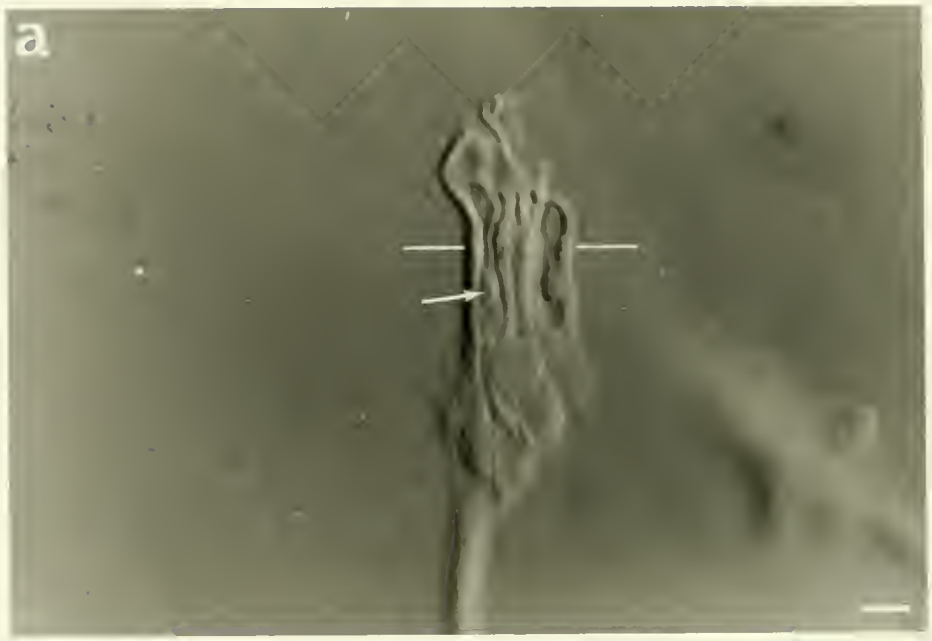
a


b

Fig. 17. (a) Photoreceptor mosaic in flatmount view at level of rod ellipsoids and tips of cone outer segments (see Fig. 16a) from central retina of lemon shark. Many cones are present; only six are indicated (arrows). Note apparent hexagonal array of six rods surrounding each cone. This area lies within the shark's visual streak. (b) Same view outside of the visual streak in peripheral retina. Fewer cones can be seen; one is indicated (arrow). NDIC optics. White bars = 10 μm.

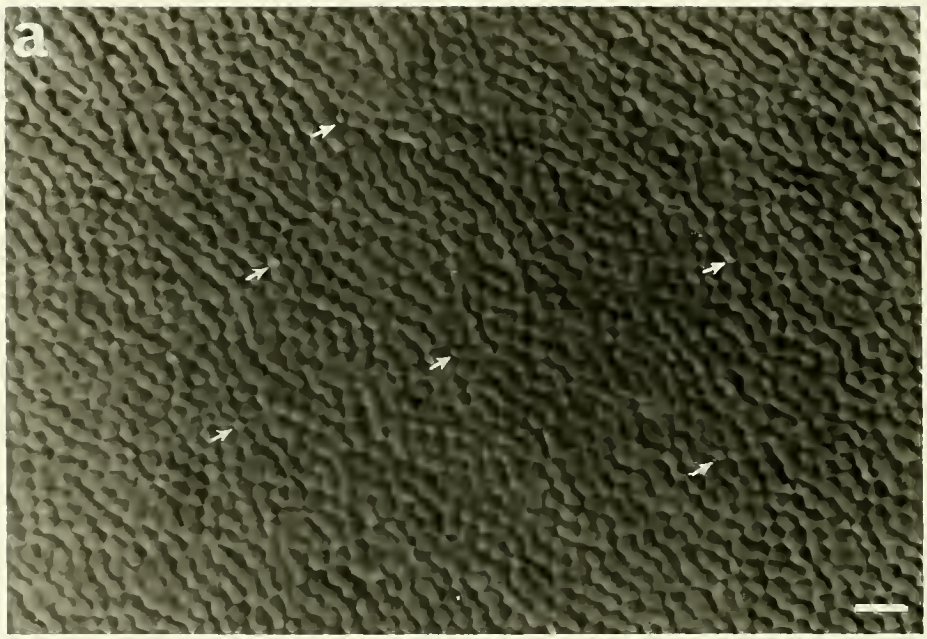
a

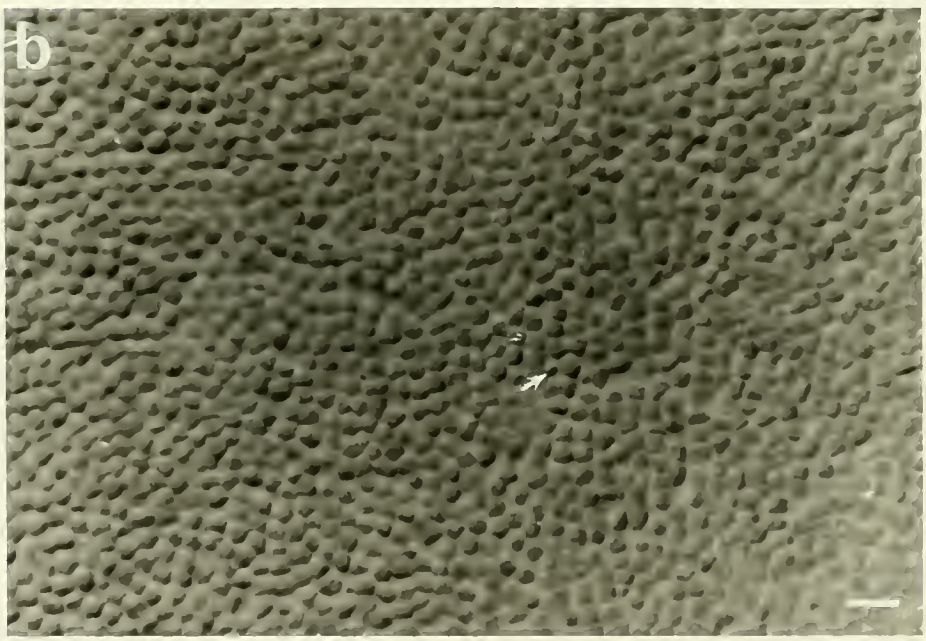
b

Fig. 18. (a) Ganglion cells in flatmount view from visual streak of lemon shark retina. A cluster of small and giant ganglion cells can be seen surrounded by parallel bundles of nerve fibers running toward the optic disc. (b) Ganglion cells from peripheral retina. Note large axonal process (arrow) from giant ganglion cell. NDIC optics. White bars = 10 μm.


a


b

Cones had the characteristic conical shape, tapering from their widest point at the ellipsoids up to the distal tips, which were positioned just above the 3.5 µm-wide rod ellipsoids (Fig. 16), in agreement with Cohen's (1980) description. Thus, the stouter cones appeared nestled among the thinner, longer rods and centered closer to the outer limiting membrane than the rods.

These features, when translated to a flat, wholemount view of the retinal photoreceptor mosaic (Fig. 17), were used to differentiate cones from rods using NDIC optics as follows. Focusing on the plane of rod ellipsoids (see Fig. 16), the tips of the cone outer segments appeared as lightly contrasting, small nodules interspersed within the sea of larger, roundish rod ellipsoids (Fig. 17). Focusing down toward the outer limiting membrane, the cone ellipsoids appeared directly below their corresponding outer segments. Besides being located deeper in the tissue, the cone ellipsoids were larger (about 5 µm diameter) and typically more oval in the flatmount plane than the overlying rod ellipsoids (about 3.5 µm diameter). Thus, both outer segment and ellipsoid conformation could be used to confirm the identification of cones in the lemon shark retina.

To identify and count ganglion cells (Fig. 18), I relied on the detailed description and classification of juvenile lemon shark ganglion cells reported by Cohen (1980), who utilized toluidine blue and Golgi staining to survey all neuronal types in this retina. Using Cohen's guidelines, I differentiated small ganglion cells (8-10 µm) from neuroglia by their perikaryon shape (spherical), nucleus shape (irregular), nucleus location within the perikaryon (eccentric), and presence of an axonal process (if visible). These ganglion cells were furthermore

differentiated from amacrine cells by their depth of location. Amacrine cells in the lemon shark retina are positioned along the proximal margin of the inner nuclear layer, and no displaced amacrine cells have been described in this retina (Cohen, 1980). Therefore, I did not count any cells that were located distal to the inner plexiform layer, unless they were giant cells over 20 μm in diameter, in which case they were included as displaced giant ganglion cells (Cohen, 1980). Any cell from the nerve fiber layer to the inner plexiform layer whose perikaryon was 20-30 μm in diameter was judged to be a giant ganglion cell, and was counted.

At best, counting ganglion cells in wholemounts is an imprecise art, and conservative investigators typically qualify their counts as being of "presumed" or "putative" ganglion cells based upon stated criteria. This is no less true in my study, and the "putative" is thus assumed to be understood in my report of "ganglion cell" distribution in the lemon shark retina.

Cone and Ganglion Cell Density

Three wholemounted retinas from the left eyes of experimental animals were systematically surveyed for both cone and ganglion cell topography. A complete grid of sampling sites arranged in 1 mm steps down 1 mm-spaced columns yielded an average of 503 sampling sites per retina. Cells were identified using the described criteria and counted in each of four quadrants within the field of view (a total area of 0.0616 mm^2), and counts were subsequently converted to cells/mm^2, so that isodensity contours could be determined. Because the ganglion cells were counted with the retina in an inverted orientation (i.e. nerve fiber layer down rather than photoreceptor layer down), the final ganglion cell maps were subsequently reversed to be topographically comparable to the cone maps.

Examples of such cone density and ganglion cell density maps from the same retina are shown in Figs. 19 and 20. The other two retinas yielded comparable results, essentially replicating the distributions shown in Figs. 19 and 20 without significant discrepancy.

A few general observations were made during the topographic surveys. In the central retina, rods and cones both appeared somewhat more tightly packed across the photoreceptor plane than in the peripheral retina. No obvious mosaic pattern to the distribution of cones along the lines of teleost or primate retina emerged during the surveys, but it appeared that cones were typically surrounded by hexagonal arrays of six rods per cone (Fig. 17). This 6+1 grouping became useful in locating and counting cones.

Both classes of ganglion cells (small and giant) were found in both central and peripheral retina (Fig. 18). In central retina, ganglion cells were sometimes seen clumped into groups surrounded by parallel bundles of nerve fibers running toward the optic disc (Fig. 18a). In peripheral retina, ganglion cells were less clumped and sometimes showed large axonal processes (Fig. 18b).

Cone density in the three retinas ranged from a high of 6496 cones/mm^2 in the central retina to a low of 454 cones/mm^2 in the extreme dorsal and ventral peripheries. A density of over 6000 cones/mm^2 extended horizontally across the central retina toward the rostral and caudal poles. This density dropped off sharply to less than 2000 cones/mm^2 in both the dorsal and caudal directions within about 2 mm from the 6000 cones/mm^2 contour. With a RMF of 0.164 mm/° visual angle for the juvenile lemon shark (Hueter, 1980), the 2000 cones/mm^2 contour was thus positioned about 18° dorsal and ventral to the horizontal

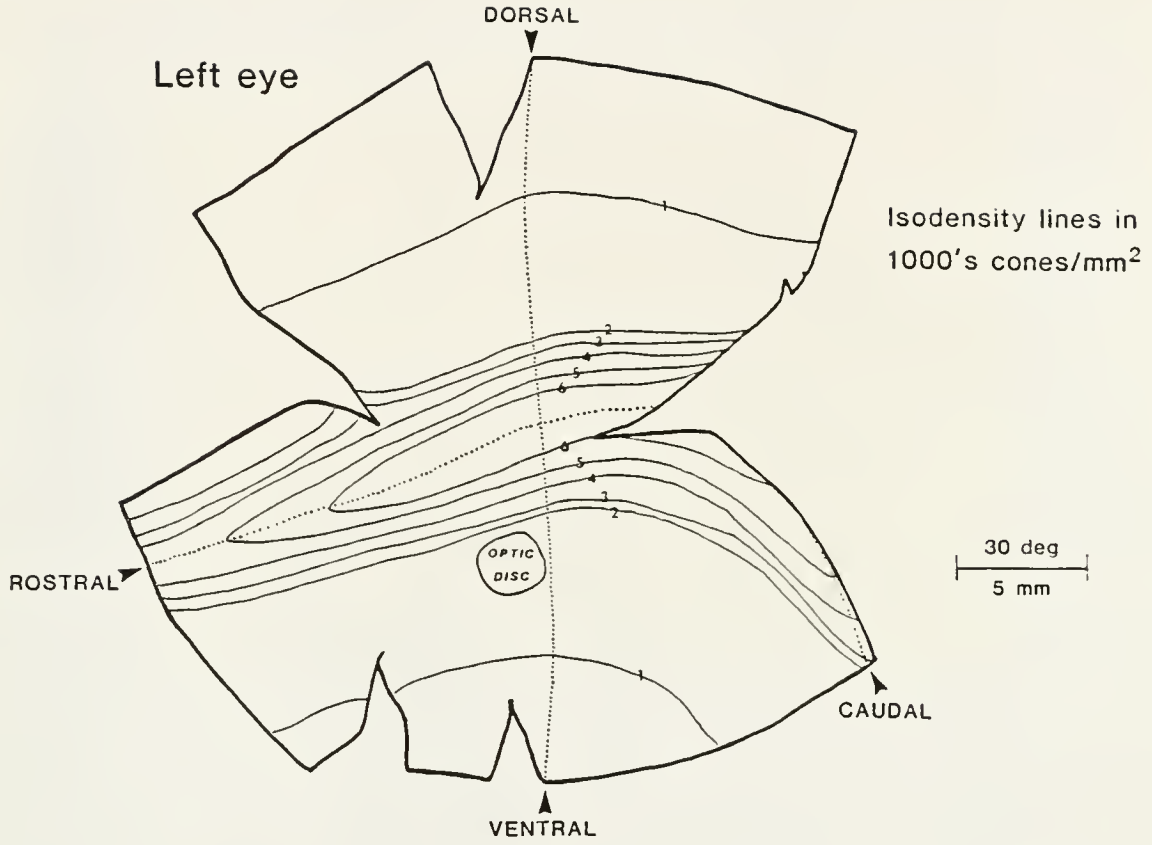

Fig. 19. Density distribution map for cone photoreceptors in lemon shark wholemounted retina. Dotted lines indicate horizontal and vertical meridians. Peak cone density is over 6000 cones/mm^2 inside the visual streak, and falls to less than 500 cones/mm^2 in the extreme dorsal and ventral peripheries. The scale indicates 30 degrees of corresponding visual angle for this retina.

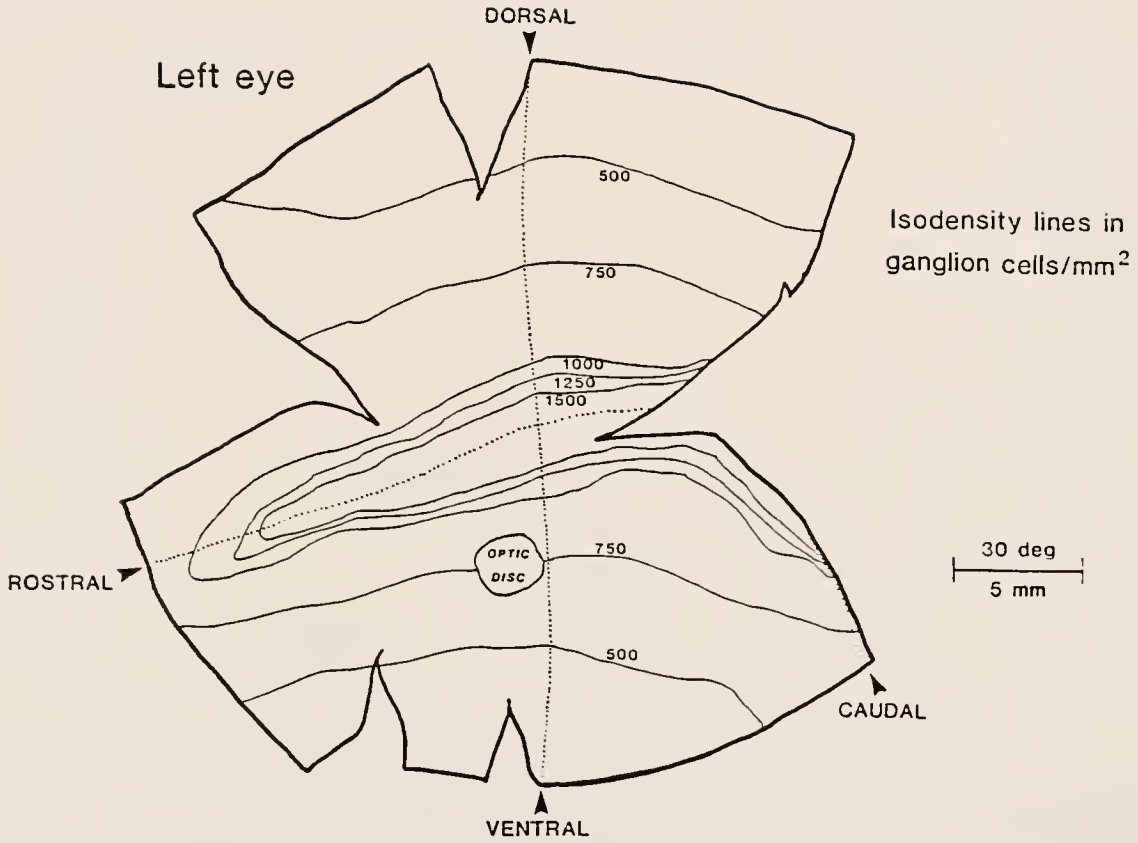

Fig. 20. Density distribution map for ganglion cells in lemon shark wholemounted retina. Dotted lines indicate horizontal and vertical meridians. Peak ganglion cell density is over 1500 cells/mm^2 inside the visual streak, and falls to less than 500 cells/mm^2 in the extreme dorsal and ventral peripheries. The scale indicates 30 degrees of corresponding visual angle for this retina.

rostro-caudal meridian; the 4000 contour was at about 13° dorsal and ventral; and the 6000 contour was at about 7° dorsal and ventral. From the 2000 contour, cone density decreased fairly evenly in dorsal and ventral directions to the low of about 450 cones/mm^2.

The ganglion cell population showed a distributional pattern similar to the cone population. Peak density was 1571 cells/mm^2 in the central retina, and the lowest density encountered was 454 cells/mm^2 in the dorsal and ventral peripheries. As with the cone distribution, the ganglion cells were arranged in a high density zone extending horizontally across the rostro-caudal meridian. In the interior of this zone, cell density remained above 1500 cells/mm^2. Within 10-20° dorsal and ventral to the horizontal meridian, density dropped off sharply from the 1500 cells/mm^2 contour to less than 1000 cells/mm^2, and then gradually decreased peripherally to the minimum density of less than 500 cells/mm^2. Thus, the ratio of ganglion cells per unit area for inside the high density band vs. in the outer periphery was approximately three-to-one.

It is evident, then, that the ganglion cell and cone populations of the lemon shark retina are organized into a well-defined visual streak extending across the horizontal meridian of the retina. The term "visual streak" is normally reserved for describing ganglion cell topography alone in those vertebrates showing a horizontal bandlike area of higher ganglion cell density (Hughes, 1977). Since it is clear that this area in the lemon shark retina is coincident with both higher cone density and retinotectal magnification, I will the use the term "visual streak" more generally to include all three specializations--retinotectal magnification, higher cone density, and higher ganglion cell density--in referring to the topographic organization of the lemon shark visual system.

DISCUSSION

The Retinotectal Pathway in the Lemon Shark

Nature of the Tectal Units

Although it is difficult to identify with absolute certainty the precise nature of the "tectal units" from which I recorded in this study, several lines of evidence lead to the conclusion that the unit responses reflected the activity of retinal ganglion cell fibers projecting to the optic tectum. First, the average depth of maximum unitary response (496 μm below the tectal surface) coincides with the level of densest degeneration of optic fibers terminating in the tectal superficial zone, following contralateral enucleation in juvenile lemon sharks (Graeber and Ebbesson, 1972a). Thus, recording depth for mapping purposes was consistent with the described anatomical location of maximum input of ganglion cell fibers in the tectum.

In addition, the general receptive field properties of the mapped units were consistent with those described by Cohen (1980) and Cohen and Gruber (1985) for extracellular recordings of ganglion cells in an eye-cup preparation of isolated lemon shark retina. The majority of units that I mapped responded maximally to the offset of light, by the introduction of a black disc over a white background, or the offset of a flashing light, within the unit's receptive field. This is consistent

with Cohen and Gruber's (1985) finding that 63% of the lemon shark ganglion cells from which they recorded were OFF units. Furthermore, the tectal units in my study displayed RF sizes of rarely smaller than 5° or larger than 10° in visual angular subtense. This also is consistent with Cohen's (1980) finding that lemon shark ganglion cells have receptive fields subtending 5.2-8.8° of visual angle.

Although no one has determined the size of tectal neuron RF's in an elasmobranch, this has been done in teleosts, and these fields are typically much larger than ganglion cell RF's. In the zebrafish (Brachydanio rerio), for example, Sajovic and Levinthal (1982) found that the tectal neurons had receptive fields averaging 25-39°, compared with retinal ganglion cell RF's of 7-13° in that species, the latter being comparable to those in the lemon shark.

Thus, it is reasonable to assume that the tectal units recorded in my mapping experiments were in fact retinal ganglion cell axons projecting to and terminating in the optic tectum, not tectal neurons. The orderly, reproducible nature of the point-to-point relationship between visual field and contralateral tectum in the lemon shark, and the similarity of the general projection pattern to those of other vertebrates, further supports this assumption. In addition, the obvious spatial correlation between ganglion cell density and retinotectal topography in this species is also consistent with the identification of the tectal units as ganglion cell fibers.

General Pattern and Functional Significance

I have demonstrated in this study that the retinotectal projection of chondrichthyans can be electrophysiologically mapped. The general

pattern of this projection--from dorsal visual field to medial tectum, ventral field to lateral tectum, rostral field to rostral tectum, and caudal field to caudal tectum--is identical to that found in teleost fishes. Indeed, this pattern is identical to that of all other vertebrates studied, with the exception of certain lizards in which the retinotectal map is rotated roughly 90° clockwise on the tectal surface (Gaither and Stein, 1979). Thus it appears that the retinotectal projection map in chondrichthyans conforms to the same general design found in the other classes of previously investigated vertebrates.

Questions concerning the functional role of the retinotectal pathway in shark spatial vision, in particular those raised by Graeber (1978), are reminiscent of similar questions raised in the past for other vertebrates. Whether or not the anatomical orderliness of the retinotectal projection is a prerequisite for spatial visual function, or merely a result of normal development, has been debated in studies ranging from specificity of neuronal connections to multimodal integration in the vertebrate brain. Recent evidence from regeneration studies that new optic projections following partial tectal ablation fill the remaining tectal space in an orderly fashion, and that functional activity of units helps to direct neuronal connections (Easter et al., 1985), argues for a functional role to the spatial projection.

This question was answered, at least for teleost fishes, by Schwassmann and Krag (1970), who used classical conditioning of heart rate to map the extent of scotomata (blind areas) following tectal lesion in the opaleye, Girella nigricans. Their results revealed a strict parallel between the anatomical orderliness of the retinotectal projection and higher-level visual function as assayed by the classically conditioned

response. Schwassmann and Krag concluded that "in the visual system of teleost fish, and probably of vertebrates in general, the precisely organized retinotectal projection is an indispensable feature for functional localization in visual space" (p. 40).

With my demonstration that the retinotectal projection in the lemon shark conforms to the same point-to-point orderliness found in teleosts and other vertebrates, I have confirmed the prominence of the mesencephalic tectum as the center for spatial visual input in elasmobranchs. The fact that tectally ablated sharks may be capable of some crude visual discrimination is interesting but, with current information, is of secondary significance in the understanding of spatial visual function in sharks. It is curiously analogous to the many studies showing that mammals continue to perform visual discrimination tasks after destruction of visual cortex, and yet the importance of this region in the spatial vision of higher vertebrates is unquestioned.

Topographical Organization of Vision in the Lemon Shark

Nonlinearity in Retinotectal Topography

The demonstration of a nonlinearity in the topographic projection of the visual field on the lemon shark's optic tectum is the first evidence that certain areas of visual space are given greater representation in higher centers of the shark nervous system. This nonlinearity in the lemon shark is organized into a prominent visual streak, a horizontal band of retinotectal magnification extending across the entire visual field and conjugate with the visual horizon. The edges of the

streak lie at approximately 15° above and 15° below the horizon, and the proportional representation on the tectum of streak vision vs. peripheral vision is approximately 3:1.

Outside of the streak, in the upper dorsal and lower ventral visual fields, vision is mediated by widely spaced units with large receptive fields, whereas inside the streak, visual receptive fields are closer together, smaller, and of a horizontally aligned elliptical shape. No further concentrated region of punctate receptive fields, as would be associated with a retinal area or fovea, is observed within the visual streak.

Similar visual streaks in the retinotectal projection pattern have been reported in a few other vertebrates. Evidence of this type of retinotectal nonlinearity was first found in the frog Rana temporaria and the toad Bufo vulgaris, both of which have proportional tectal representations of approximately 2.7:1 in streak vs. periphery (Jacobson, 1962). Among teleosts, the surface-swimming "four-eyed fish" (Anableps microlepis) has a visual streak of retinotectal magnification associated with aerial vision just above the surface of the water (Schwassmann and Kruger, 1965b). The lower edge of the streak is conjugate with the water surface, and the upper edge is located about 25° into the aerial field. Proportional tectal representation is approximately 2.4:1 between the streak and the peripheral aerial field in this species.

The American alligator (Alligator mississippiensis) also appears to have a visual streak in its retinotectal projection (Heric and Kruger, 1965). The streak in this case is 20° wide and aligned about 10° above and 10° below the horizontal meridian. Retinotectal magnification factors for the alligator were not reported.

It is noteworthy that in the above cases in which receptive field sizes and shapes were reported (four-eyed fish and alligator), RF's appear to show a pattern similar to those in the lemon shark. That is, peripheral RF's are larger and rather irregular in shape, whereas streak RF's are not only smaller but are also compressed horizontally into an elliptical shape. Since ganglion cell dendritic spread has been correlated with receptive field size (Brown, 1965), it would be interesting to examine the arborization pattern of streak vs. peripheral ganglion cells in four-eyed fish, lemon shark, and alligator retina.

Anatomical Basis in the Retina

My finding of an anatomical visual streak in the lemon shark retina, as revealed in the cone and ganglion cell populations, is consistent with previous reports of spatial correlations between retinal topography and tectal representation. Jacobson (1962) first demonstrated a close correlation between the retinotectal magnification factor and ganglion cell density with retinal eccentricity, in anurans with visual streaks. Schwassmann and Kruger (1965b) also indicated that the visual streak of Anableps is associated with a greater density of cones, interneurons, and ganglion cells. Retinal foveas receive a substantially magnified representation on the tectum of teleosts (Schwassmann, 1968) and reptiles (Stein and Gaither, 1981) as well. Five times more tectal surface is devoted to foveal vision than to peripheral vision in the marine teleost Paralabrax (Schwassmann, 1968).

Such correlations extend to the representation of retinal areas on the striate cortex of mammals. In primates, this representation is nonlinear in that more cortex is devoted to equivalent areas of central

retina than peripheral retina (Daniel and Whitteridge, 1961). Cone and ganglion cell densities in primate retina reflect a similar topographic distribution, which is furthermore correlated with cortical magnification factor, although not by a simple arithmetic relationship (Perry and Cowey, 1985).

Thus, the striking similarities in cone, ganglion cell, and retinotectal topography in the lemon shark are clearly not coincidental, but must reflect an anatomical basis in retinal architecture for the patterns revealed physiologically on the tectal surface. That both photoreceptor and ganglion cell populations reflect this basis in the lemon shark's visual streak is not surprising: in other vertebrates, including turtles, rabbits, and cats, when a visual streak is present in the ganglion cell layer, the underlying photoreceptor distribution also shows an increased density within the streak (Hughes, 1977).

The heterogeneity in cone density which I have observed in the wholemounted lemon shark retina would seem to bear out Cohen's (1980) report of variable rod:cone ratios in histological sections of this retina, although his finding of a lower ratio (i.e. greater cone density) in "dorsal" retina is enigmatic. The peak density of cones in the center of the visual streak reflects a greater than 14:1 increase in the packing of cones in comparable retinal areas of the streak vs. the periphery. This is not to imply, however, that although indicative of enhanced spatial vision within the streak compared with the periphery, the peak cone density in the juvenile lemon shark retina is high among vertebrates. With a RMF of .164 mm/°, the peak density of about 6500 cones/ mm^2 converts to about 175 cones/$°^2$. This is less than the lowest density of cones in the most peripheral human retina (Østerberg, 1935).

The 3:1 concentration of ganglion cells in visual streak vs. periphery of the lemon shark retina mirrors the 3:1 ratio of proportional tectal representation for the two areas. It is tempting to conclude that this numerical difference in total ganglion cell density is directly responsible for the resulting differences in retinotectal magnification factors, without further complications. But considering that all retinal ganglion cells are not equal, such that they are broken down into various classifications based upon specific morphological and physiological criteria (Stone, 1983), this is most likely too simplistic. A case in point is the foveate teleost Paralabrax: although the fovea receives five times more tectal representation than the periphery, the ratio between foveal and peripheral ganglion cell densities is over 10:1 (Schwassmann, 1968).

As with the cone density, the peak ganglion cell density of about 1600 cells/mm^2 (43 cells/$°^2$) in the juvenile lemon shark is comparatively low among the vertebrates. In the visual streak of the rabbit, for example, maximum density is about 5000 cells/mm^2 (153 cells/$°^2$), and the retina of the cat contains as many as 10,000 cells/mm^2 (424 cells/$°^2$) at the area centralis (Hughes, 1985). However, ganglion cell density in the lemon shark is comparable to that of the horn shark, Heterodontus francisci, as reported by Peterson and Rowe (1980). Peak density in the horn shark retina is about 500 ganglion cells/mm^2 within its streaklike area, and density drops to between 50 and 100 cells/mm^2 in the periphery.

Interestingly, the ganglion cell density of marine mammals appears to be more comparable to that of sharks than to terrestrial mammals. Maximum cell density in dolphins, for example, averages between 500 and 800 cells/mm^2. In the harbor porpoise, Phocoena phocoena, ganglion cell

distribution is organized into two higher-density zones, one nasal and one temporal, each of which contains a peak density of only about 705 cells/mm^2 (Mass and Supin, 1986).

Even with a relatively low ganglion cell density, however, the lemon shark retina is topographically heterogeneous, and the ganglion cell distribution clearly indicates the presence and location of the visual streak.

Implications for the Visual Ecology of Sharks

Function of the Visual Streak

The term "visual streak" is thought to have been first used by Davis (1929) to refer to an elongated, horizontally oriented region of retinal specialization (Stone, 1983), although interpretations of streak function appeared earlier (Johnson, 1901). When present, the streak is sometimes visible on the macroscopic level in features such as the distribution of retinal blood vessels or the relative thickness of the retina. The possession of a streak skips across phylogenetic lines, having been found in certain species from most of the classes of vertebrates. An analogue even exists in the compound eyes of certain invertebrates (Wehner, 1987).

In the vertebrates, visual streaks have been previously described in some teleost fishes (Butcher, 1938; Munk, 1970), anurans (Jacobson, 1962), turtles (Brown, 1969), birds (Duijm, 1958), and mammals (Hughes, 1977; Stone, 1983). If the definition of the term is expanded to include a horizontal band of magnification in the retinotectal projection pattern,

then the examples of the four-eyed fish (Schwassmann and Kruger. 1965b) and alligator (Heric and Kruger, 1965) must be added to the list. Among the sharks, it would appear that the previously described cases of Scyliorhinus canicula, Mustelus spp., and Heterodontus francisci (although detailed topographic information is only available for Heterodontus) qualify them as visual streak species (see Table 1), now along with the lemon shark.

The functional significance of the visual streak has been discussed in depth by Munk (1970), Hughes (1977), and Wehner (1987). In general, all hypotheses correlating the presence of a streak with other biological features--including the possession of laterally vs. frontally directed eyes, or nonpredatory vs. predatory lifestyle--have been rejected, except for one. This hypothesis has been formalized into the "terrain" theory by Hughes (1977).

The terrain theory proposes that animals with visual worlds dominated by the two-dimensional horizon--an open grassland, a desert, the water surface, the sea bottom, for example--benefit from a visual streak by concentrating ganglion cells in the region of the retina that is normally conjugate with that horizon, along which the majority of visual "action" takes place. This seemingly ensures that the visual machinery, of which there must be a finite number of components, is economically utilized to better detect stimuli within the space just above and below the horizontal meridian, across the entire visual field. It is in this space where the majority of new visual targets appear, either by their movement across the horizontal plane toward the observer, or by the movement of the observer across the horizontal plane. Objects located far above or far below the horizon are, relatively speaking, of "peripheral" significance.

Among the mammals, one of the best developed visual streaks is found in the cheetah, Acinonyx jubatus (Hughes, 1977), a visual predator par excellence of the open grasslands. Tree kangaroos (Dendrolagus dorriana), an arboreal species, have a radially symmetrical distribution of retinal ganglion cells, whereas the plains kangaroo (Megalia rufa) has a prominent visual streak (Hughes, 1975). In birds, visual streaks are found particularly in sea birds, such as the herring gull, Larus argentatus (Duijm, 1958). Reptiles that orient visually to water surfaces, such as the turtle Pseudemys scripta (Brown, 1969) and the alligator Alligator mississippiensis (Heric and Kruger, 1965), have visual streaks, as do species of frogs (Jacobson, 1962). And in fishes, the most highly developed streaks are found in the surface-oriented killifishes, such as Fundulus heteroclitus (Butcher, 1938) and Aplocheilus lineatus (Munk, 1970), the mudskippers Boleophthalmus and Periophthalmus spp. (Munk, 1970), and the four-eyed fish Anableps microlepis (Schwassmann and Kruger, 1965b).

Hughes (1977) established some criteria for determining the validity of the terrain theory in functional interpretations of the visual streak, beyond simply the terrain habitat for a given species. When a visual streak is present in the ganglion cell layer, then the underlying photoreceptor distribution--which is, after all, the first to deal with the horizontal bias of the visual field--should also show an increased density organized into a band-shaped region. This receptor array must furthermore be kept in a relatively fixed position with respect to the retinal image of the terrain and horizon. To do so, this necessitates that the streak be horizontal under normal conditions, and that displacement of the streak be resisted when head orientation is changed.

Notes on Visual Behavior in the Juvenile Lemon Shark

In assessing the functional role of the visual streak in sharks, it is important to not only examine the demands of habitat and lifestyle, as outlined in the Introduction for the juvenile lemon shark, but behavior as it relates to visual function as well. During the course of collecting lemon sharks in the field and maintaining them in captivity for this study, I periodically took advantage of the opportunity to observe the sharks' behavior as it relates to vision. This was done on an unstructured basis through hours of underwater observation of the sharks in the field (Florida Bay) and in semi-natural conditions (Whitney Lab pond), in addition to watching the animals from above the water as they moved, fed, and interacted within the Whitney pond. Behaviors were occasionally recorded on film with a 35 mm underwater camera. The following constitutes my general observations of juvenile lemon shark behavior under these conditions. This is in no way meant to substitute for a proper ethological analysis of lemon shark behavior, which is sorely needed.

Juvenile lemon sharks are constantly patrolling, benthically orienting animals. They typically cruise just over the bottom, maintaining a constant distance of a few centimeters over the substrate. They do not avoid extreme shallows, sometimes investigating areas in which there is just enough water for them to stay submerged. While patrolling, they do not often make depth changes, but tend to maintain their position with respect to the bottom. Although they are capable of resting on the bottom, they spend most of their time slowly swimming, both night and day. Actually, these sharks have to expend about 9% more energy in resting than in slow swimming, apparently due to the energetic costs of actively pumping water over the gills vs. passive ram ventilation (Gruber, 1981).

As this shark swims over the benthos, the slow, side-to-side sweep of the body is accompanied by small, strictly horizontal shifts of eye position with respect to the head. These would appear to maintain some stability of the visual field during swimming and turning movements, in the manner described by Harris (1965) for the spiny dogfish, Squalus acanthias. I have never observed a juvenile lemon shark making voluntary eye movements while at rest under natural conditions.

Lemon sharks do not appear to stop and fixate a visual target, either monocularly or binocularly. They show initial visual interest in an object by swimming past and returning to the object, keeping it within range. When at rest, they will respond to a new, presumably visual stimulus by initiating patrolling behavior. In Florida Bay, where turbidity due to sediment disturbance can be high (Ginsburg, 1956), I have watched these sharks swim up a chum line toward an observer until just within the underwater range of visibility, then abruptly veer off. In the Whitney pond, the sharks readily acclimated to an underwater observer, allowing a slow approach up to about 1 m away before moving off. A non-moving observer was sometimes approached by the sharks to within less than 1 m distance.

In the pond, the sharks would take food at the surface, at mid-depths, and on the bottom. It was my impression that they responded primarily to acoustic cues in reacting to food striking the surface, and to primarily olfactory cues in localizing small pieces of prepared food lying still on the bottom. But the use of visual cues could not be ruled out under any of these conditions. They did not generally respond to visual stimuli originating high above the water surface, but were quick to react to new objects placed underwater in the pond.

The Visual Niches of Sharks

From the standpoint of visual streak function, the juvenile lemon shark seems to meet all of the criteria of the terrain theory. In Florida Bay, its habitat of shallow grass flats and mangrove-fringed shoals presents a world that is restricted to the narrow column between the water's surface and the sea bottom. It is truly a two-dimensional world. As the shark moves through this space, relevant visual stimuli appear just above and below the horizontal meridian in the visual field.

The increase in cone density within the juvenile lemon shark's visual streak implies that photopic acuity, as mediated by the cones, should be higher in the streak zone of the visual field than in the periphery. With a peak density of about 6500 cones/mm^2, and a RMF of 164 μm/°, the average intercone separation can be no greater than 12.4 μm, corresponding to 4.5' of visual angle. In the periphery, where cone density decreases to a low of about 450 cones/mm^2, average intercone separation expands to about 47.1 μm or 17.2' of visual angle--almost a 4X drop in theoretical resolving power of the retina.

The functional relevance of these numbers can only be established with real measures, not predictions, of visual acuity, in itself a "blurry" term referring to an animal's maximum ability to visually resolve the spatial details of an object under certain conditions of illumination. Visual acuity is not a concrete specification of a visual system, but rather is an operationally defined feature of an animal's behavior that may vary with measurement conditions, and it is determined by optical as well as neural factors (Hughes, 1977).

Still, the increase in cone density in the lemon shark's visual streak satisfies terrain theory criteria, and the necessity of horizontal

alignment of the streak under normal conditions seems to be satisfied as well. This shark's strict orientation to the benthos, and its horizontal, compensatory eye movements during movement, should keep the streak concentrated on the horizon during patrolling activity.

But this raises a new point. Might locomotory behavior also affect the adaptive value of the visual streak? I suggest that it does in the lemon shark. As constantly patrolling predators, these sharks operate in a world in near-continual motion, but that motion tends to be congruent with the visual terrain--that is, horizontal. The swimming mode of the lemon shark, therefore, further exaggerates the visual tasks located near the horizontal plane, and makes the development of a visual streak all the more adaptive.

Thus, the spatial characteristics of the visual niche occupied by the juvenile lemon shark are affected by the terrain-type habitat, predatory lifestyle, and mode of locomotion of the species. Because the adult lemon sharks remain patrolling, benthic predators even in deeper water, the adaptive value of the visual streak would seem to continue throughout this shark's life.

Not surprisingly, the other species of sharks so far described to have some development of a visual streak are also benthically oriented animals not unlike the juvenile lemon shark. Mustelus in particular has been described as "a very active shark, constantly patrolling the bottom for food" (Compagno, 1984: p. 406). Heterodontus is a strict bottom dweller, but it also spends much more time sitting on the bottom than does Negaprion. This locomotory difference, along with its more nocturnal lifestyle (Compagno, 1984), perhaps explains the weaker nature of the horn shark's visual streak compared with that of the lemon shark, as manifested in absolute ganglion cell density.

Because the benthic species of sharks tend to be more easily captured and maintained in captivity, we have a sampling bias skewed toward these sharks vs. more pelagic species. All of the sharks listed in Table 1, for example, are bottom-dwelling sharks, with the notable exception of the white shark (Carcharodon carcharias). It is doubtful that the spatial vision of pelagic sharks is without topographic specialization, and it would be enlightening to explore the trends present in retinal and retinotectal topography of more active, pelagic species, such as the blue (Prionace glauca), mako (Isurus oxyrinchus), or white sharks. It may be that the preliminary indication of a higher cone concentration in the center of the white shark retina (Gruber and Cohen, 1985) will ultimately lead to the discovery of a high acuity zone in the vision of this diurnal species. Perhaps this magnificent predator has in its great black eye a true visual axis, which, when all is said and done, I never found in the lemon shark.

SUMMARY AND CONCLUSIONS

1) The organization of spatial vision in juvenile lemon sharks (Negaprion brevirostris) collected in Florida Bay was investigated. Data were collected from a total of 46 animals of less than two years of age.

2) For the first time in a chondrichthyan vertebrate, the retinotectal projection pattern from left visual field to right mesencephalic (optic) tectum was electrophysiologically mapped, in 20 animals. Tectal unit responses were evoked by photic stimuli. Average recording depth in mapping was 496 μm below the tectal surface.

3) The tectal units recorded in mapping were identified as retinal ganglion cell fibers terminating in the superficial contralateral tectum, based upon depth of recording and receptive field properties.

4) The overall projection pattern is from dorsal visual field to medial tectum, ventral visual field to lateral tectum, rostral visual field to rostral tectum, and caudal visual field to caudal tectum. This conforms with the general design found in almost all other vertebrates.

5) A precise point-to-point relationship exists between areas in the visual field and projection sites on the tectum, such that the complete visual field is represented on the tectal surface in an orderly spatial arrangement. This is consistent with the optic tectum as being the primary center for spatial visual input in elasmobranchs.

6) The projection pattern in the juvenile lemon shark is organized into a visual streak, a horizontal band of proportionately greater retinotectal magnification, located within 15° above and 15° below the horizontal meridian in the visual field. This area comprising only 26% of the total visual field is represented by 52% of the tectal surface. Three times more tectum is devoted to vision in the streak than to equal-sized areas in the peripheral visual field.

7) Receptive fields of streak units tend to be smaller, elliptical, and horizontally oriented. Peripheral fields are larger and more irregular in shape. Field sizes range from about 5° inside the streak to 10° or more at the periphery.

8) Retinal cell distribution, as mapped using a retinal wholemount technique, also is organized into a visual streak coincident with the retinotectal streak.

9) Ganglion cell density ranges from a high of over 1500 cells/mm^2 inside the streak to less than 500 cells/mm^2 in the periphery. Cone density is approximately 6500 cones/mm^2 inside the streak and less than 500 cones/mm^2 in the extreme periphery. Average intercone separation is calculated to be 12.4 μm at peak cone density, which corresponds to a visual angle of 4.5'.

10) The visual streak of the juvenile lemon shark conforms with the terrain theory of visual streak function. According to this theory, the streak enhances spatial vision along the visual horizon in animals whose habitats are dominated by a two-dimensional horizontal terrain. In the juvenile lemon shark, the locomotory mode of constant patrolling over the benthos may further add to the adaptive value of the visual streak in this shark species.

REFERENCES

Akert, K. (1949) Der visuelle Greifreflex. Helv. Physiol. Acta 7: 112-134.

Ali, M.A. (1978) General introduction. In Sensory Ecology: Review and Perspectives (Ali, M.A., ed.), pp. 3-8. Plenum Press, New York.

Apter, J.T. (1945) Projection of the retina on superior colliculus of cats. J. Neurophysiol. 8: 123-134.

Ariëns-Kappers, C.U., Huber, G.C. and Crosby, E.C. (1936) The Comparative Anatomy of the Nervous System, including Man. Macmillan, N.Y.

Aronson, L.R. (1963) The central nervous system of sharks and bony fishes with special reference to sensory and integrative mechanisms. In Sharks and Survival (Gilbert, P.W., ed.), pp. 165-241. D.C. Heath, Boston.

Aronson, L.R., Aronson, F.R. and Clark, E. (1967) Instrumental conditioning and light-dark discrimination in young nurse sharks. Bull. Mar. Sci. 17: 249-256.

Baldridge, H.D. (1974) Shark attack: a program of data reduction and analysis. Contrib. Mote Marine Lab. 1: 1-98.

Bastian, J. (1982) Vision and electroreception: integration of sensory information in the optic tectum of the weakly electric fish Apteronotus albifrons. J. Comp. Physiol. 147: 287-297.

Brown, A.M., Dobson, V. and Maier, J. (1987) Visual acuity of human infants at scotopic, mesopic and photopic luminances. Vision Res. 27: 1845-1858.

Brown, J.E. (1965) Dendritic fields of retinal ganglion cells of the rat. J. Neurophysiol. 28: 1091-1100.

Brown, K.T. (1969) A linear area centralis extending across the turtle retina and stabilized to the horizon by non-visual cues. Vision Res. 9: 1053-1062.

Bullock, T.H. (1984) Physiology of the tectum mesencephali in elasmobranchs. In Comparative Neurology of the Optic Tectum (Vanegas, H., ed.), pp. 47-68. Plenum Press, New York.

Butcher, E.O. (1938) The structure of the retina of Fundulus heteroclitus and the regions of the retina associated with different chromatophoric responses. J. Exp. Zool. 79: 275-297.

Clark, E. (1959) Instrumental conditioning of sharks. Science 130: 217-218.

Clark, E. (1961) Visual discrimination in lemon sharks. Abstr. Symposium Papers, Tenth Pacific Science Congress, Honolulu: 175-176.

Clark, E. (1963) Maintenance of sharks in captivity with a report on their instrumental conditioning. In Sharks and Survival (Gilbert, P.W., ed.), pp. 115-149. D.C. Heath, Boston.

Clark, E. and von Schmidt, K. (1965) Sharks of the central gulf coast of Florida. Bull. Mar. Sci. 15: 13-83.

Cohen, J.L. (1980) Functional organization of the retina of the lemon shark (Negaprion brevirostris, Poey): an anatomical and electrophysiological approach. Ph.D. diss., Univ. Miami, Coral Gables, Florida.

Cohen, J.L. and Gruber, S.H. (1985) Spectral input to lemon shark (Negaprion brevirostris) ganglion cells. J. Comp. Physiol. A 156: 579-586.

Cohen, J.L., Gruber, S.H. and Hamasaki, D.I. (1977) Spectral sensitivity and Purkinje shift in the retina of the lemon shark, Negaprion brevirostris (Poey). Vision Res. 17: 787-792.

Compagno, L.J.V. (1977) Phyletic relationships of living sharks and rays. Amer. Zool. 17: 303-322.

Compagno, L.J.V. (1984) FAO species catalogue. Vol. 4. Sharks of the world. An annotated and illustrated catalogue of shark species known to date. Part 2. Carcharhiniformes. FAO Fish. Synop. (125) 4: 251-655.

Curcio, C.A., Packer, O. and Kalina, R.E. (1987) A whole mount method for sequential analysis of photoreceptor and ganglion cell topography in a single retina. Vision Res. 27: 9-15.

Daniel, P.M. and Whitteridge, D. (1961) The representation of the visual field on the cerebral cortex of monkeys. J. Physiol. 159: 203-221.

Davis, F.A. (1929) The anatomy and histology of the eye and orbit of the rabbit. Trans. Am. Ophthalmol. Soc. 27: 401-441.

Dawson, W.W., Hawthorne, M.N., Parmer, R., Hope, G.M. and Hueter, R.E. (1987) Very large neurons of the human inner retina. Submitted for publication.

Dawson, W.W. and Maida, T.M. (1984) Relations between the human retinal cone and ganglion cell distributions. Ophthalmologica, Basel 188: 216-221.

Dowling, J.E. and Ripps, H. (1970) Visual adaptation in the retina of the skate. J. Gen. Physiol. 56: 491-520.

Duijm, M. (1958) On the position of a ribbon-like central area in the eyes of some birds. Archs. Néer. Zool. 13 Suppl.: 128-145.

Duke-Elder, W.S. (1958) System of Ophthalmology, Vol. 1: The Eye in Evolution. Henry Kimpton, London.

Easter, S.S., Jr., Purves, D., Rakic, P. and Spitzer, N.C. (1985) The changing view of neural specificity. Science 230: 507-511.

Ebbesson, S.O.E. and Ramsey, J.S. (1968) The optic tracts in two species of sharks (Galeocerdo cuvieri and Ginglymostoma cirratum). Brain Res. 8: 36-53.

Ewert, J.-P. (1967) Electrische Reizung des retinalen Projektionsfeldes im Mittelhirn der Erdkröte (Bufo bufo L.). Pflügers Arch. ges. Physiol. 295: 90-98.

Ewert, J.-P. (1980) Neuroethology. Springer-Verlag, Berlin.

Ewert, J.-P. and Borchers, H.W. (1971) Reaktionscharakteristik von Neuronen aus dem Tectum opticum und Subtectum der Erdkröte Bufo bufo (L.). Z. vergl. Physiol. 71: 165-189.

Fernald, R.D. (1977) Quantitative behavioural observations of Haplochromis burtoni under semi-natural conditions. Animal Behaviour 25: 643-653.

Fernald, R.D. (1983) Neural basis of visual pattern recognition in fish. In Advances in Vertebrate Neuroethology (Ewert, J.-P., Capranica, R.R. and Ingle, D.J., eds.), pp. 569-580. Plenum Press, New York.

Forster, R.P., Goldstein, L. and Rosen, J.K. (1972) Intrarenal control of urea reabsorption by renal tubules of the marine elasmobranch, Squalus acanthias. Comp. Biochem. Physiol. 42A: 3-12.

Franz, V. (1931) Die Akkommodation des Selachierauges und seine Abblendungsapparate, nebst Befunden an der Retina. Zool. Jb. Abt. allg. Zool. u. Physiol. 49: 323-462.

Franz, V. (1934) Vergleichende Anatomie des Wirbeltierauges. In Handbuch der vergleichenden Anatomie der Wirbeltiere, Vol. 2 (Bolk, L., Göppert, E., Kallius, E. and Lubosch, W., eds.), pp. 989-1292. Urban & Schwarzenberg, Berlin.

Gaither, N.S. and Stein, B.E. (1979) Reptiles and mammals use similar sensory organizations in the midbrain. Science 205: 595-597.

Gaze, R.M. (1958) The representation of the retina on the optic lobe of the frog. Quart. J. exp. Physiol. 43: 209-214.

Gaze, R.M. and Jacobson, M. (1962) The projection of the binocular visual field on the optic tecta of the frog. Quart. J. exp. Physiol. 47: 273-280.

Gaze, R.M., Jacobson, M. and Szekely, G. (1963) The retino-tectal projection in Xenopus with compound eyes. J. Physiol. 165: 484-499.

Gilbert, P.W. (1963) The visual apparatus of sharks. In Sharks and Survival (Gilbert, P.W., ed.), pp. 283-326. D.C. Heath, Boston.

Gilbert, P.W., Hodgson, E.S. and Mathewson, R.F. (1964) Electroencephalograms of sharks. Science 145: 949-951.

Gilbert, P.W. and Wood, F.G. (1957) Methods of anaesthetizing large sharks and rays safely and rapidly. Science 126: 212.

Ginsburg, R.N. (1956) Environmental relationships of grain size and constituent particles in some South Florida carbonate sediments. Bull. Am. Assoc. Petrol. Geol. 40: 2384-2427.

Grace, A.A. and Llinás, R. (1985) Morphological artifacts induced in intracellularly stained neurons by dehydration: circumvention using rapid dimethyl sulfoxide clearing. Neurosci. 16: 461-475.

Graeber, R.C. (1978) Behavioral studies correlated with central nervous system integration of vision in sharks. In Sensory Biology of Sharks, Skates, and Rays (Hodgson, E.S. and Mathewson, R.F., eds.), pp. 195-225. Off. Nav. Res., Arlington, Virginia.

Graeber, R.C. and Ebbesson, S.O.E. (1972a) Retinal projections in the lemon shark. Brain, Behav. Evol. 5: 461-477.

Graeber, R.C. and Ebbesson, S.O.E. (1972b) Visual discrimination learning in normal and tectal-ablated nurse sharks (Ginglymostoma cirratum). Comp. Biochem. Physiol. 42A: 131-139.

Graeber, R.C. Ebbesson, S.O.E. and Jane, J.A. (1973) Visual discrimination in sharks without optic tectum. Science 180: 413-415.

Graeber, R.C., Schroeder, D.M., Jane, J.A. and Ebbesson, S.O.E. (1978) Visual discrimination following partial telencephalic ablations in nurse sharks (Ginglymostoma cirratum). J. Comp. Neurol. 180: 325-344.

Green, J.D. (1958) A simple microelectrode for recording from the central nervous system. Nature 182: 962.

Gruber, S.H. (1967) A behavioral measurement of dark adaptation in the lemon shark, Negaprion brevirostris. In Sharks, Skates and Rays (Gilbert, P.W., Mathewson, R.F. and Rall, D.P., eds.), pp. 479-490. Johns Hopkins Press, Baltimore.

Gruber, S.H. (1975) Duplex vision in the elasmobranchs: histological, electrophysiological and psychophysical evidence. In Vision in Fishes: New Approaches in Research (Ali, M.A., ed.), pp. 525-540. Plenum Press, New York.

Gruber, S.H. (1980) Keeping sharks in captivity. J. Aquariculture 1: 6-14.

Gruber, S.H. (1981) Lemon sharks: supply-side economists of the sea. Oceanus 24: 56-64.

Gruber, S.H. (1982) Role of the lemon shark, Negaprion brevirostris (Poey) as a predator in the tropical marine environment: a multidisciplinary study. Florida Sci. 45: 46-75.

Gruber, S.H. and Cohen, J.L. (1978) Visual system of the elasmobranchs: state of the art 1960-1975. In Sensory Biology of Sharks, Skates, and Rays (Hodgson, E.S. and Mathewson, R.F., eds.), pp. 11-105. Off. Nav. Res., Arlington, Virginia.

Gruber, S.H. and Cohen, J.L. (1985) Visual system of the white shark, Carcharodon carcharias, with emphasis on retinal structure. Mem. S. Cal. Acad. Sci. 9: 61-72.

Gruber, S.H., Gulley, R.L. and Brandon, J. (1975) Duplex retina in seven elasmobranch species. Bull. Mar. Sci. 25: 353-358.

Gruber, S.H., Hamasaki, D.I. and Bridges, C.D.B. (1963) Cones in the retina of the lemon shark (Negaprion brevirostris). Vision Res. 3: 397-399.

Gruber, S.H. and Keyes, R.S. (1981) Keeping sharks for research. In Aquarium Systems (Hawkins, A.D., ed.), pp. 373-402. Academic Press, London.

Gruber, S.H. and Myrberg, A.A., Jr. (1977) Approaches to the study of behavior in sharks. Amer. Zool. 17: 471-486.

Gruber, S.H. and Schneiderman, N. (1975) Classical conditioning of the nictitating membrane response of the lemon shark (Negaprion brevirostris). Behav. Res. Meth. Inst. 7: 430-434.

Gruber, S.H. and Stout, R.G. (1983) Biological materials for the study of age and growth in a tropical marine elasmobranch, the lemon shark, Negaprion brevirostris (Poey). In Proceedings of the International Workshop on Age Determination of Oceanic Pelagic Fishes: Tunas, Billfishes, and Sharks (Prince, E.D. and Pulos, M., eds.), pp. 193-205. NOAA Tech. Rep. NMFS 8.

Hairston, N.G., Li, K.T. and Easter, S.S., Jr. (1982) Fish vision and the detection of planktonic prey. Science 218: 1240-1242.

Hamasaki, D.I. and Bridges, C.D.B. (1965) Properties of the electroretinogram in three elasmobranch species. Vision Res. 5: 483-496.

Hamasaki, D.I. and Gruber, S.H. (1965) The photoreceptors of the nurse shark, Ginglymostoma cirratum and the sting ray, Dasyatis sayi. Bull. Mar. Sci. 15: 1051-1059.

Hamdi, F.A. and Whitteridge, D. (1953) The representation of the retina on the optic lobe of the pigeon and the superior colliculus of the rabbit and goat. J. Physiol. 121: 44P-45P.

Hamdi, F.A. and Whitteridge, D. (1954) The representation of the retina on the optic tectum of the pigeon. Quart. J. exp. Physiol. 39: 111-118.

Harris, A.J. (1965) Eye movements of the dogfish Squalus acanthias L. J. Exp. Biol. 43: 107-130.

Hartline, P.H., Kass, L. and Loop, M.S. (1978) Merging of modalities in the optic tectum: infrared and visual integration in rattlesnakes. Science 199: 1225-1229.

Hebel, R. (1976) A method of preparing whole mounts of the retina for studies on ganglion cells. Mikroscopie 32: 96-99.

Heric, T.M. and Kruger, L. (1965) Organization of the visual projection upon the optic tectum of a reptile (Alligator mississippiensis). J. Comp. Neurol. 124: 101-112.

Hess, W.R., Bürgi, S. and Bucher, V.M. (1946) Motorische Funktion des Tectal und Tegmentalgebietes. Monats. für Psychiat. Neurol. (Basel) 112: 1-52.

Hester, F.J. (1968) Visual contrast thresholds of the goldfish (Carassius auratus). Vision Res. 8: 1315-1336.

Hoffman, R. and Basinger, S. (1977) The effect of MS-222 on rhodopsin regeneration in the frog. Vision Res. 17: 335-336.

Houser, G.L. (1901) The neurons and supporting elements of the brain of a selachian. J. Comp. Neurol. 11: 65-175.

Hueter, R.E. (1980) Physiological optics of the eye of the juvenile lemon shark (Negaprion brevirostris). M.S. thesis, Univ. Miami, Coral Gables, Florida.

Hueter, R.E. and Gruber, S.H. (1982) Recent advances in studies of the visual system of the juvenile lemon shark (Negaprion brevirostris). Florida Sci. 45: 11-25.

Hughes, A. (1975) A comparison of retinal ganglion cell topography in the plains and tree kangaroo. J. Physiol. 244 : 61P-63P.

Hughes, A. (1977) The topography of vision in mammals of contrasting life-style: comparative optics and retinal organisation. In Handbook of Sensory Physiology, Vol. VII/5: The Visual System in Vertebrates (Crescitelli, F., ed.), pp. 613-756. Springer-Verlag, Berlin.

Hughes, A. (1985) New perspectives in retinal organisation. In Progress in Retinal Research (Osborne, N.N. and Chader, G.J., eds.), 4: 243-313. Pergamon Press, Oxford.

Ingle, D. (1973) Evolutionary perspectives on the function of the optic tectum. Brain, Behav. Evol. 8: 211-237.

Jacobson, M. (1962) The representation of the retina on the optic tectum of the frog. Correlation between retinotectal magnification factor and retinal ganglion cell count. Quart. J. exp. Physiol. 47: 170-178.

Jacobson, M. and Gaze, R.M. (1964) Types of visual response from single units in the optic tectum and optic nerve of the goldfish. Quart. J. exp. Physiol. 49: 199-209.

Jaeger, R.G. (1978) Ecological niche dimensions and sensory functions in amphibians. In Sensory Ecology: Review and Perspectives (Ali, M.A., ed.), pp. 169-196. Plenum Press, New York.

Jen, L.S., So, K.-F., Yew, D.T. and Lee, M. (1983) An autoradiographic study of the retinofugal projections in the shark, Hemiscyllium plagiosum. Brain Res. 274: 135-139.

Johnson, G.L. (1901) Contributions to the comparative anatomy of the mammalian eye, chiefly based on ophthalmoscopic examination. Phil. Trans. B194: 1-82.

Kahmann, H. (1934) Über das Vorkommen einer Fovea centralis im Knochenfischauge. Zool. Anz. 106: 49-55.

Kahmann, H. (1936) Über das foveale Sehen der Wirbeltiere. I. Über die Fovea centralis und die Fovea lateralis bei einigen Wirbeltieren. v. Graefes Arch. Ophthal. 135: 265-276.

Karamian, A.I., Veselkin, N.P., Belekhova, M.G. and Zagorulko, T.M. (1966) Electrophysiological characteristics of tectal and thalamocortical divisions of the visual system in lower vertebrates. J. Comp. Neurol. 127: 559-576.

Klatzo, I. (1967) Cellular morphology of the lemon shark brain. In Sharks, Skates and Rays (Gilbert, P.W., Mathewson, R.F. and Rall, D.P., eds.), pp. 341-359. Johns Hopkins Press, Baltimore.

Knudsen, E.I. (1985) Experience alters the spatial tuning of auditory units in the optic tectum during a sensitive period in the barn owl. J. Neurosci. 5: 3094-3109.

LaTouche, Y. and Kimeldorf, D. (1978) An effect of tricaine methanesulfonate on the electroretinogram of Taricha granulosa. Life Sci. 22: 597-602.

Leghissa, S. (1951) Il sostrato anatomico dei riflessi ottico-oculomotori nei teleostei. Monit. zool. ital. Suppl. 59: 1-11.

Lettvin, J.Y., Maturana, H.R., McCulloch, W.S. and Pitts, W.H. (1959) What the frog's eye tells the frog's brain. Proc. Inst. Radio Engrs. 47: 1940-1951.

Longval, M.J., Warner, R.M. and Gruber, S.H. (1982) Cyclical patterns of food intake in the lemon shark Negaprion brevirostris under controlled conditions. Florida Sci. 45: 25-33.

Lubsen, J. (1921) Over de projectie van het netvlies op het tectum opticum bij een beenvisch. Nederl. Tijds. v. Geneesk. 2: 1258-1261.

Luiten, P.G.M. (1981) Two visual pathways to the telencephalon in the nurse shark (Ginglymostoma cirratum). I. Retinal projections. J. Comp. Neurol. 196: 531-538.

Mass, A.M. and Supin, A.Y. (1986) Topographic distribution of sizes and density of ganglion cells in the retina of a porpoise, Phocoena phocoena. Aquatic Mammals 12: 95-102.

Müller, H. (1856) Anatomisch-physiologische Untersuchungen über die Retina des Menschen und der Wirbeltiere. Leipzig.

Munk, O. (1970) On the occurrence and significance of horizontal band-shaped retinal areae in teleosts. Vidensk. Meddr dansk naturh. Foren. 133: 85-120.

Murray, R.W. (1962) The response of the ampullae of Lorenzini of elasmobranchs to electrical stimulation. J. Exp. Biol. 39: 119-128.

Myrberg, A.A., Jr. (1976) Behavior of sharks--a continuing enigma. Nav. Res. Revs. 29: 1-11.

Northcutt, R.G. (1977) Elasmobranch central nervous system organization and its possible evolutionary significance. Amer. Zool. 17: 411-429.

Northcutt, R.G. (1978) Brain organization in the cartilaginous fishes. In Sensory Biology of Sharks, Skates, and Rays (Hodgson, E.S. and Mathewson, R.F., eds.), pp. 117-193. Off. Nav. Res., Arlington, Virginia.

Northcutt, R.G. (1979) Retinofugal pathways in fetal and adult spiny dogfish, Squalus acanthias. Brain Res. 162: 219-230.

Østerberg, G. (1935) Topography of the layer of rods and cones in the human retina. Acta ophthal. Suppl. 6: 1-102.

Penfield, W. and Rasmussen, T. (1950) The Cerebral Cortex of Man. Macmillan, New York.

Penzlin, H. and Stubbe, M. (1977) Untersuchungen zur Sehschärfe des Goldfisches (Carassius auratus L.). Zool. Jb. Physiol. 81: 310-326.

Perry, V.H. and Cowey, A. (1985) The ganglion cell and cone distribution in the monkey's retina: implications for central magnification factors. Vision Res. 25: 1795-1810.

Peterson, E.H. and Rowe, M.H. (1980) Different regional specializations of neurons in the ganglion cell layer and inner plexiform layer of the California horned shark, Heterodontus francisci. Brain Res. 201: 195-201.

Pettigrew, J.D. (1986a) Flying primates? Megabats have the advanced pathway from eye to midbrain. Science 231: 1304-1306.

Pettigrew, J.D. (1986b) The evolution of binocular vision. In Visual Neuroscience (Pettigrew, J.D., Sanderson, K.J. and Levick, W.R., eds.), pp. 208-222. Cambridge Univ. Press, Cambridge.

Platt, C.J., Bullock, T.H., Czéh, G., Kovačević, N., Konjević, D. and Gojković, M. (1974) Comparison of electroreceptor, mechanoreceptor, and optic evoked potentials in the brain of some rays and sharks. J. Comp. Physiol. 95: 323-355.

Polyak, S. (1957) The Vertebrate Visual System. Univ. Chicago Press, Chicago.

Rapp, L.M. and Basinger, S.F. (1982) The effects of local anaesthetics on retinal function. Vision Res. 22: 1097-1103.

Repérant, J., Micelli, D., Rio, J.P., Peyrichoux, J., Pierre, J. and Kirpitchnikova, E. (1986) The anatomical organization of retinal projections in the shark Scyliorhinus canicula with special reference to the evolution of the selachian primary visual system. Brain Res. Rev. 11: 227-248.

Rochon-Duvigneaud, A. (1943) Les Yeux et la Vision des Vertébrés. Masson et Cie, Paris.

Sajovic, P. and Levinthal, C. (1982) Visual cells of zebrafish optic tectum: mapping with small spots. Neurosci. 7: 2407-2426.

Schlag, J. (1978) Electrophysiological mapping techniques. In Neuroanatomical Research Techniques (Robertson, R.T., ed.), pp. 385-404. Academic Press, New York.

Schmidt, J.T. (1982) The formation of retinotectal projections. Trends Neurosci. 5: 111-115.

Schneider, D. (1971) Specialized odor receptors in insects. In Gustation and Olfaction (Ohloff, O. and Thomas, A.F., eds.), pp. 45-60. Academic Press, New York.

Schneider, G.E. (1969) Two visual systems. Science 163: 895-902.

Schultze, M. (1866) Zur Anatomie und Physiologie der Retina. Arch. mikr. Anat. 2: 175-286.

Schwassmann, H.O. (1968) Visual projection upon the optic tectum in foveate marine teleosts. Vision Res. 8: 1337-1348.

Schwassmann, H.O. (1975) Central projections of the retina and vision. In Vision in Fishes: New Approaches in Research (Ali, M.A., ed.), pp. 113-126. Plenum Press, New York.

Schwassmann, H.O. and Krag, M.H. (1970) The relation of visual field defects to retinotectal topography in teleost fish. Vision Res. 10: 29-42.

Schwassmann, H.O. and Kruger, L. (1965a) Organization of the visual projection upon the optic tectum of some freshwater fish. J. Comp. Neurol. 124: 113-126.

Schwassmann, H.O. and Kruger, L. (1965b) Experimental analysis of the visual system of the four-eyed fish Anableps microlepis. Vision Res. 5: 269-281.

Schwassmann, H.O. and Meyer, D.L. (1971) Refractive state and accommodation in the eye of three species of Paralabrax (Serranidae, Pisces). Vidensk. Meddr dansk naturh. Foren. 134: 103-108.

Schweitzer, J. (1986) Functional organization of the electroreceptive midbrain in an elasmobranch (Platyrhinoidis triseriata). J. Comp. Physiol. A 158: 43-58.

Sharma, S.C. (1972) Reformation of retinotectal projections after various tectal ablations in adult goldfish. Exp. Neurol. 34: 171-182.

Siminoff, R., Schwassmann, H.O. and Kruger, L. (1966) An electrophysiological study of the visual projection to the superior colliculus of the rat. J. Comp. Neurol. 127: 435-444.

Sivak, J.G. (1974) Accommodation of the lemon shark eye (Negaprion brevirostris). Vision Res. 14: 215-216.

Sivak, J.G. (1978) Refraction and accommodation of the elasmobranch eye. In Sensory Biology of Sharks, Skates, and Rays (Hodgson, E.S. and Mathewson, R.F., eds.), pp. 107-116. Off. Nav. Res., Arlington, Virginia.

Smeets, W.J.A.J. (1981) Retinofugal pathways in two chondrichthyans, the shark Scyliorhinus canicula and the ray Raja clavata. J. Comp. Neurol. 195: 1-11.

Smeets, W.J.A.J., Nieuwenhuys, R. and Roberts, B.L. (1983) The Central Nervous System of Cartilaginous Fishes. Springer-Verlag, Berlin.

Springer, S. (1950) Natural history notes on the lemon shark, Negaprion brevirostris. Texas J. of Sci. 2: 349-359.

Starck, W.A. (1968) Life history and ecology of the lemon shark, Negaprion brevirostris (Poey), in Florida Bay. Abstr. Curr. Invest. U.S. Elas. Fish., AIBS Shark Research Panel, Washington.

Stein, B.E. and Gaither, N.S. (1981) Sensory representation in reptilian optic tectum: some comparisons with mammals. J. Comp. Neurol. 202: 69-87.

Stell, W.K. and Witkovsky, P. (1973a) Retinal structure in the smooth dogfish, Mustelus canis: general description and light microscopy of giant ganglion cells. J. Comp. Neurol. 148: 1-32.

Stell, W.K. and Witkovsky, P. (1973b) Retinal structure in the smooth dogfish, Mustelus canis: light microscopy of photoreceptor and horizontal cells. J. Comp. Neurol. 148: 33-46.

Stone, J. (1981) The Wholemount Handbook: A Guide to the Preparation and Analysis of Retinal Wholemounts. Maitland Publs., Sydney, Australia.

Stone, J. (1983) Parallel Processing in the Visual System: The Classification of Retinal Ganglion Cells and its Impact on the Neurobiology of Vision. Plenum Press, New York.

Tamura, T. (1957) A study of visual perception in fish, especially on resolving power and accommodation. Bull. Jap. Soc. sci. Fish. 22: 536-557.

Tamura, T. and Wisby, W.J. (1963) The visual sense of pelagic fishes especially the visual axis and accommodation. Bull. Mar. Sci. 13: 433-448.

Tester, A.L. and Kato, S. (1966) Visual target discrimination in blacktip sharks (Carcharhinus melanopterus) and grey sharks (C. menisorrah). Pac. Sci. 20: 461-471.

Ulinski, P.S. (1984) Design features in vertebrate sensory systems. Am. Zool. 24: 717-731.

Van Buren, A. (1963) The Retinal Ganglion Cell Layer. Thomas, Springfield, Illinois.

Van der Meer, H.J. and Anker, G.C. (1984) Retinal resolving power and sensitivity of the photopic system in seven haplochromine species. Neth. J. Zool. 34: 197-209.

Vanegas, H. (1983) Organization and physiology of the teleostean optic tectum. In Fish Neurobiology, Vol. 2: Higher Brain Areas and Functions (Davis, R.E. and Northcutt, R.G., eds.), pp. 43-90. Univ. Mich. Press, Ann Arbor, Michigan.

Verrier, M.-L. (1930) Contribution à l'étude de la vision chez les sélaciens. Ann. Sci. Nat. Zool. 13: 5-54.

Veselkin, N.P. (1966) Electrical reactions in midbrain, medulla and spinal cord of lamprey to visual stimulation. Fedn. Proc. Fedn. Am. Socs. exp. Biol. 25: 957-960.

Veselkin, N.P. and Kovačević, N. (1973) Non-olfactory telencephalic afferent projections in elasmobranch fishes. Zh. Evol. Biokh. Fiziol. 9: 585-592.

Von Helmholtz, H. (1924) Treatise on Physiological Optics (trans. from 3rd German ed. of 1909 by Southall, J.P.C.). Amer. Opt. Soc.

Walls, G.L. (1942) The Vertebrate Eye and its Adaptive Radiation. Hafner Publ. Co., New York (reprinted 1967).

Wang, C.-S.J. (1968) The eye of fishes with special reference to pigment migration. Ph.D. diss., Cornell Univ., Ithaca, New York.

Wehner, R. (1987) 'Matched filters'--neural models of the external world. J. Comp. Physiol. A 161: 511-531.

Witkovsky, P., Powell, C.C. and Brunken, W.J. (1980) Some aspects of the organization of the optic tectum of the skate Raja. Neurosci. 5: 1989-2002.

Wolken, J.J. (1975) Photoprocesses, Photoreceptors and Evolution. Acad. Press, New York.

Wright, T. and Jackson, R. (1964) Instrumental conditioning of young sharks. Copeia 1964: 409-412.

Wyszecki, G.W. and Stiles, W.S. (1967) Color Science: Concepts and Methods, Quantitative Data and Formulas. Wiley, New York.

Yew, D.T., Chan, Y.W., Lee, M. and Lam, S. (1984) A biophysical, morphological and morphometrical survey of the eye of the small shark (Hemiscyllium plagiosum). Anat. Anz., Jena 155: 355-363.

BIOGRAPHICAL SKETCH

Robert Edward Hueter was born in Baltimore, Maryland, on April 13, 1952. His parents are Edward M. Hueter, Jr. and Patricia C. Hueter of Naples, Florida. He completed his secondary education at Dulaney Senior High School in Timonium, Maryland, and in 1974 graduated magna cum laude with the Bachelor of Science degree in biology with general honors from the University of Miami, Coral Gables, Florida. In 1980 he was granted the degree of Master of Science in marine biology by the Rosenstiel School of Marine and Atmospheric Science of the University of Miami and was awarded the degree of Doctor of Philosophy in zoology from the University of Florida, Gainesville, in 1988.

Concurrent with his graduate studies, he was employed as chief scientist and instructor aboard R/V Geronimo, a shark-fishing vessel based in Newport, Rhode Island; science correspondent for National Public Radio in San Francisco; editorial researcher for the International Oceanographic Foundation, Miami; interviewer of marine sportfishermen for the National Marine Fisheries Service; and teacher of lower and upper division courses in zoology and marine science at the University of Miami and the University of Florida. Following his Ph.D. degree, he was awarded the position of Postdoctoral Research Associate at the Mote Marine Laboratory in Sarasota, Florida.

I certify that I have read this study and that in my opinion it conforms to acceptable standards of scholarly presentation and is fully adequate, in scope and quality, as a dissertation for the degree of Doctor of Philosophy.

Horst O. Schwassmann, Chairman
Professor of Zoology

I certify that I have read this study and that in my opinion it conforms to acceptable standards of scholarly presentation and is fully adequate, in scope and quality, as a dissertation for the degree of Doctor of Philosophy.

Carter R. Gilbert
Professor of Zoology

I certify that I have read this study and that in my opinion it conforms to acceptable standards of scholarly presentation and is fully adequate, in scope and quality, as a dissertation for the degree of Doctor of Philosophy.

David H. Evans
Professor of Zoology

I certify that I have read this study and that in my opinion it conforms to acceptable standards of scholarly presentation and is fully adequate, in scope and quality, as a dissertation for the degree of Doctor of Philosophy.

William W. Dawson
Professor of Neuroscience

I certify that I have read this study and that in my opinion it conforms to acceptable standards of scholarly presentation and is fully adequate, in scope and quality, as a dissertation for the degree of Doctor of Philosophy.

Paul J. Linser
Associate Professor of Anatomy and
Cell Science

This dissertation was submitted to the Graduate Faculty of the Department of Zoology in the College of Liberal Arts and Sciences and to the Graduate School and was accepted as partial fulfillment of the requirements for the degree of Doctor of Philosophy.

April 1988

Dean, Graduate School